Research Report from the National Institute for Environmental Studies, Japan, No.89, 1986.
国立公害研究所研究報告　第89号

Measuring the Water Quality of Lake Kasumigaura by LANDSAT Remote Sensing

LANDSATリモートセンシングによる霞ケ浦の水質計測

Tadakuni MIYAZAKI
宮崎　忠国

Environmental Information Division
環境情報部

環境庁　国立公害研究所
THE NATIONAL INSTITUTE FOR ENVIRONMENTAL STUDIES

Preface

The quality of the environment varies both spatially and with time. Since remote sensing is a technology suitable for simultaneous observation of the physical state of the target with spatial extent, it can be an adequate technique to obtain information on the spatial structure of the quality of environment at a moment. With a view to obtaining the basic knowledge for constructing the environmental information system, a series of remote sensing experiment has been carried out both in laboratory and field by the National Institute for Environmental Studies since 1977. In this report, water quality measurement of Lake Kasumigaura by spacecraft (LANDSAT) remote sensing is described, and emphasis is being placed on problem-oriented approaches, development of operational interpretation methods and techniques of water quality measurement by remote sensing.

It is hoped that the results obtained here and the techniques developed in this study would be of much use to researchers of the environmental sciences and environment planners.

Shota HIROSAKI
Director of the
Environmental Information
Division,
March 1986

CONTENTS

Abstract

Measuring the water quality of Lake Kasumigaura from LANDSAT multispectral scanner data is reported herein.

To investigate the nature of suspended solid or chlorophyll-spectral reflectance relationships, a portable high-speed spectroradiometer for measuring spectral reflectance of water surface was developed. This instrument uses a monochromatic grating and a photomultiplier system for light detection and sweeps over the 400 to 850 nm wavelength spectral range within one second.

Both reflected and incident solar radiation at the water surface and water quality parameters were measured at ground truth points on Lake Kasumigaura. Linear regression analysis shows that the best-fit for the relationship between Secchi depth transparency or suspended solid concentration in the surface water and radiance reflectance at the water surface is in the 500 to 800 nm wavelength range.

Statistical models to estimate water quality parameters from LANDSAT data are developed using linear regression analysis between the various water quality parameters and LANDSAT data. The results show a significant correlation between Secchi depth transparency or concentration of suspended solids and LANDSAT band 4, 5 or 6 data.

The effect of the light transmittance and path radiance of the atmosphere on LANDSAT data is also evaluated. The transmittance and the path radiance are estimated by a linear regression analysis between the radiance detected by LANDSAT and the upwelling radiance observed at the water surface. Then the distribution of the radiance reflectance of the entire surface of the lake are estimated from LANDSAT data. The estimated path radiance included in LANDAST band 4 data on 3 March 1982 was 0.26 mW/cm·sr and the transmittance 0.86.

From the spectral radiance reflectance of the water surface estimated from LANDSAT data, water quality models independent of different weather conditions are developed.

Finally, distribution maps for concentration of suspended solids in Lake Kasumigaura are presented.

CHAPTER 1

Introduction

1.1 GENERAL INTRODUCTION

Remote sensing is used to gather and record information about terrain and ocean surfaces without making actual contact with the object or area being investigated. Each type of surface material, for example, soil, rocks, vegetation and ocean surface, absorb and reflect solar energy in some characteristic manner which depends on its atomic and molecular structure. In addition, a certain amount of internal energy is emitted independently of the solar flux from the surface material. The absorbed, reflected, and internally emitted energy in the electromagnetic spectrum can be detected by remote sensing of the object or phenomenon of interest. The instruments used provide the charateristic spectral signatures and images. These spectral signatures can then usually be correlated with other known spectral signatures of rock, soil, crop, terrain, or ocean surface features. By selecting specific ranges of the electromagnetic spectrum to be used, useful information can be obtained about the terrain or ocean to be examined.

In the past decade, with industrial growth and the increase in urbanization, human pollution has expanded exponentially. Water quality particularly have been seriously degenerated by organic waste in many rivers, lakes, estuaries, and inland seas. The increasing complexity of water pollution problems has forced planners to seek new methodologies for determining alternative resource management plans. To meet this challenge and to satisfy certain planning needs, techniques for remote sensing of natural aquatic bodies have been developed. Measurements by remote sensing may have two distinctive contributions: (1) monitoring macroscopic environmental conditions and (2) simultaneous measurement of a large surface. Such measurements provide an aid in the understanding, management, and control of natural water bodies.

Remotely sensed data may be interpreted by two approaches. The first approach is qualitative in nature and has been used to map features, such as river plumes and pollution patterns without concurrent ground truth measurements. The second approach is quantitative analysis in which ground truth collected at a limited number of locations is used to calibrate the remotely sensed data and to extend the results to the remotely sensed scene. Results of the quantitative analysis, calibrated regression equation, have been used to develop maps showing quantitative distributions of some water quality parameters such as the amount of suspended solids or chlorophyll-*a*. A key problem is to determine whether the relationships between suspended solids or chlorophyll-*a* and spectral reflectance are unchanging. If these relationships are variable with location and time, then extensive ground truth must be obtained at each monitoring site for calibration, thus greatly reducing the utility of remote sensing methods.

In this report, the water quality measurement of Lake Kasumigaura by

satellite (LANDSAT) remote sensing is described. Throughout our experiments, we especially tried to determine the degree of variability in relationships between concentrafion of suspended solids or chlorophyll-*a* and spectral reflectance at water surface to determine whether it is possible to make remote measurement with sufficient accuracy to permit monitoring with few or no ground truth measurements. A spectroradiometer designed for spectral reflectance measurement in remote sensing is described in Chapter 2. Relationships between water quality and radiance reflectance at water surface are described in Chapter 3. Water quality measurements from LANDSAT MSS data are described in Chapter 4. Finally, an estimation of path radiance and transmittance of the atmosphere together with atmospheric correction of LANDSAT MSS data are described in Chapter 5.

Chapter 2 is a revised version of the report of Miyazaki *et al.* (1981) and reports the additional laboratory expriments (Miyazaki & Watanabe, 1984) and field measurements. Chapter 3 is based on a paper by Okami *et al.* (1982). Chapter 4 is based on technical data from a series of experments of Lake Kasumigaura reported by Yasuoka and Miyazaki (1979, 1982 a, 1982 b). Chapter 5 is a revision of work by Yasuoka and Miyazaki (1982c).

1.2 AIM OF THE PRESENT EXPERIMENT

Here water quality measurements of Lake Kasumigaura by LANDSAT MSS data are described.

When measuring terrain or ocean objects by remote sensing techniques, it is essential to know the spectral characteristics of the objects. To investigate the relationship between water quality and spectral reflectance a portable high-speed spectroradiometer was developed. Utilizing this instrument at Lake Kasumigaura, we obtained the relationships between water quality parameters and radiance reflectance of the water surface and path radiance and the transmittance of the air between the water surface and the remote sensor.

Many investigators have tried to measure water quality parameters qualitatively or quantitatively in various bodies of water, the resulting water quality distribution maps showed reasonable results with sufficient accuracy. These results, however, were not independent of particular bodies of water, the nature of the water quality, and weather conditions. Consequently the development of generalized water quality models adapted to remote sensing are desired.

The aim of the present experiment is to develop a technique for estimating the effects of the atmosphere on LANDSAT MSS data and to develop a water quality model which will make it feasible to use quantitave remote measurements of water bodies without accompaning ground truth for monitoring purposes.

The steps in the project are as follows:

(1) To develop a high-speed spectroradiometer to measure the spectral characteristics of surface objects which are applicable to remote sensing;

(2) To investigate the relationships between the water quality parameters and the spectral characteristics of Lake Kasumigaura;

(3) To measure water quality parameters from LANDSAT MSS data utilizing regression analysis;

(4) To evaluate the effects of the atmosphere on LANDSAT MSS data;

(5) To estimate the surface radiance reflectance of Lake Kasumigaura from

LANDSAT MSS data;

(6) Finally, to develop a water quality model suggested by the experiments and then to evaluate the aptness of this model.

CHAPTER

2

The instrumentation for measuring spectral reflectance

2.1 INTRODUCTION

In recent years, in various scientific disciplines, techniques for collecting remotely sensed data have progressed very rapidly, but many problems still remain in the utilization of this data. One of the main problems is the lack of good techniques to obtain satisfactry samples of ground data. Since remote sensors operate by detecting or sensing energy levels of emitted and/or reflected radiation over various ranges of the electromagnetic spectrum, it is necessary to make ground measurements of the reflectance from natural surfaces in order to understand the relationships between spectral reflectance and other surface parameters. The spectral signatures of field samples may be obtained by laboratory measurement, but these data will not, in general, be typical of outdoor situations. There was, therefore, a need to develop a spectroradiometer with adequate wavelength resolution which could be used to obtain typical values of spectral reflectance in the field. Several types of spectroradiometer have been used to measure the spectral reflectance of natural surfaces in the field. Miller *et al.* (1971) developed a four channel scanning photometer for remote sensing and this instrument provided spectral information about water surface in the spectral ranges of 440 to 460, 550 to 590, 680 to 700, and 720 to 750 nm. Burr and Dancan (1972), on the other hand, developed a submersible spectroradiometer for measuring upwelling and downwelling irradiance spectra underwater. The instrument consists of a submersible probe, cable, and control box. Within the probe, there is a rotating wheel holding 16 interference filters allowing the detection of irradiance from 400 to 700 nm at every 20 nm intervals. Rouse and Coleman (1976) used a radiometer (International Light IL 700 Research Radiometer) to investigate relationships between concentration of suspended solids and reflected radiation in laboratory experiments. A compact spectrometer Model DA, two channel (380 and 500 nm) was developed by Doda and Green (1978) to obtain spectral atmospheric turbidity. Viollier *et al.* (1978) developed a radiometer which uses four interference filters, 446, 500, 525, and 600 nm with a half bandwidth of 10 nm. The upwelling and downwelling radiations are directed into the interference filters by two optical fibers. Booth and Dustan (1979) developed a submersible multi-channel irradiance meter (MER-1000). This instrument covers the wavelength range from 410 to 694 nm with 11 interchangeable interference filters. For ground data collection in remote sensing, Milton (1980) introduced a low-cost, portable multi-band radiometer that measures the spectral reflectance of ground objects in four bands simultaneously. The spectral coverage of each band is determined by interchangable absorption filters. Myrabφ *et al.* (1982) designed and constructed a portable field spectroradiometer to measure the spectral reflectance signatures of terrain and ocean objects. This instrument employs a chopping technique which makes it possible to measure simultaneously both the irradiance from the sun and sky and the

radiance from a scene. Three interchangeable gratings ruled at 500, 1000, and 2000 nm cover the entire spectral region of 340 to 2500 nm, and the monochromatic slit is adjusted to give waveband halfwidths of 10, 20, and 40 nm for the 500, 1000, and 2000 nm gratings, respectively. Adams *et al.* (1985) introduced a lightweight, portable two-band radiometer which used the reflectance ratio of infrared to red or some linear combination of these characteristics for estimating standing crop biomass values. The instrument employs two interchangeable filters and photo detectors which, with the aid of a neutral beam spilitter mounted at angle of 45° to the optical axis of the collecting lens, simultaneously monitors the intensity of the radiation with the two filter/photodetector assemblies.

None of these instruments, however, meet all of the requirements for ground or ocean measurements in specific fields. Some surface conditions are so dynamic that they may change within one second. Under such conditions, ground data collected at the instant the remote sensor flies over is absolutely necessary to verify what was actually present and what the acquired imagery may subsequently reveal. This ground data collection is very expensive and often requires special instrumentation, planning and logistical support. As a result, there is a need for high-speed spectroradiometric instruments, specifically designed for collecting ground data. The following properties are desirable for such instruments:

(1) The wavelength range covered should be the same as that of the remote sensors;
(2) A spectral resolution of about 2 nm is generally sufficient for most spectrophotometric measurement at the ground level;
(3) The sampling speed of the scanning cycle should be less than one second;
(4) The instrumentation should also have a data storage system such as a digital magnetic cassette tape or a mini-floppy disk system;
(5) The instrumentation should operate with either line or battery power for either laboratory or field use;
(6) The instrumentation should be compact, light and versatile;
(7) The electronic and mechanical reliability should be very high.

This chapter describes the design of a newly developed high-speed spectroradiometer for ground data collection and discusses its applicability to the remote sensing sessions.

2.2 THE HIGH-SPEED SPECTRORADIOMETER

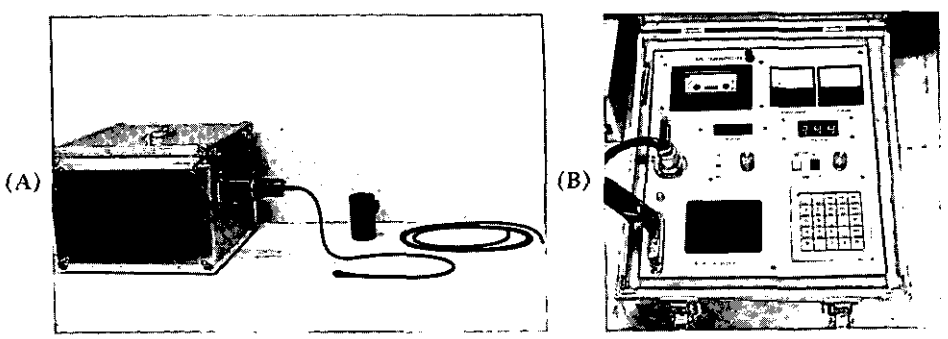

Fig. 2.1 Photographs of the high-speed spectroradiometer.
(A): Sensor unit. (B): Control unit.

Fig. 2.1 shows photographs of our newly developed spectroradiometer, the instrument consists of a sensor unit and a control unit. Fig. 2.2 shows the block diagram for optical and electrical systems of the spectroradiometer.

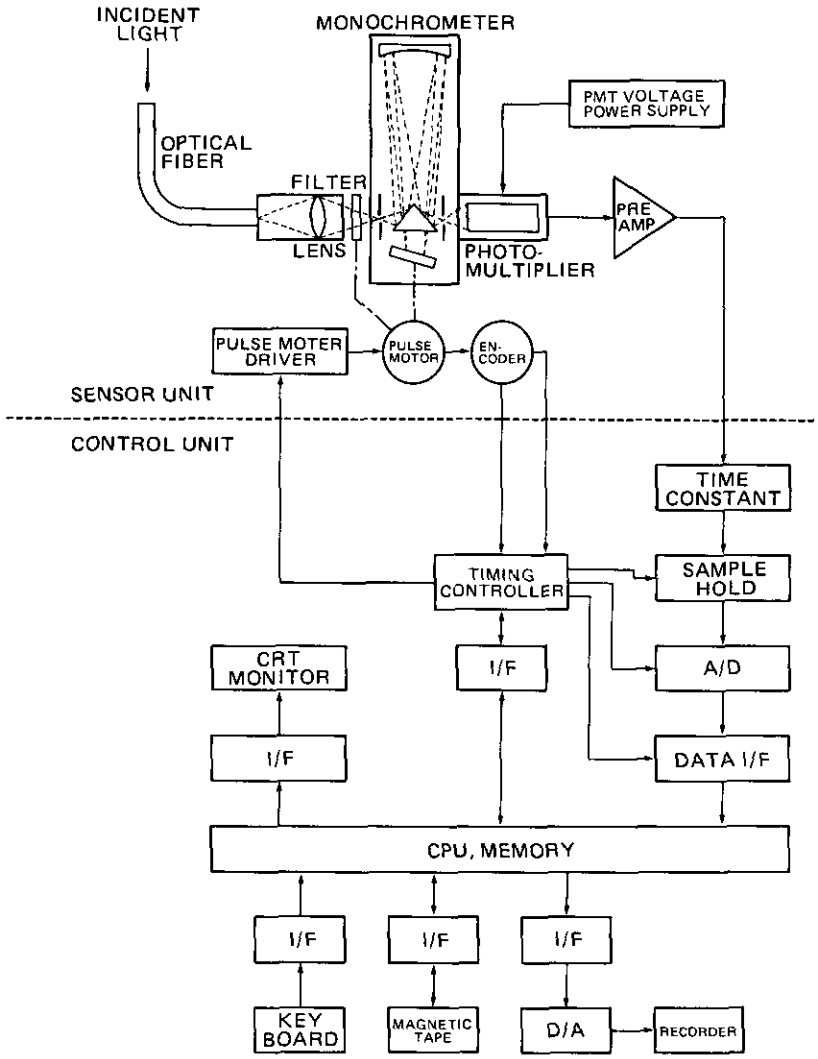

Fig. 2.2 Block diagram of the high-speed spectroradiometer.

2.2.1 The sensor unit

The sensor unit contains an optical system and a photomultiplier system. The optical system consists of an optical fiber, a light collecting lens, and a monochrometer system. The optical fiber is glass of 7 mm dimeter; its efficiency for light transmittance is about 0.8 for a length of 1 m in the visible wavelength range while the light collecting lens is a commercially available camera lens with a diameter of 52 mm, focal length of 50 mm, and f-value of 2.0. We used an off-plane

Ebert type of monochrometer with a focal length of 300 mm, slit width of 0.357 mm, and a reciprocal dispersion of 5.4 nm/mm for a 600-line/nm grating with an f-value of 6. The photomultiplier tube (PMT) used is a side-on S-20 type PMT which has a relatively wide and uniform response to light in the wavelength range of interest.

Fig. 2.3 shows a schematic drawing of the three types of optical arrangements of the sensor unit. In practice, the optical arrangement (B) in Fig. 2.3 is most convenient for field and laboratory use because of the flexibility of optical fiber and adjustable length of the optical fiber. All spectral measurements with the instrument reported here have been taken with optical arrangement (B). Fig. 2.4 shows three variations of sensor head for the optical fiber system. Heads (A) and (B) are for radiance measurement; the field of view of each sensor is determined by the

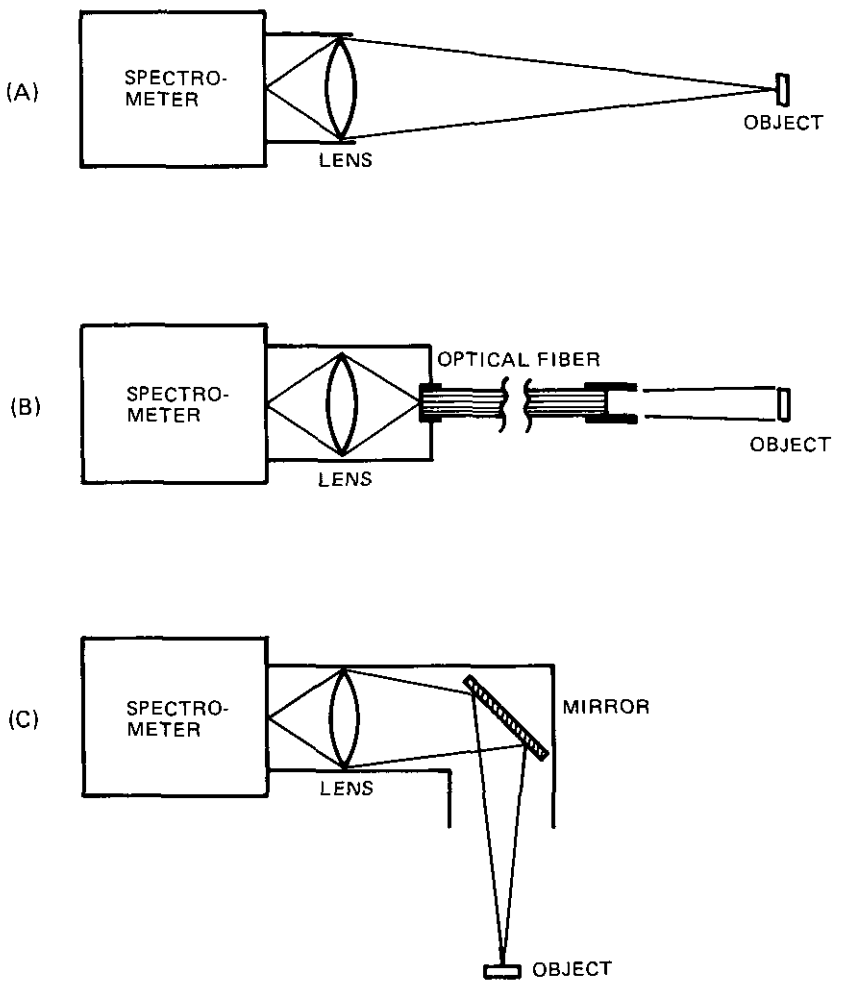

Fig. 2.3 Optical arrangement of light collecting system.
(A): Standard arrangement. (B): Optical fiber.
(C): Downword attachment.

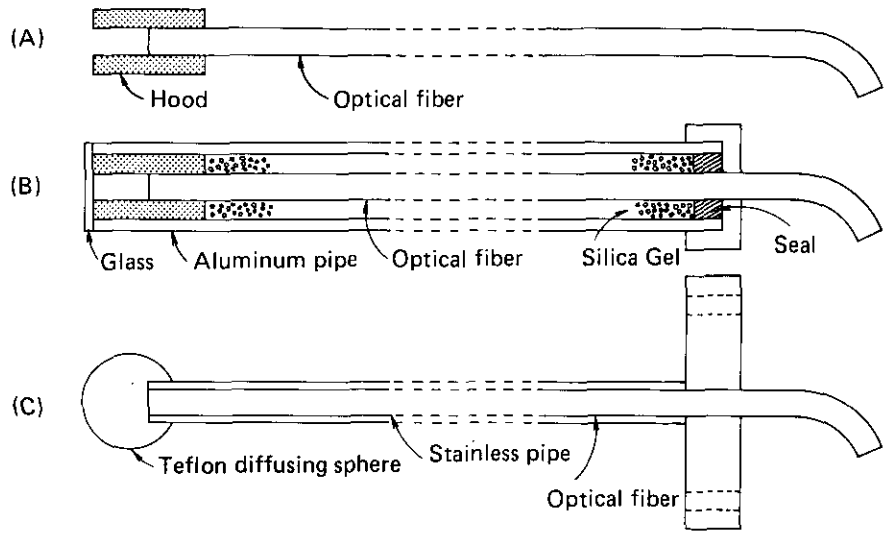

Fig. 2.4 Schematic picture of three sensor heads.

adjustable-length hood in front of the optical fiber. Sensor head (C) in Fig. 2.4 uses a Teflon diffusing sphere for irradiance measurement. Sensor head (B) and (C) are installed in a metal pipe to measure the spectral characteristics of both underwater and ground objects. Figs. 2.5 and 2.6 show the dependence of the light detection efficiency of the sensor heads on the directional angle of the light source. Fig. 2.5 indicates detection efficiency of the sensor head (A) and (B) in Fig. 2.4; Fig. 2.6 shows the detection efficiency of sensor head (C).

The unit weighs about 22 kg and is 44 cm long, 44 cm wide, and 35 cm high. The parameters and specifications for the sensor unit are listed in Table 2.1.

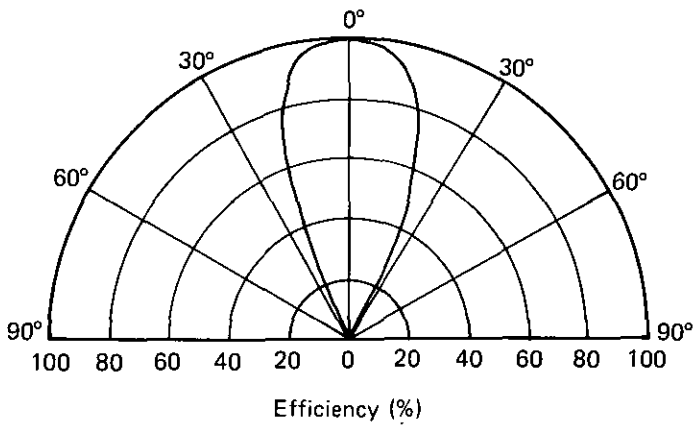

Fig. 2.5 Directional efficiency of the sensor head (A) and (B) in Fig. 2.4.

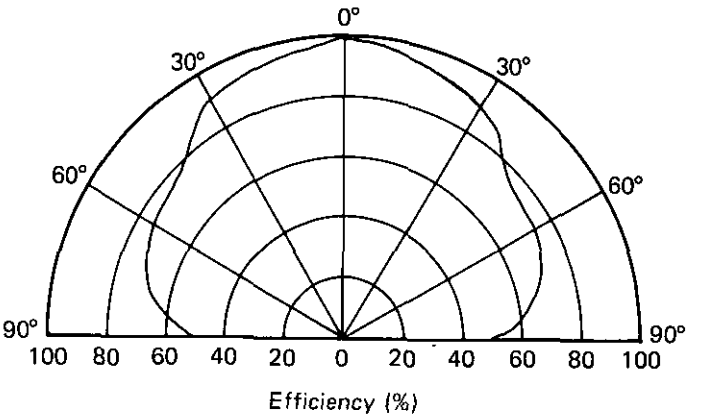

Fig. 2.6 Directional efficiency of the sensor head (C) in Fig. 2.4.

Table 2.1 Parameters and specification of the sensor unit.

Light collecting system	
Method of light collection	Plane mirror and lens
Optical fiber	Glass made, 7mm
Diffraction grating	
Method of mounting system	Off-plane Ebert type
Focal length	300mm
Slit width	0.8mm
Reciprocal dispersion	1200 line/mm
F-value	6
Method of driving system	Vibrating grating
Light detecting system	
PMT	S-20 side on type
Pre amplifire	
Range of frequency	DC-2kHz
Linearity	0.1%
Temperature stability	10μV/℃
Out put power	±10V

2.2.2 The control unit

The control unit consists of a PMT high voltage power supply and a micro-processor with keyboard, a 5 inch CRT display and a cassette tape unit. With a potentiometer the PMT voltage is adjusted between 100 and 999 volts. The supply voltage is displayed on a 3-digit LED indicator. The micro-processor is an 8085, with a 16 KByte ROM and a 4 KBite RAM to control the total interactive operation of the instrument. The operation is divided into 6 subsystems:

(1) Keying in the chart data of a standard lamp for calibration;

(2) Measurement of the standard lamp, this routine calculates the correction factor for each wavelength and stores them on the RAM;

(3) Measurement, measured values are stored on the RAM after having been multiplied by the correction factors to obtain absolute intensity;

(4) Display the chart data, correction factors, and results of the measurement;

(5) Read the cassette tape;
(6) Initialization of the cassette tape.

The control unit weighs about 20 kg and is 35 cm long, 39 cm wide, and 45 cm high. The specifications of the control unit are listed in Table 2.2.

Table 2.2 Parameters and specification of the control unit.

Operating system	
A/D converter	
Resolution	12 bit
Conversion time	10 μs
Micro-processor	
CPU	8080
Memory	ROM 4 K bite, RAM 16 K bits
Input device	Key board
Cassette tape unit	
Method of recording	PE system
Recording density	800 BPI
Speed of data exchange	12 K bit/s
CRT display	
Screen size	5 inch CRT
Number of character	24×80 characters
Density of screen	240×320 dotts
Pen recorder	
A/D converter	12 bit
Recording width	120 mm

2.2.3 System performance

The optical system is first carefully lined up by using a monochromatic light beam. The linearity of the instrument is tested by comparison with an absolutely calibrated linear radiometer. The deviation from linearity was less than 0.5% over a wavelength range of operation. This deviation was considered to be no practical significane. The slit of the monochrometer was adjusted to give a wave half-band width of 2 nm for 500 blased gratings. The scanning time for the entire wavelength range from 400 to 850 nm is about one second and measured data are accumulated up to 99 scan cycles. The time to store the data in the magnetic cassette tape is approximately 30 seconds, including the time to calculate the absolute intensity with the correction coefficient.

2.2.4 Calibration procedures

In order to measure spectral reflectance accurately, the instrument sholud be calibrated at regular intervals. The calibration can shift due to factors such as the collection of dust in the optical system or from a variety of other random factors. The most convenient way to calibrate the instrument is to make use of a standard light source which produces a known amount of radiant energy at various wavelengths. The standard light source used here is a 5 W Halogen lamp and the shape of its spectral distribution curve is very close to that of black body radiation at the apparent color temerature of the lamp. This lamp is commercially available with a calibration chart giving radiant energy output at some photometric distance

(50 cm) from the lamp at a specified lamp voltage. A regulated power supply, also commercially available, has both an accurate ammeter and voltmeter to enable one to reproduce the standard operating condition of the lamp. The procedure for the calibrating the instrument are as follows:

(1) Key in the chart data of the standard lamp, the data are stored in either memory or cassette tape as "Table data";

(2) Measure the standard lamp at the photometric distance (50cm) with adequate PMT voltage, correction coefficients at every wavelength can be formed by determining the ratios of the actual spectral intensity listed in calibration chart of the standard lamp, divided by the actually measured spectral intensity of the standard lamp.

This calculation is done automatically by the micro-processor and the correction coefficients are stored either in its memory or in cassette tape as "Reference data". Some typical correction coefficients are snown in Fig. 2.7.

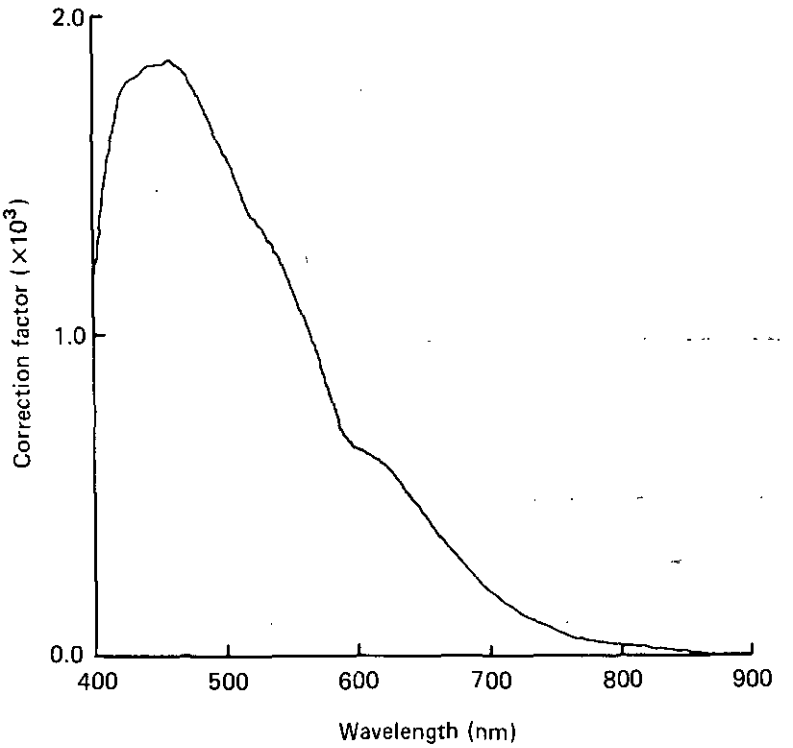

Fig. 2.7 Correction coefficient of the system.

2.3 LABORATORY EXPERIMENTS

The instrument was used to study the spectral characteristics of natural water containing suspended solids and phytoplankton. Fig. 2.8 showed the setup for measuring the spectral signatures of water samples. The water is placed into a 20 × 20 mm glass cell and illuminated by a 500 W Halogen lamp which is operated by a power supply having a stabilized voltage and current. The results shown in Figs. 2.9 and 2.10 give the resulting spectral signatures for different concentrations of suspended solids or chlorophyll-*a* in the water. Fig. 2.9 shows typical spectral output measurements for three different concentrations of suspended solids; Fig. 2.10 shows the same for chlorophyll-*a*. In Fig. 2.9, as the concentration increases, the intensity of the reflectance of water surface increases over the entire wavelength range of 500 to 850 nm. In Fig. 2.10, the highest concentration of chlorophyll-*a* has the lowest reflectance in the wavelength range of 430 and 680 nm, the ranges known to have chlorophyll-*a* absorption bands.

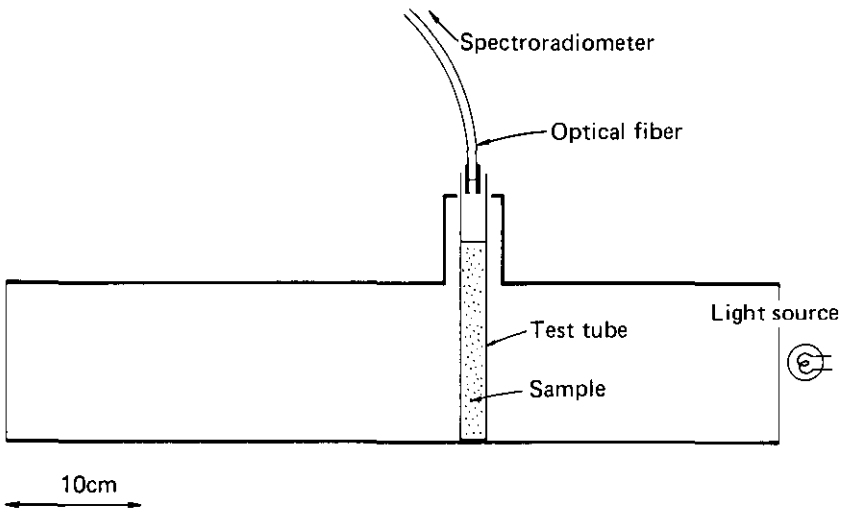

Fig. 2.8 Measuring system for radiance of water sample.

The instrument was also used to measure irradiance underwater with a Teflon 4π light collector. The Teflon 4π sensor is illustrated in Fig. 2.4 (C). The vertical distribution of photosynthetically active irradiance was measured in microcosm (Miyazaki & Watanabe, 1984), where an axenic clonal culture of red tide alga, *Heteroshiguma Akashiwo*, grew and accumulated at the water surface due to vertical migration. Fig. 2.11(A) shows the vertical distribution of the irradiance of pure sea water and Fig. 2.11 (B) shows the vertical distribution of irradiance of sea water

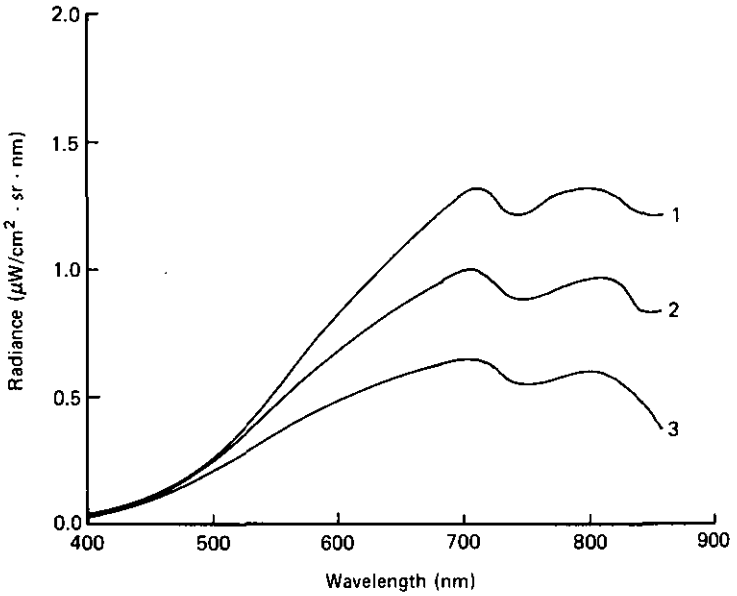

Fig. 2.9 Spectral characteristics of water with different concentration of suspended solids. 1: 52.8mg/*l*. 2: 26.4mg/*l*. 3: 13.2mg/*l*.

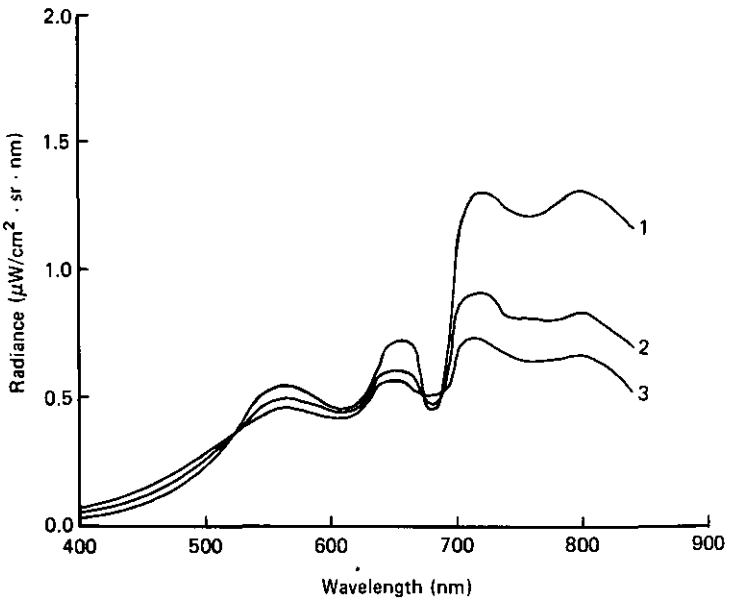

Fig. 2.10 Spectral characteristics of water with different concentration of chlorophyll-*a*. 1: 23.5μg/*l*. 2: 15.4μg/*l*. 3: 7.69μg/*l*.

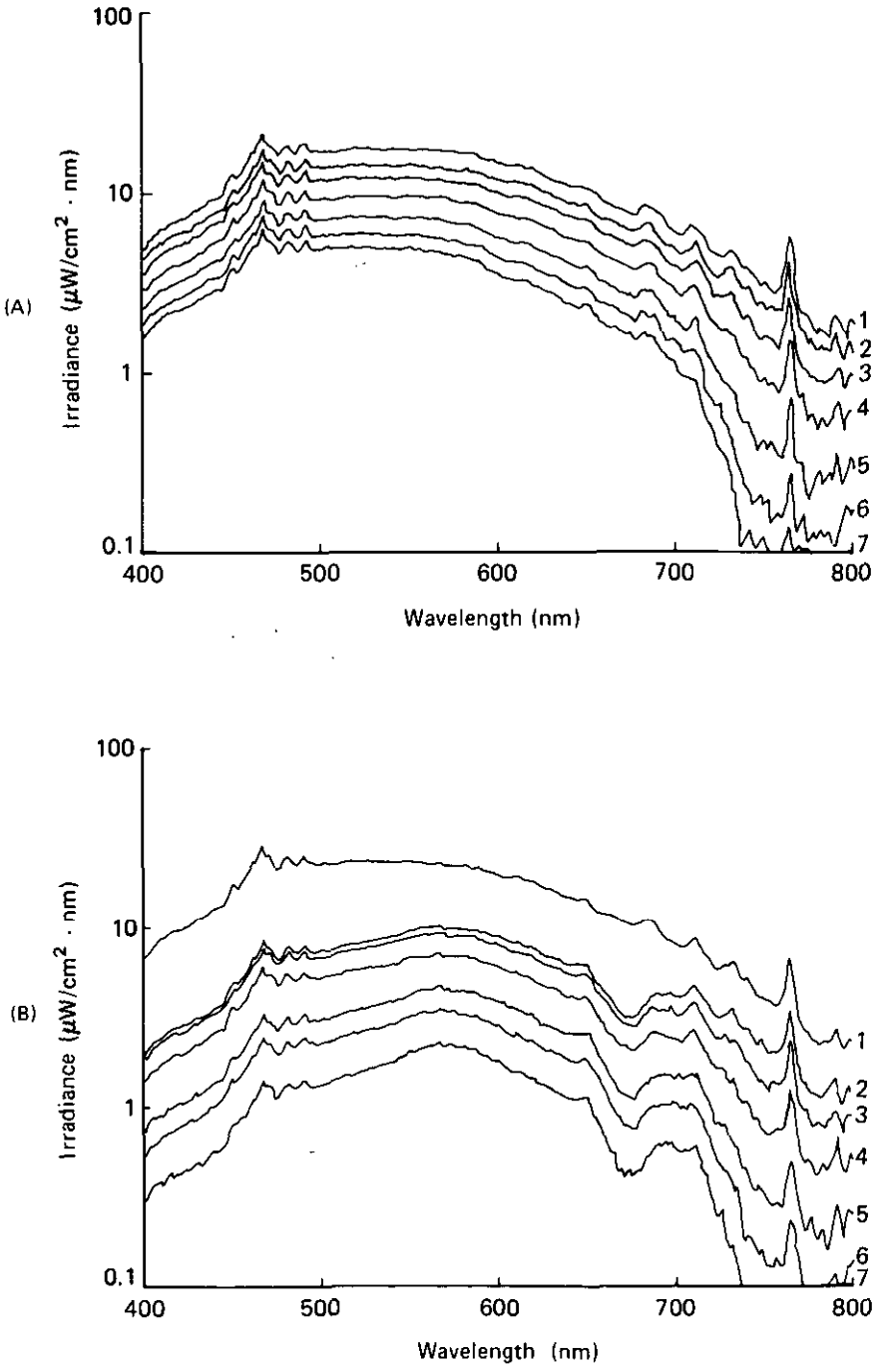

Fig. 2.11 Spectral characteristics of under water irradiance in Microcosm.
(A): Pure sea water. (B): Sea water contaminated by *H. Akashiwo* of 137,544 cells/m*l*.
1: At water surface. 2: 0cm underwater. 3: 10cm. 4: 20cm. 5: 40cm. 6: 60cm. 7: 80cm.

contaminated by *H. Akashiwo* at 137,544 cells/m*l*. Fig. 2.12 shows the underwater irradiance with different concentrations of *H. Akashiwo* at 10 cm depth from the water surface of microcosm. In Fig. 2.12, it can be seen that a higher concentration of *H. Akashiwo* results in a lower recorded irradiance in the spectral range of 400 to 710 nm.

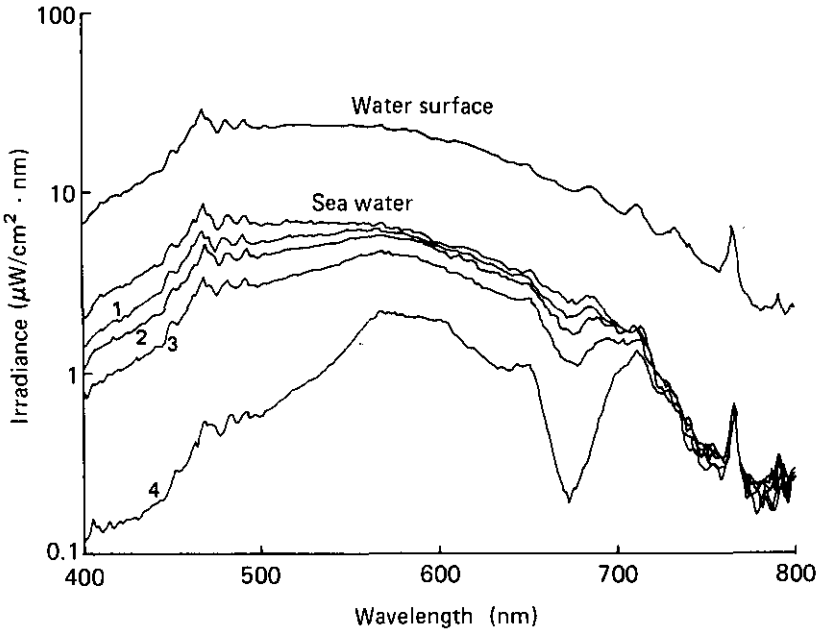

Fig. 2.12 Spectral characteristics of underwater irradiance with different concentration of *H. Akashiwo* measured at the depth of 10cm from the water surface.
1: 32, 822 cells/m*l*. 2: 63, 518 cells/m*l*. 3: 137, 544 cells/m*l*.
4: 272, 832 cells/m*l*.

2.4 FIELD EXPERIMENTS

The high-speed spectroradiometer has been used to measure the spectral characteristics of the water of Lake Kasumigaura in Ibaraki prefecture. The measurement was carried out at the water surface and underwater at a time coinciding with the overflight of a remote sensor. The recorded results were used to the estimate water quality of the lake, the effect of the atmosphere between the remote sensor and the water surface, and the effects of light reflected from the water surface. Fig. 2.13 shows the measured spectral characteristics of the surface of Lake Kasumigaura and Fig. 2.14 gives the underwater radiance distributions.

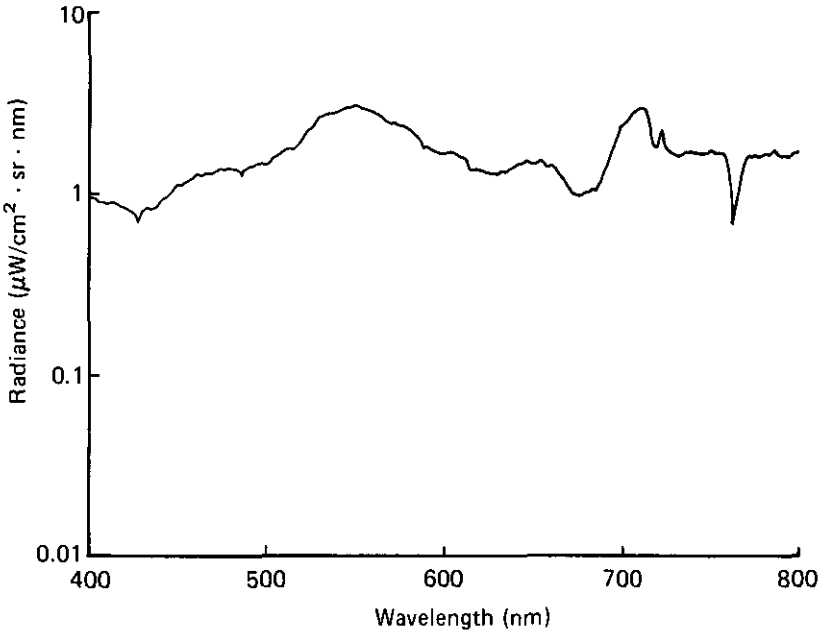

Fig. 2.13 Spectral signature of water surface of Lake Kasumigaura.

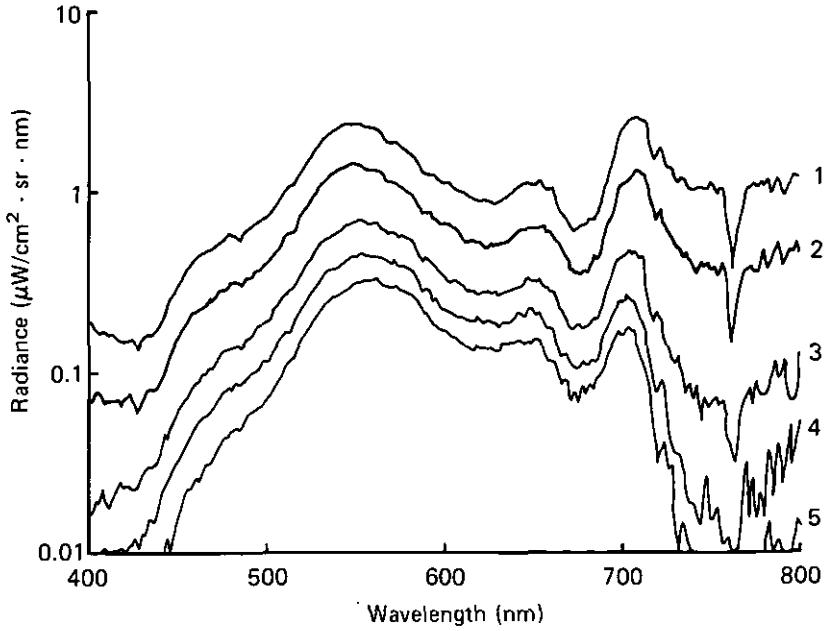

Fig. 2.14 Spectral signature of under water radiance of Lake Kasumigaura.
1: 10cm underwater. 2: 20cm. 3: 40cm. 4: 60cm. 5: 80cm.

2.5 CONCLUSIONS

The development of a spectroradiometer suitable for collecting data from fast moving surfaces like water with wave motion in remote sensing has been described and some applications of its use in laboratory and field experiment have been also presented. This instrument has been constrcted to supply the need for a portable and high-speed spectroradiometer for ground reflectance measurements over the visible and the near infrared wavelength range. It is designed to be used especially for water surface reflectance measurements during remote sensing sessions. This spectroradiometer fulfills the above needs. Its principal components are a light collection system, a light chopper, a monochromatic grating, a photomultiplier, an electronic amplification system, a micro-processor with an analog-to-digital converter I/O channel, a cassette tape unit and a CRT display. We have estimated the measurement accuracy to be about 0.5%.

Tests and measurements have shown that the instrument works as originally conceived and that potentially variable spectral signatures can be established for terrain targets. From a series of careful spectral measurements of a certain terain target, optimum sensor bandpasses and suitable overflight conditions for remote sensors can be determined, taking into account the natural limitations on target discrimination posed by surface variability.

The major drawbacks of this spectroradiometer are the limited wavelength range of measurement, the time for data storage to cassette tape, and the high cost of construction. It may be possible to extend the wavelength range to shorter wavelengths by using a quartz optical fiber and lens system. For extension to longer wavelengths, however, an entirely new system for longer wave light detection is needed. To shorten the data storage time (it now takes about 30 seconds to record measurement data onto casstte tape) a mini-floppy disk system will be faster because of its randam access data filing.

The high-speed spectroradiometer described in this chapter meets the criteria we proposed for spectral measurements and would seem to be an appropriate instrument for ground data collection during remote sensing.

CHAPTER

3

Regression analysis between water quality parameters and radiance reflectance of water surface

3.1 INTRODUCTION

Suspended solids and phytoplankton in natural water bodies present major environmental problems. Thus, monitoring this type of pollution from non-localized sources by remote multispectral techniques is increasingly being considered by local governments. As explained before, the multispectral scanner detects the energies of absorbed, reflected and emitted electromagnetic spectrum of objects; therefore, to interpret this data the spectral characteristics of water surfaces must be understood. Some chemical compounds discharged from homes give origin to substances such as chlorophyll, phaeophytin and yellow substance which alter the optical properties of the water surface. These substances are complex organic molecules found in a varitety of phytoplankton. Furthermore, the suspended solids (SS) in the water body also affect the spectra of the irradiance upwelling from the water surface. For aquatic remote sensing, the key question is whether the relationships between substances (for example, suspended solids and phytoplankton) in the water body and spectral reflectance are universal. If these relationships should be variable with location and time, then extensive ground truth would be required at each monitoring site for calibration purposes, thus greatly reducing the utility of remote sensing.

The basic physical concepts which have led to the presently existing technolgy of remote sensing were developed by a number of investigators, some of whom were Duntley (1960) and Williams (1970). The early work on the spectral response of chlorophyll was done by many investigators such as Clarke *et al.* (1969, 1970), Polcyn (1972), Mueller (1972), and Suits (1973). Suits analyzed the effects of sand and chlorophyll concentration on reflectance and pointed out the relatively high green and low red reflectance of chlorophyll, as contrasted with the very flat or uniform reflectance of sand. Suits further explored the effect on the reflectance of water of increasing phytoplankton concentration. For a given concentration of the yellow substance and sand, he plotted five different values for the extinction coefficient of phytoplankton to show changes in reflectance for various chlorophyll concentrations. The values of reflectance near 0.5 μm appears like a hinge; lower reflectance is observed in the blue, with increasing reflectance toward the green and red regions. Rouse and Coleman (1976) performed a laboratory experiment to measure reflected spectral relationships versus concentration of suspended solids. The reflectance measurements were made on several concentrations of Mississippi River sediment and Kaolinite (a white clay). Measurements for the Mississippi River sediment showed approximately linear relationships between reflected radiance values and sediment concentrations up to 500 mg/l. Above 500 mg/ l the radiance increases much more slowly with increasing sendiment concentration. Viollier *et al.*

(1978) obtained measurements of downwelling and upwelling radiance with a two-band radiometer in the Gulf of Guinea and concluded that the low values of the difference between 446 and 525 nm albedos, and the high value of the difference between 550 and 600 nm albedos give two criteria to discriminate zones rich in phytoplankton from poor water. Aranuvachapun and Perry (1981) measured integrated downwelling irradiance (from 400 to 700 nm) at 2 m depth intervals from the water surface to a depth of 10 m along the coast of British Columbia, Canada and showed that there is a greater attenuation of irradiance at wavelength 420 nm than at 540 nm, a result which agrees with absorption maximum and minimum of phytoplankton pigments. Bukata *et al.* (1983) measured optical cross-sections of Lake Ontario water masses, and these optical cross-sections have been utilized to study the use of chromaticity analysis for estimating water quality parameters in a body of water containing chlorophyll and suspended solids. They concluded that chromaticity analysis is only applicable on a very restricted range. In laboratory experiments, McKim *et al.* (1984) measured the spectral reflectance from suspensions of orgnic and inorganic sediments, individually and in combination, in a water tank with a Chiu-Collins Spectrometer (Chiu & Collins, 1978) and they concluded that a difference of 5 ppm for inorganic suspensions can be detected by the spectrometer and that the response to organic suspensions is sensitive to the order of 100 mg/ *l* in shallow water. Kishino *et al.* (1984) used a submersible spectral irradiance meter to obtain the spectral characteristics of pure and sea water, and calculated the contribution of quanta absorbed by phytoplankton. Gower *et al.* (1984) reported the spectral measurement of coastal water off British Columbia, Canada in order to analyze relationships between chlorophyll concentration and upwelling radiance at the water surface.

In this chapter we examine the variablity of reflectance of polluted water to determine whether it is sufficiently accurate to use quantitative remote measurements of water bodies with little or no concomitant ground truth. Water quality parameters and spectral signatures of water surface were measured in Lake Kasumigaura and relationships between the water quality parameters and the optical characteristics of the water surface of Lake Kasumigaura were determined. We also discuss the optimum wavelength for quantitatively measuring the water quality of the surface water from LANDSAT satellite data.

3.2 MEASUREMENT OF SPECTRAL REFLECTANCE OF LAKE KASUMIGAURA

Ground truth measurent of water quality and spectral reflectance of water were takn on Lake Kasumigaura exactly during the overflight of LANDSAT. The data acquired in these Kasumigaura experiments are summarized in Table 3.1. Lake Kasumigaura is the second largest lake in Japan and has an area of 167.7 km^2 with the depth ranging from 0 to 7 meters. The lake water serves as a reservoir for domestic, industrial and agricultural uses as well as being a fishing ground. Due to the growth of population and industrial activities in the drainage area of the lake, the water quality of the lake has been degraded by eutrophication. The annual average values of COD (chemical oxygen demand) reached as much as 11.5 ppm in 1978. Fig. 3.1 shows photographs of the polluted surface of Lake Kasumigaura during a typical summer. Hence, an assessment of the water quality of the lake, particularly of the

pattern of water quality distribution of the lake was long overdue.

Table 3.1 Summary of data acquisition at Lake Kasumigaura.

Date	25 October 1983
Spectral measurement	Water surface, Underwater, White reflector
Water quality measurement	Temperature, Transparency, Suspended solids, Chlorophyll-*a*, Phaeophytin
Number of ground truth point	12
LANDSAT	LANDSAT-4, MSS, Path 107, Row 35

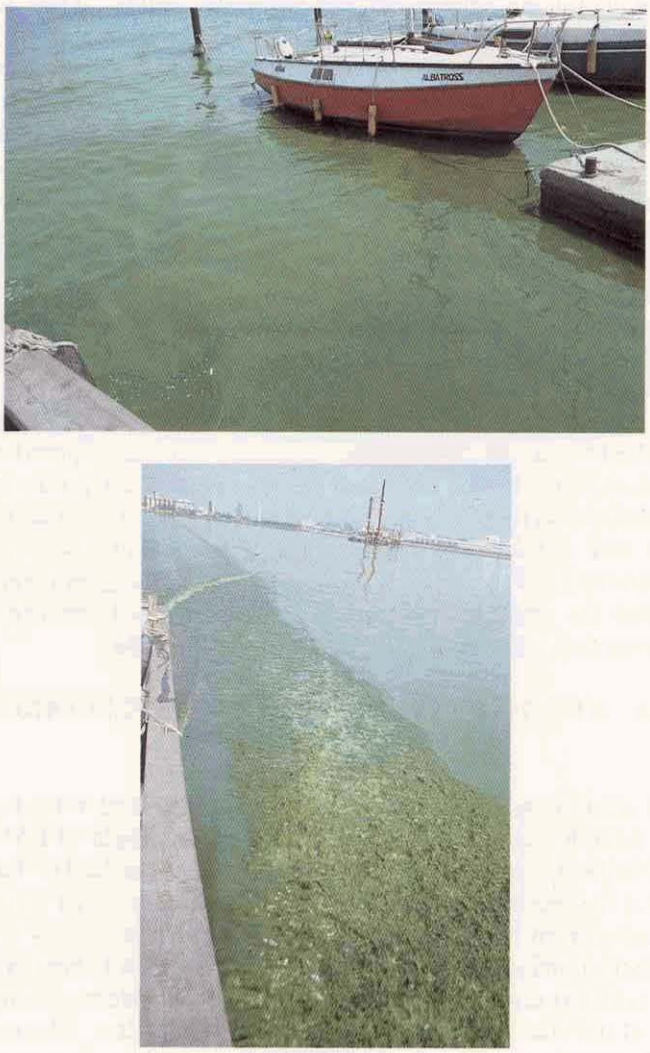

Fig. 3.1 Photographs of Lake Kasumigaura polluted by massive growth of blue green algae.

The upwelling (nadir) radiance of the lake was measured at the water surface and at several depth layers underwater. The measurements covers the wavelength interval 400 to 850 nm with a resolution of 2 nm; water quality parameters such as chlorophyll-*a*, phaeophytin, suspended solids, transparency, and water temperature were also measured at the same ground truth point. The spectrum of incident light from the sun and sky was measured on the observation ship immediately before or after a series of surface and underwater measurements by recording the light reflected from a horizontally placed Eastman Kodak white coating (Grum & Luckey, 1968). The observed readings of the reflected light from the white coating were used to calibrate the spectral sensitivity change due to the different sun angels at each ground truth point. Reflected solar radiation data at the water surface or at the white board were measured about 30 cm above the surface, and the angle of the field of view of the sensor head was about 30 degrees. Photographs of spectral measurement being taken at a ground truth site in the lake are shown in Fig. 3.2. All

(A)

(B)

Fig. 3.2 Photographs of spectral measurement at a ground truth point.
(A): Radiance measurement at water surface. (B): Radiance measurement of white reflector.

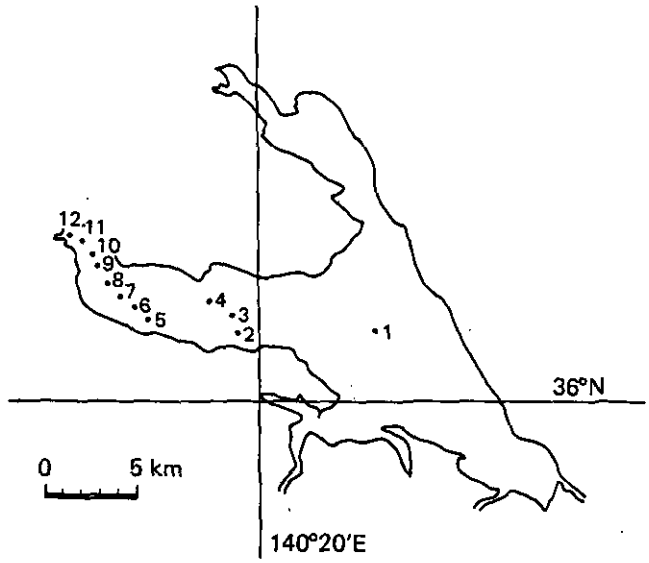

Fig. 3.3 Ground truth points of the experiment (25 Oct. 1983).

measurements were made within 2 hours of the overflight time of LANDSAT and the sun angle was calculated for each set of ground truth measurements. The typical ground truth points of the lake are marked on the map of Fig. 3.3.

At each ground truth point, the incident radiation of the sun and sky were measured first, then the upwelling radiance from the water surface, and finally the underwater radiance at depths of 5, 10, 20, 40, 60, and 80 cm from the water surface. To make one set of these measurements takes about 20 minutes. Simultaneously, the surface water temperature, the Secchi depth transparency, and fundamental meteorological conditions such as temperature, humidity, wind direction and speed, visibility etc. were measured. To measure concentration of suspended solids and chloroplyll-*a*, 2 liters of surface water of the lake were collected at each ground truth site.

Table 3.2 gives some typical data for water surface reflectance. These data are plotted in Fig. 3.4; the radiance due to the total solar radiation upwelling from a white reflector is shown in Table 3.3 and Fig. 3.5. The upwelling radiance from a white reflector by sky light is shown in Fig. 3.6, and the radiance underwater is shown in Fig. 3.7. Table 3.4 shows data on water quality in Lake Kasumigaura.

Table 3.2 Spectral radiance measured at water surface of Lake Kasumigaura.

STATION NO. : 2 TIME : 09:15:00 WATER SURFACE DATA CODE : 3

DATA NO. : 111 REP TIME : 10 GAIN : 20 MAX DATA VAL : 1.61896 AT 580
MIN DATA VAL : 0.13917 AT 762 (MICRO W/CM**2.SR.NM)

	0	2	4	6	8
400	0.48809	0.52210	0.47312	0.48051	0.46277
410	0.49141	0.51954	0.49335	0.49269	0.47718
420	0.52423	0.49754	0.49206	0.46872	0.43582
430	0.47831	0.51751	0.55845	0.54983	0.54405
440	0.57008	0.61499	0.62826	0.67346	0.70973
450	0.74931	0.77689	0.75559	0.78534	0.79473
460	0.80936	0.83710	0.80519	0.81240	0.84343
470	0.84533	0.84471	0.87881	0.89076	0.92560
480	0.94350	0.96210	0.92166	0.86813	0.89242
490	0.94757	0.95855	0.98703	0.98864	0.99178
500	0.98305	0.98868	1.01431	1.06180	1.06874
510	1.10672	1.08915	1.10313	1.06201	1.10966
520	1.19118	1.20998	1.23545	1.21467	1.31919
530	1.32829	1.33045	1.37178	1.41662	1.38695
540	1.42258	1.46131	1.50267	1.49251	1.50270
550	1.52048	1.54469	1.52290	1.56299	1.55032
560	1.56519	1.60828	1.55364	1.52054	1.57128
570	1.60217	1.60649	1.56450	1.55330	1.59207
580	1.61896	1.57796	1.58718	1.50027	1.49498
590	1.56266	1.57758	1.49665	1.51835	1.45500
600	1.48628	1.43973	1.47122	1.50762	1.42932
610	1.46363	1.43367	1.39814	1.39595	1.40548
620	1.41042	1.39279	1.47873	1.42518	1.40271
630	1.39991	1.37683	1.41676	1.38834	1.46342
640	1.46241	1.50617	1.53539	1.53917	1.49638
650	1.49293	1.53208	1.57204	1.53066	1.36253
660	1.44437	1.38397	1.33168	1.33472	1.30874
670	1.31465	1.25081	1.29705	1.24602	1.25702
680	1.24234	1.27705	1.25653	1.10000	1.07792
690	1.21578	1.29359	1.39877	1.43928	1.43386
700	1.49442	1.48499	1.51035	1.38397	1.40757
710	1.33335	1.31960	1.25823	1.27531	1.06153
720	1.01191	1.01271	0.93855	0.88233	0.92342
730	0.83354	0.76048	0.77557	0.69795	0.63191
740	0.65763	0.64619	0.58423	0.61297	0.65929
750	0.60717	0.63466	0.58450	0.60564	0.55037
760	0.35446	0.13917	0.26017	0.36205	0.43528
770	0.49467	0.45570	0.49172	0.45197	0.46074
780	0.45676	0.49171	0.53042	0.53234	0.50206
790	0.51697	0.43098	0.48765	0.47255	0.52288
800	0.48482	0.44524	0.45947	0.43155	0.49205
810	0.51008	0.53371	0.46503	0.41543	0.37416
820	0.42497	0.40718	0.31932	0.32044	0.32504
830	0.30036	0.29296	0.31949	0.26962	0.26190
840	0.29101	0.28443	0.26314	0.24383	0.23497
850	0.23902				

Table 3.4 Water quality samples collected on 25 October 1983.

Ground Truth point	Temperature (℃)	Transparency (cm)	Suspended solids (mg/l)	Chlorophyll-a ($\mu g/l$)	Phaeophytin ($\mu g/l$)
1	16.8	90.0	12.7	56.3	10.3
2	16.1	50.0	31.8	50.5	13.9
3	16.3	55.0	27.3	49.2	7.1
4	16.6	55.0	25.3	53.6	8.0
5	16.0	45.0	36.5	55.4	6.4
6	16.0	45.0	36.0	60.4	4.6
7	16.2	43.0	34.8	55.5	2.6
9	16.3	43.0	35.2	47.2	3.3
10	16.2	42.0	39.5	58.2	3.6
11	16.2	40.0	39.8	38.9	3.8
12	16.3	50.0	26.5	16.2	0.2
13	16.7	45.0	29.0	26.9	2.0

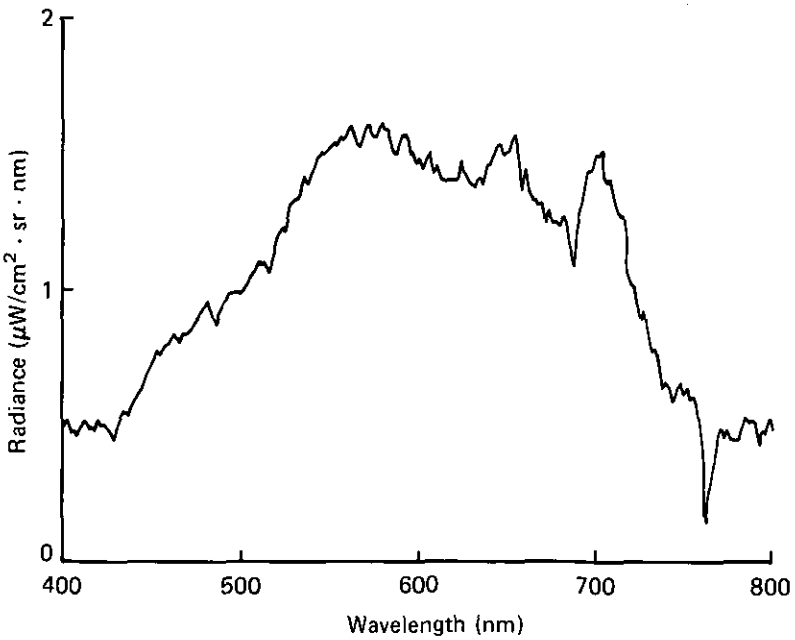

Fig. 3.4 Spectral radiance measured at water surface at ground truth point 2.

Table 3.3 Upwelling radiance of white reflector due to total solar radiation.

STATION NO. : 2 TIME : 09:13:00 WHITE BOARD DATA CODE : 1

DATA NO. : 109 REP TIME : 10 GAIN : 1 MAX DATA VAL : 30.00909 AT 482
MIN DATA VAL : 6.64357 AT 762 (MICRO W/CM**2.SR.NM)

	0	2	4	6	8
400	19.69266	21.20923	20.95103	20.35385	20.96988
410	21.65121	22.27159	22.20111	21.95308	21.68828
420	21.99661	21.64883	21.87419	20.75662	18.70169
430	20.53539	22.41074	23.63333	23.61960	23.48679
440	25.14153	25.88797	26.10626	26.88046	28.20369
450	28.74237	28.24091	28.12372	28.82222	28.64259
460	29.22517	29.33394	28.98383	28.58632	28.45946
470	28.89259	28.98911	29.55891	29.13580	29.56134
480	29.95619	30.00909	28.58134	26.71432	28.04628
490	29.08405	28.91685	29.50520	29.30586	29.08160
500	28.03575	27.93065	28.57800	28.89673	28.84616
510	28.71155	28.08249	27.49704	25.68716	26.67278
520	28.03568	27.75290	27.81522	27.39050	28.97101
530	28.49503	28.17030	28.55655	28.51630	27.82538
540	27.96216	28.16313	28.37189	28.27534	28.24893
550	28.24539	28.36171	28.16382	27.60162	27.11237
560	27.66977	27.82538	27.22862	27.20618	26.79697
570	26.88535	27.10286	26.69165	26.50281	27.24792
580	27.69737	27.35951	27.25647	26.46883	25.81812
590	26.37451	26.50197	26.28040	26.47688	26.04988
600	26.26422	26.47363	26.36017	26.55388	26.26361
610	26.02428	25.82909	25.43083	25.40822	26.00249
620	26.37402	25.74118	25.25493	25.29997	24.88847
630	24.91002	24.98587	25.35040	25.55867	25.68578
640	26.25960	26.20018	25.83368	25.98322	25.35629
650	25.46820	25.19720	25.69690	24.33212	23.30269
660	25.49971	25.63831	25.66759	25.62715	25.69539
670	25.48904	25.12294	25.59360	25.42468	25.36038
680	24.80484	24.98160	24.52507	20.55986	19.95087
690	21.62486	23.24530	23.31712	23.69620	23.37576
700	23.09476	23.21268	24.19266	23.97818	23.80611
710	23.61043	23.59737	23.22615	22.19026	19.71417
720	19.41211	21.38562	20.08978	20.13007	20.21722
730	20.54074	20.74190	22.50327	22.38930	21.98557
740	22.30624	21.90855	22.71689	22.90472	23.28291
750	22.31360	22.88432	22.49673	22.21100	21.34851
760	12.60595	6.64357	8.96745	13.19932	18.23759
770	20.56380	21.19485	21.52054	21.24593	21.11037
780	20.74297	21.30756	21.10507	21.02730	20.69562
790	20.55757	20.01578	19.58955	20.05005	19.70331
800	20.18164	19.42435	18.99141	18.74832	20.04073
810	19.56610	19.31262	18.54611	16.96109	15.43793
820	15.45921	16.15999	15.73077	16.40938	17.23444
830	16.52007	16.25697	15.97426	17.62888	17.60858
840	17.08929	16.79495	15.94780	16.43608	15.59377
850	15.34743				

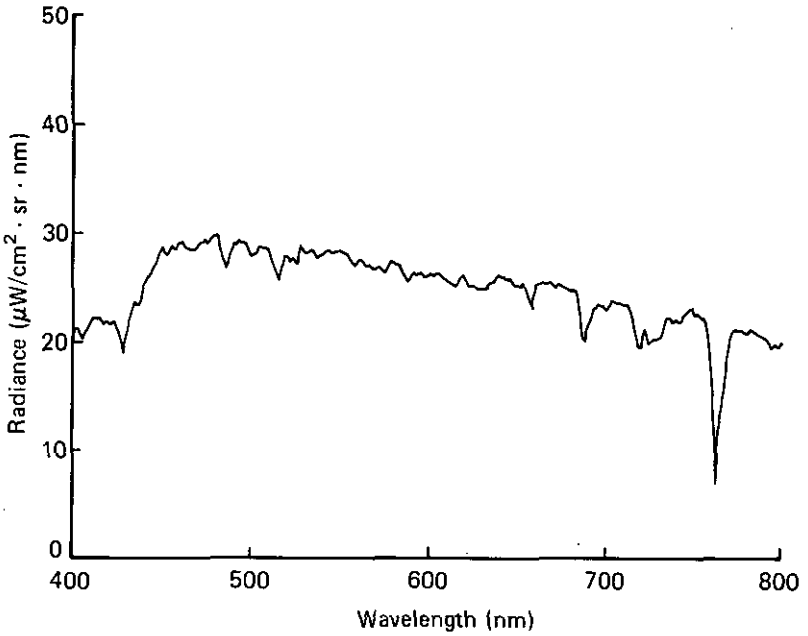

Fig. 3.5 Upwelling radiance of white reflector due to total solar radiation at ground truth point 2.

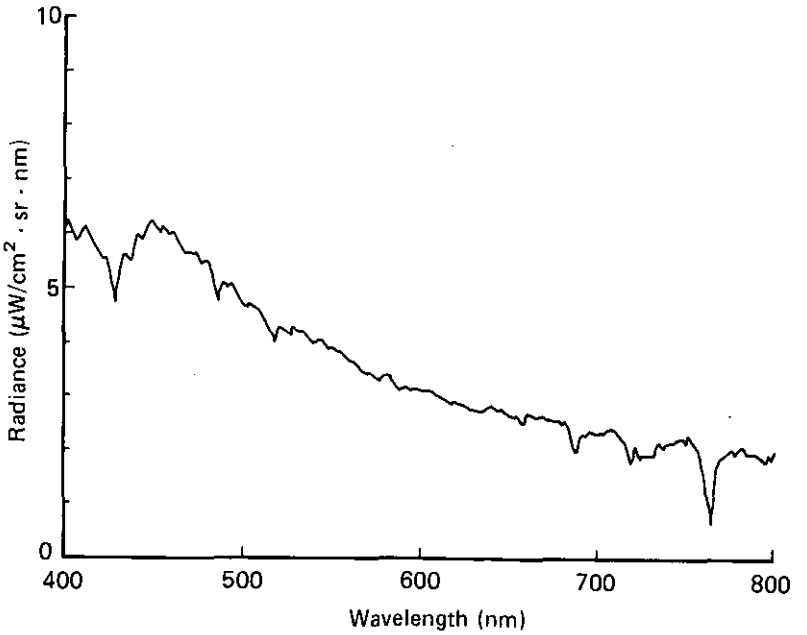

Fig. 3.6 Upwelling radiance of white reflector due to skylight at ground truth point 2.

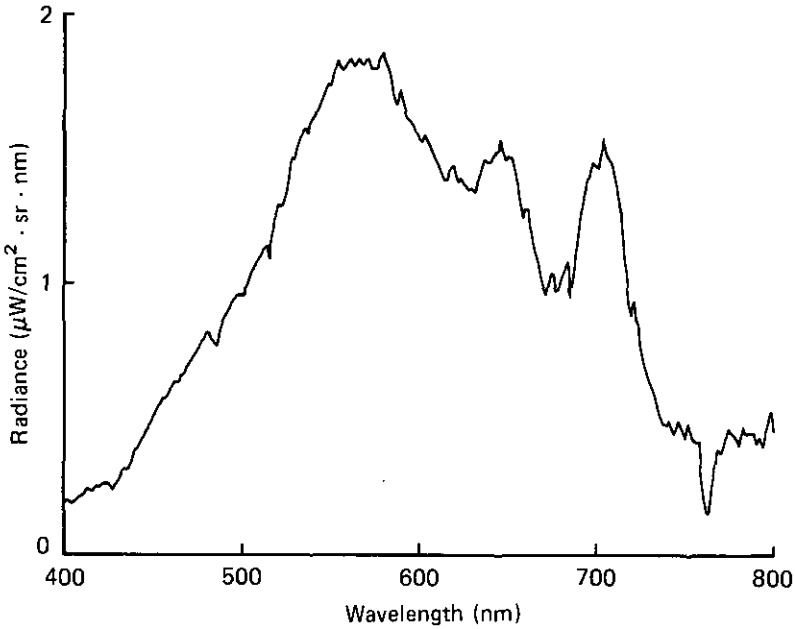

Fig. 3.7 Spectral radiance of 10cm under water at ground truth point 2.

3.3 ESTIMATING THE RADIANCE REFLECTANCE JUST ABOVE THE WATER SURFACE

Solar radiation reflected by the water surface varied with the amount of suspended solids or chlorophyll-*a* in the water. This suggests that a change in the water quality causes a change in the amount of radiation reflected from the water surface.

The spectral radiance reflectance or ratio of radiance to irradiance ratio R_o at the water surface is defind by

$$R_o = \frac{L_o}{H} \qquad 3.1$$

$$U_o = U_W + U_R \qquad 3.2$$

$$H = H_{SUN} + H_{SKY} \qquad 3.3$$

where U_o is the upwelling spectral radiance from the water surface. H is the spectral irradiance onto the water surface from total solar radiation. U_W is the upwelling spectral radiance just above water surface, and U_R is the upwelling spectral radiance from water surface due to sky light (see Fig. 3.8). The spectral radiance reflectance just above the water surface R_W is also defind by

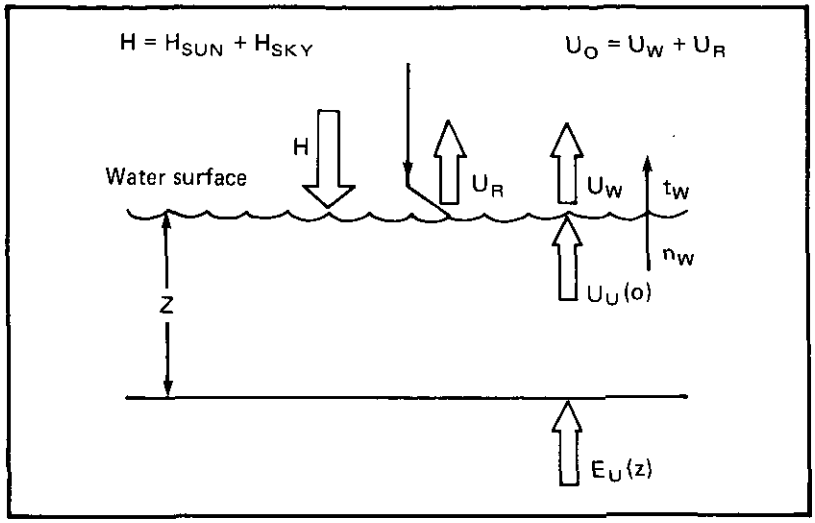

Fig. 3.8 Optical processes through the water surface.

$$R_w = \frac{U_w}{H} \quad . \tag{3.4}$$

As shown in Fig. 3.8, $U_u(0)$ is the upwelling spectral radiance just below the water surface. Then the relation between U_w and $U_u(0)$ is

$$U_w = \frac{t_w}{n_w^2} \cdot U_u(0) \tag{3.5}$$

where t_w/n_w^2 accounts for the transmittance t_w of irradiance from water of index of reflection n_w, to air (Note: $t_w/n_w^2 \fallingdotseq 0.544$).

If Q is defined by the ratio of the upwelling irradiance $E_u(0)$ just below the water surface to upwelling radiance $U_u(0)$ just below water surface, Eq. 3.5 can be rewritten as

$$U_w = \frac{t_w}{n_w^2 \cdot Q} \cdot E_u(0). \tag{3.6}$$

The value of Q may be computed for a variety of water conditions. Austin (1974) obtained a value ranging from 4.4 to 5.4 in the wavelength range 425 to 600 nm. In this report, we assume that the body of water is a lambertian reflector and the angular distribution of radiance in the lower hemisphere of the water surface is uniform for radiance traveling upward. Then, $Q \fallingdotseq \pi$, and U_w is

$$U_w = \frac{t_w}{n_w^2 \cdot \pi} \cdot E_u(0). \tag{3.7}$$

In Eq. 3.7, however, actual measurement of $E_u(0)$ is impossible in practice. Therefore, $E_u(0)$ was estimated from the upwelling irradiance at the depth of z using the relation

$$E_u(0) = E_u(z)e^{K_u \cdot z} \tag{3.8}$$

where K_u is the extinction coefficient for the upwelling irradiance of the water, expressed as

$$K_u = \frac{1}{z_2 - z_1} \log_e \frac{E_u(z_1)}{E_u(z_2)} \qquad 3.9$$

therefore, U_w is expressed as

$$\begin{aligned} U_w &= \frac{t_w}{n_w^2 \cdot \pi} E_u(z) e^{K_u \cdot z} \\ &\fallingdotseq 0.174 E_u(z) e^{K_u \cdot z}. \end{aligned} \qquad 3.10$$

The upwelling irradiance $E_u(z)$ at the depth of z underwater was calculated by

$$E_u(z) = \pi \cdot U_u(z) \qquad 3.11$$

where $U_u(z)$ is the upwelling radiance measured at the depth of z underwater. Using Eqs. 3.4 and 3.10, the radiance reflectance R_w just above the water surface can be expressed as

$$R_w = 0.174 \frac{E_u(z) e^{K_u \cdot z}}{H} \quad . \qquad 3.12$$

The total irradiance H onto the water surface is estimated with the following expression

$$H = \pi \cdot \rho \cdot w \qquad 3.13$$

where w is the upwelling radiance reflected by a white reflector horizontally placed at the ground truth point. The surface of the white reflector is assumed to be a lambertian surface and ρ is the reflectivity of the reflector and the value of ρ is supposed to be 1.0.

The type of light from the water surface which is most important for remote measurements is the upwelling radiance U_w just above the water surface because the upwelling radiance U_w contains only optical information of the water or of substances in the body of water, on the other hand, upwelling radiance U_o consists of light from underwater and the light reflected by water surface. In this experiment, upwelling radiance U_o and upwelling radiance $U_u(z)$ underwater were measured at Lake Kasumigaura to deduce the radiance U_w just above the water surface. The extinction coefficient K_u may change its value with the wavelength, water quality, or the position of the ground truth site. The extinction confficient of Lake Kasumigaura water could be measured with a spectrophotometer such as a HITAC-220 double beam spectrophotometer. In this report, the extinction coefficient K_u and the upwelling radiance U_w just above the the water surface were calculated using Eqs. 3.9, 3.10 and 3.11 with the values for z, z_1, and z_2 were 10, 10, and 60 cm, respectively. Then the radiance reflectance R_o at the water surface and R_w just above the water surface were calculated from the Eqs. 3.1, 3.11, 3.12, and 3.13. All terms in Eqs. 3.1 to 3.13 except t_w/n_w^2 are dependent on the wavelength.

The results are listed in Tables 3.5, 3.6, and 3.7. Fig. 3.9 shows the spectral distribution of the extinction coefficient K_u; Fig. 3.10, the radiance reflectance R_o at the water surface; Fig. 3.11, the radiance reflectance R_w just above water surface.

Table 3.5 Calculated extinction coefficients at ground truth point 2.

KU (1/CM)

STATION NO. : 2

	0	2	4	6	8
400	0.09687	0.10088	0.10377	0.09859	0.09267
410	0.09101	0.08553	0.09234	0.09367	0.09561
420	0.09144	0.08705	0.08612	0.08070	0.08437
430	0.09865	0.08159	0.08209	0.07909	0.08184
440	0.07722	0.07883	0.07439	0.07244	0.07200
450	0.07233	0.06803	0.06919	0.06825	0.06627
460	0.06618	0.06495	0.06333	0.06320	0.06355
470	0.06169	0.06078	0.05930	0.06045	0.05752
480	0.05936	0.05659	0.05574	0.05764	0.05573
490	0.05487	0.05543	0.05463	0.05395	0.05185
500	0.05185	0.05177	0.05140	0.04961	0.04840
510	0.04785	0.04857	0.04728	0.04620	0.04453
520	0.04600	0.04397	0.04322	0.04270	0.04209
530	0.04103	0.04155	0.04077	0.04005	0.03942
540	0.03927	0.03877	0.03811	0.03730	0.03761
550	0.03746	0.03657	0.03724	0.03667	0.03560
560	0.03530	0.03511	0.03509	0.03481	0.03450
570	0.03462	0.03507	0.03456	0.03444	0.03417
580	0.03485	0.03489	0.03373	0.03335	0.03321
590	0.03402	0.03433	0.03332	0.03482	0.03506
600	0.03436	0.03510	0.03564	0.03591	0.03495
610	0.03546	0.03615	0.03445	0.03658	0.03584
620	0.03447	0.03536	0.03587	0.03536	0.03607
630	0.03438	0.03571	0.03505	0.03550	0.03419
640	0.03504	0.03281	0.03390	0.03603	0.03574
650	0.03513	0.03464	0.03330	0.03453	0.03445
660	0.03598	0.03661	0.03626	0.03716	0.03786
670	0.03758	0.03991	0.04011	0.03887	0.03999
680	0.03876	0.04041	0.03721	0.03516	0.03970
690	0.03473	0.03423	0.03388	0.03143	0.03209
700	0.03167	0.03004	0.03249	0.03279	0.03237
710	0.03334	0.03653	0.03358	0.03443	0.03638
720	0.03716	0.03857	0.04180	0.04165	0.04384
730	0.05038	0.04962	0.04649	0.06161	0.05525
740	0.05254	0.05521	0.05470	0.05504	0.05018
750	0.05451	0.05774	0.05551	0.06080	0.06795
760	0.06819	0.05669	0.04961	0.05808	0.06578
770	0.05328	0.05343	0.05201	0.05771	0.05834
780	0.04870	0.05828	0.05794	0.05571	0.05515
790	0.04903	0.04379	0.05065	0.05722	0.05477
800	0.04752				

N = 201 MEAN = 0.04960

Table 3.6 Calculated radiance reflectance at water surfact at ground truth point 2.

R (%/SR)

STATION NO. : 2

	0	2	4	6	8
400	0.78895	0.78358	0.71881	0.75147	0.70246
410	0.72245	0.74254	0.70734	0.71438	0.70034
420	0.75861	0.73159	0.71604	0.71879	0.74178
430	0.74141	0.73504	0.75217	0.74096	0.73730
440	0.72177	0.75618	0.76603	0.79749	0.80101
450	0.82983	0.87566	0.85520	0.86752	0.88320
460	0.88152	0.90836	0.88429	0.90461	0.94335
470	0.93130	0.92752	0.94636	0.97316	0.99666
480	1.00255	1.02051	1.02645	1.03441	1.01285
490	1.03707	1.05514	1.06483	1.07383	1.08554
500	1.11612	1.12675	1.12977	1.16962	1.17932
510	1.22656	1.23453	1.27700	1.31601	1.32425
520	1.35244	1.38778	1.41381	1.41158	1.44942
530	1.43360	1.50335	1.52907	1.56129	1.58661
540	1.61941	1.65103	1.68588	1.68020	1.69324
550	1.71349	1.73354	1.72120	1.80249	1.82014
560	1.80058	1.83980	1.81625	1.77902	1.86645
570	1.89690	1.88675	1.86574	1.86958	1.85986
580	1.86057	1.83585	1.85556	1.80420	1.84315
590	1.88595	1.89480	1.81275	1.82939	1.77790
600	1.80130	1.73108	1.77656	1.80723	1.73231
610	1.79021	1.76681	1.75001	1.74082	1.72052
620	1.70224	1.72229	1.86378	1.79308	1.79398
630	1.78887	1.75402	1.77894	1.72905	1.81354
640	1.77269	1.82947	1.89184	1.88557	1.87848
650	1.86592	1.93544	1.94730	2.00239	1.86119
660	1.80300	1.71626	1.65144	1.65784	1.62124
670	1.64174	1.58479	1.61315	1.55999	1.57774
680	1.59425	1.62720	1.63085	1.70304	1.71979
690	1.78958	1.77130	1.90950	1.93336	1.95249
700	2.05973	2.05634	1.98721	1.83722	1.88205
710	1.79760	1.78004	1.72439	1.82938	1.71398
720	1.65926	1.50755	1.48708	1.59521	1.45388
730	1.24169	1.16706	1.09704	0.99228	0.91489
740	0.93844	0.93635	0.81863	0.85186	0.90135
750	0.86615	0.88278	0.82701	0.86796	0.82061
760	0.80504	0.86652	0.92349	0.67312	0.75972
770	0.76570	0.86439	0.72730	0.87715	0.69472
780	0.70092	0.73456	0.79999	0.80585	0.77220
790	0.80047	0.68559	0.79236	0.75020	0.84472
800	0.76468				

N = 201 MEAN = 1.53383

Table 3.7 Calculated radiance reflectance just above water surface at ground truth point 2.

RW (%/SR)

STATION NO. : 2

	0	2	4	6	8
400	0.36692	0.43049	0.45570	0.42955	0.38578
410	0.41629	0.36957	0.41608	0.44858	0.47532
420	0.46960	0.44009	0.47000	0.42800	0.44615
430	0.54570	0.47123	0.49336	0.48205	0.54256
440	0.52778	0.55129	0.54679	0.55015	0.57507
450	0.60286	0.59424	0.64453	0.65043	0.64203
460	0.66957	0.66575	0.67279	0.70327	0.73979
470	0.72686	0.73272	0.73415	0.78837	0.76533
480	0.79348	0.79272	0.78499	0.84058	0.83490
490	0.83333	0.87860	0.89458	0.90133	0.89734
500	0.93048	0.95268	0.98883	0.98787	0.99033
510	1.01749	1.06895	1.09661	1.11908	1.13342
520	1.20884	1.18375	1.21439	1.26442	1.28616
530	1.28484	1.35622	1.35336	1.37035	1.38272
540	1.40536	1.44649	1.44312	1.44483	1.49486
550	1.48928	1.50415	1.57229	1.57807	1.58284
560	1.57605	1.58255	1.58446	1.58509	1.60238
570	1.60207	1.64017	1.60522	1.61750	1.58345
580	1.59356	1.59766	1.54053	1.50559	1.49034
590	1.51338	1.51041	1.43993	1.45347	1.45538
600	1.40628	1.39206	1.40512	1.40754	1.32519
610	1.33597	1.35069	1.29537	1.32475	1.31324
620	1.29958	1.24035	1.32908	1.29449	1.33079
630	1.30054	1.31777	1.32195	1.35563	1.32272
640	1.33774	1.29966	1.36367	1.45224	1.42781
650	1.39451	1.38884	1.32307	1.32191	1.26646
660	1.24175	1.19699	1.08395	1.05602	0.99285
670	0.98657	0.97874	0.99130	0.99431	0.96678
680	0.99498	1.07215	1.06328	1.09786	1.33199
690	1.23661	1.29965	1.40558	1.33146	1.41909
700	1.43260	1.33497	1.46271	1.45367	1.40599
710	1.37647	1.41014	1.31400	1.19482	1.17957
720	1.11989	1.01937	1.03925	0.96732	0.87719
730	0.86617	0.79352	0.83611	0.75521	0.62206
740	0.54436	0.61048	0.57271	0.58550	0.52279
750	0.54556	0.61648	0.52874	0.58645	0.72078
760	0.66728	0.69282	0.46295	0.57594	0.66880
770	0.47805	0.51035	0.51291	0.57090	0.60638
780	0.48756	0.65643	0.64142	0.61795	0.62938
790	0.57755	0.51149	0.54122	0.64372	0.78461
800	0.59092				

N = 201 MEAN = 1.01259

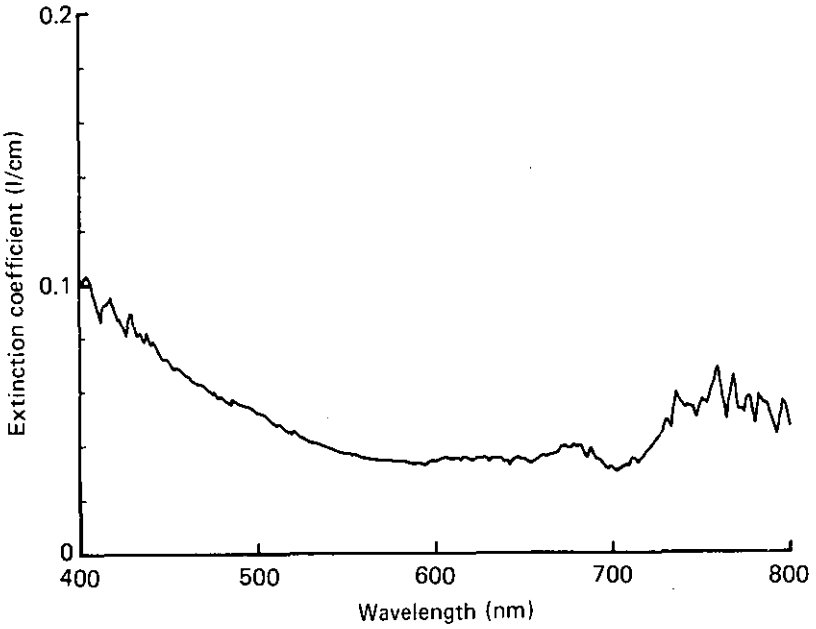

Fig. 3.9 Calculated extinction coefficient.

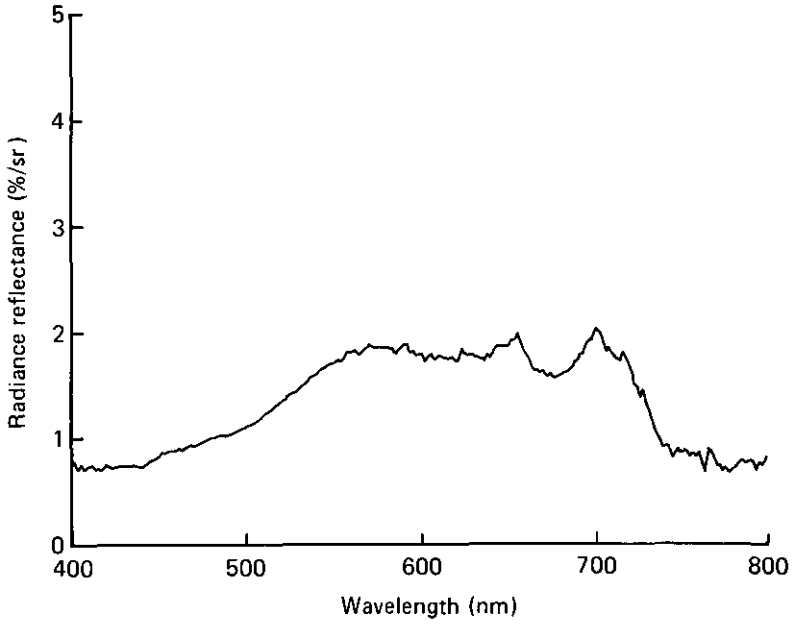

Fig. 3.10 Calculated radiance reflectance at the water surface.

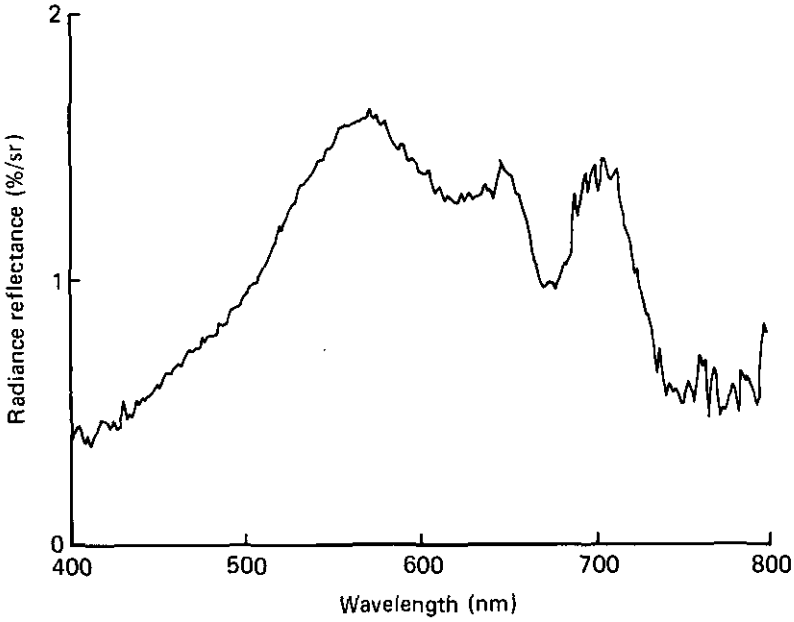

Fig. 3.11 Calculated radiance reflectance just above the water surface.

3.4 REGRESSION ANALYSIS BETWEEN WATER QUALITY PARAMETERS AND RADIANCE REFLECTANCE

A change in the concentration of suspended solids or phytoplankton caused a change in the amount of radiation reflected from water surface, and so linear least-square regression analysis was used to evaluate the relationship between various water quality parameters and solar radiation reflected by water surface at different wavelengths.

The data sets taken at 12 ground truth points were used to form a linear regression model for the water quality parameters from the radiation reflected at the water surface. The dependent variables (y) were the measured values of Secchi depth transparency, suspended solids and chlorophyll-*a*, listed in Table 3.4; the independent variables (x) were the radiance reflectance R_o at the water surface and the radiance reflectance R_w just above the water surface calculated (see previous section) from the extinction coefficient K_u, the upwelling irradiance $E_u(z)$ underwater, and the spectral irradiance H onto the water surface. The range of the radiance reflectance was 400 to 800 nm and the resolution was 2 nm, and so, for suspended solids, for example, and radiance reflectance at the water surface, 201 regression models were constructed.

In standard linear regression analysis, the following assumptions are made about the relation between (y) and (x): (1) For each specific (x), there is a normal distribution of (y) from which the sample values of (y) are assumed to be drawn at random; (2) The normal distribution of (y) corresponding to a specific (x) has a mean

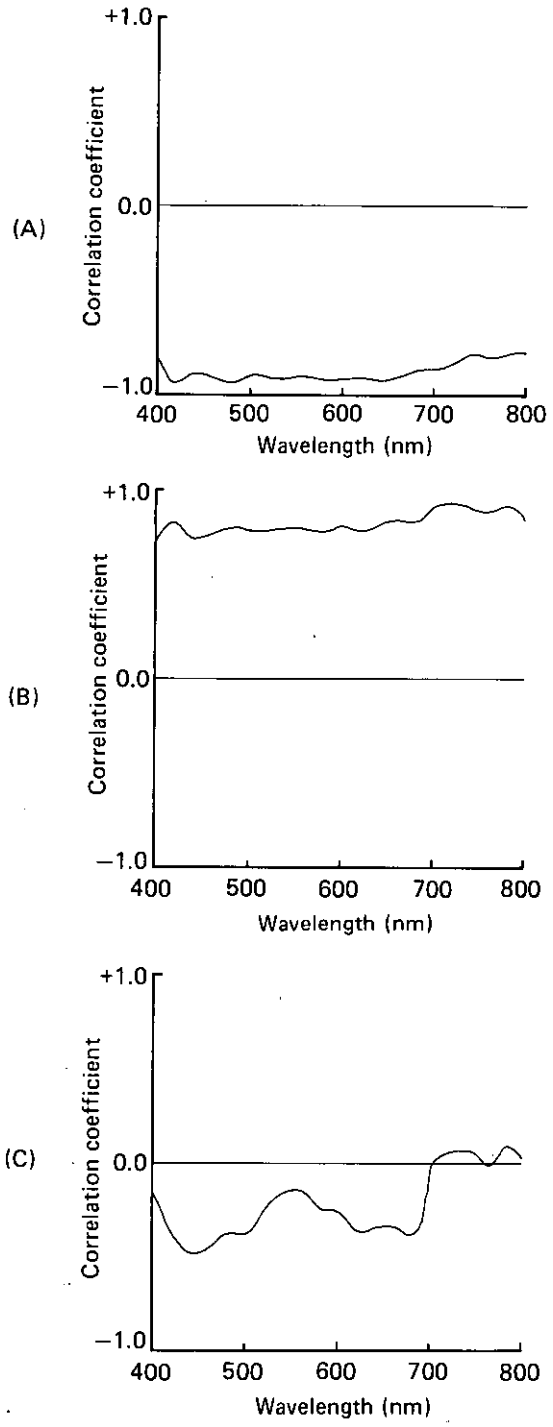

Fig. 3.12 Correlation coefficient between water quality and radiance reflectance at water surface.
(A): Transparency. (B): Suspended solids. (C): Chlorophyll-*a*.

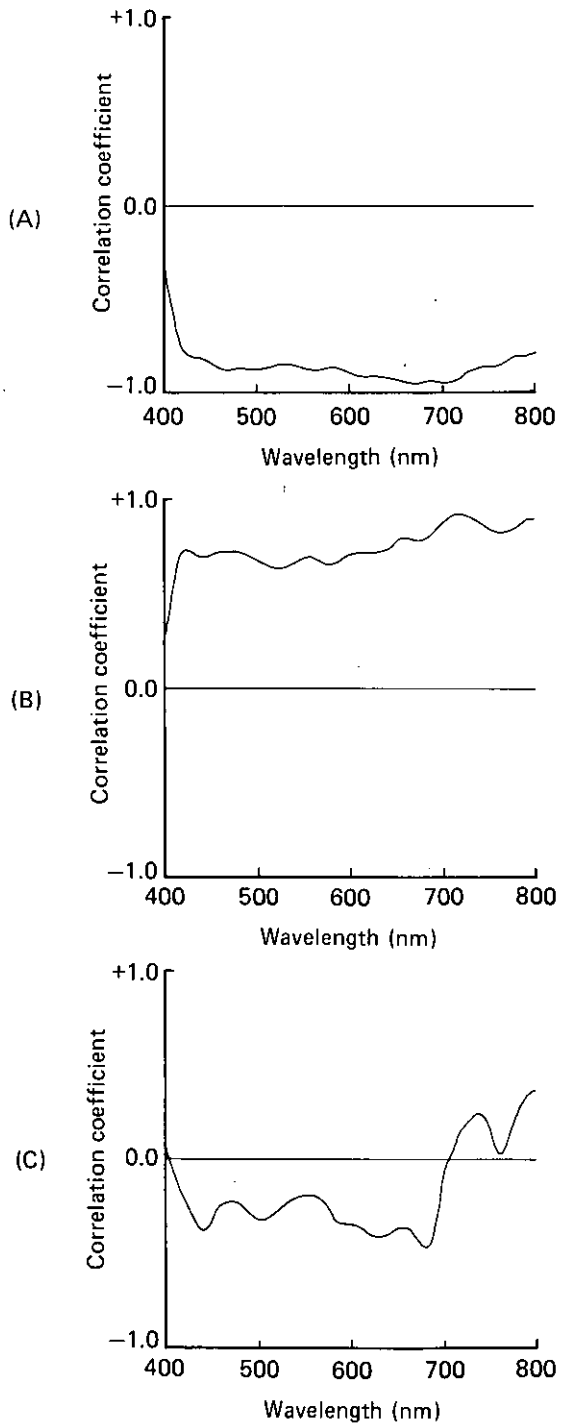

Fig. 3.13 Correlation coefficient between water quality and radiance reflectance just above water surface.
(A): Transparency. (B): Suspended solids. (C): Chlorophyll-*a*.

that lies on the straight line; (3) The normal distributions of (y) for any specific (x) are independent of each other and each have the same variance. We, therefore, assumed that the values used here have a normal distribution for each pair of measurements. The correlation coefficients between various water quality parameters and radiance reflectance at the water surface are plotted in Fig. 3.12. Those between water quality parameters and radiance reflectance just above water surface are plotted in Fig. 3.13. The significance test used here is a two-tailed test (Snedecor & Cochran, 1980) to determine the minimum value of the correlation coefficient (r_c) which will reject the hypothesis of independence for all paris of variables. The minimum value of the correlation coefficient (r_c) was calculated to be 0.58 at the 95% level of confidence. Therefore, our results confirm that a significant negative correlation was found between transparency and the radiance raflectance, while a positive correlation was found between the concentration of suspended solids and the radiance reflectance. On the other hand, chlorophyll-*a* showed a poor fit for the wavelength range. The correlation coefficients between the water quality parameters and the radiance reflectance just above the water surface which are shown in Fig. 3.13 did not improve significantly expect for chlorophyll-*a* in the wevelength range 440 and 680 nm.

Data equivalent to that of LANDAST for spectral radiance at water surface between 500 to 600, 600 to 700, and 700 to 800 nm were calculated by integrating the spectral radiance curves. Again regression analysis was applied to the water quality

Table 3.8 Coefficients of correlation between water quality parameters and radiance at water surface.

Water quality	Spectral range (nm)		
	500-600	600-700	700-800
Transparency	<u>−0.92</u>	<u>−0.92</u>	<u>−0.92</u>
Suspended solids	<u>0.79</u>	<u>0.84</u>	<u>0.91</u>
Chlorophyll-*a*	−0.24	−0.32	−0.16

Underscored values are statistically significant at the 5% level.

Table 3.9 Coefficients of correlation between water quality parmeters and radiance reflectance just above water surface.

Water quality	Spectral range (nm)		
	500-600	600-700	700-800
Transparency	<u>−0.88</u>	<u>−0.94</u>	<u>−0.98</u>
Suspended solids	<u>0.68</u>	<u>0.76</u>	<u>0.87</u>
Chlorophyll-*a*	−0.25	−0.38	−0.18

Underscored values are statistiscally significant at the 5% level.

parameters and this integrated spectral radiance. The resulting correlation coefficients are listed in Tables 3.8 and 3.9; the underscored values are statistically significant at the 5% level. It can be seen that the regression analysis between chlorophyll-*a* and radiance reflectance shows weak correlation. Also, there was no improvement in the correlation between the radiance reflectance at the water surface and the radiance reflectance just above the water surface. Derived linear

regression equations for transparency and the concentration of suspended solids are shown in Figs. 3.14 to 3.17. As can be seen from these figures, one measurement value shows abnormally low radiance value when compared with the other values. This point (point 1 in Fig. 3.3) in the lake is the most clear place and the measured radiance at the water surface was supposed to be very low, and so this value of water quality parameter was expected to appear as an outlier in the regression analysis.

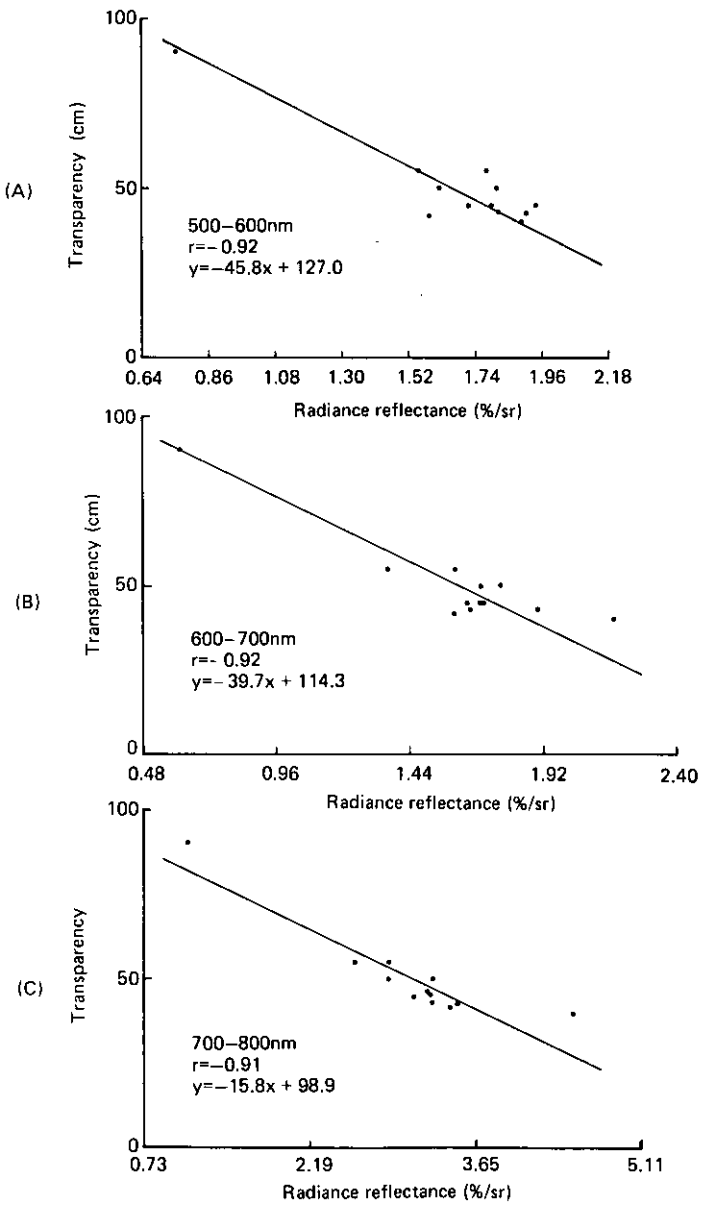

Fig. 3.14 Relation between transparency and radiance reflectance at water surface.
(A): 500-600nm. (B): 600-700nm. (C): 700-800nm.

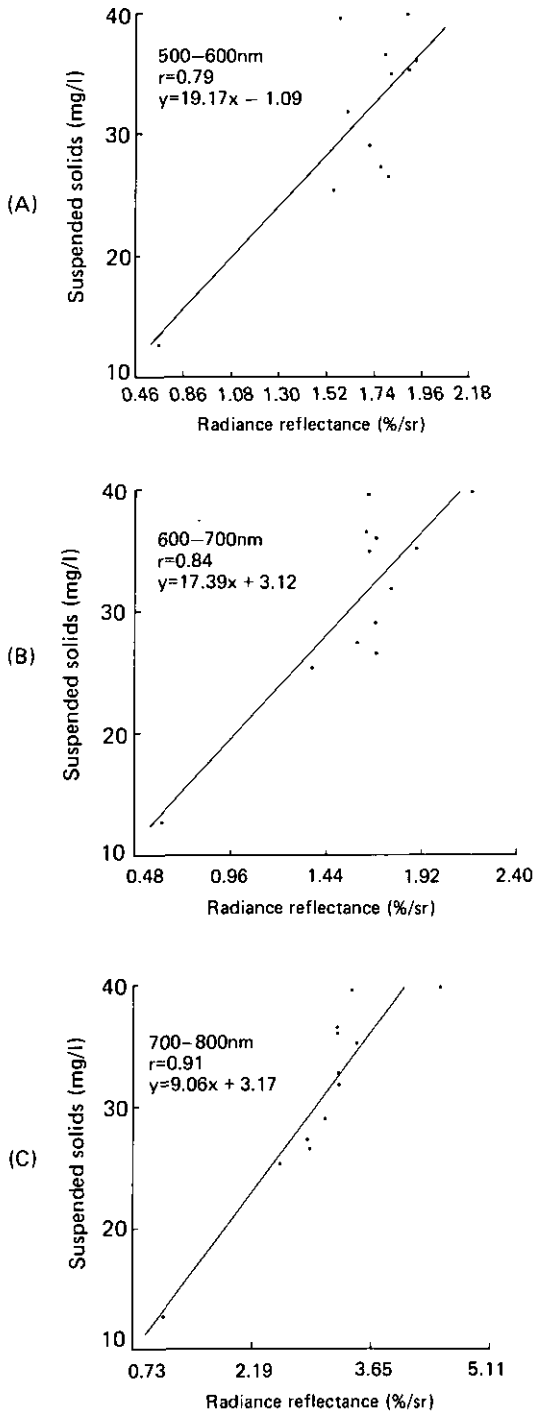

Fig. 3.15 Relation between suspended solids and radiance reflectance at water surface.
(A): 500-600nm. (B): 600-700nm. (C): 700-800nm.

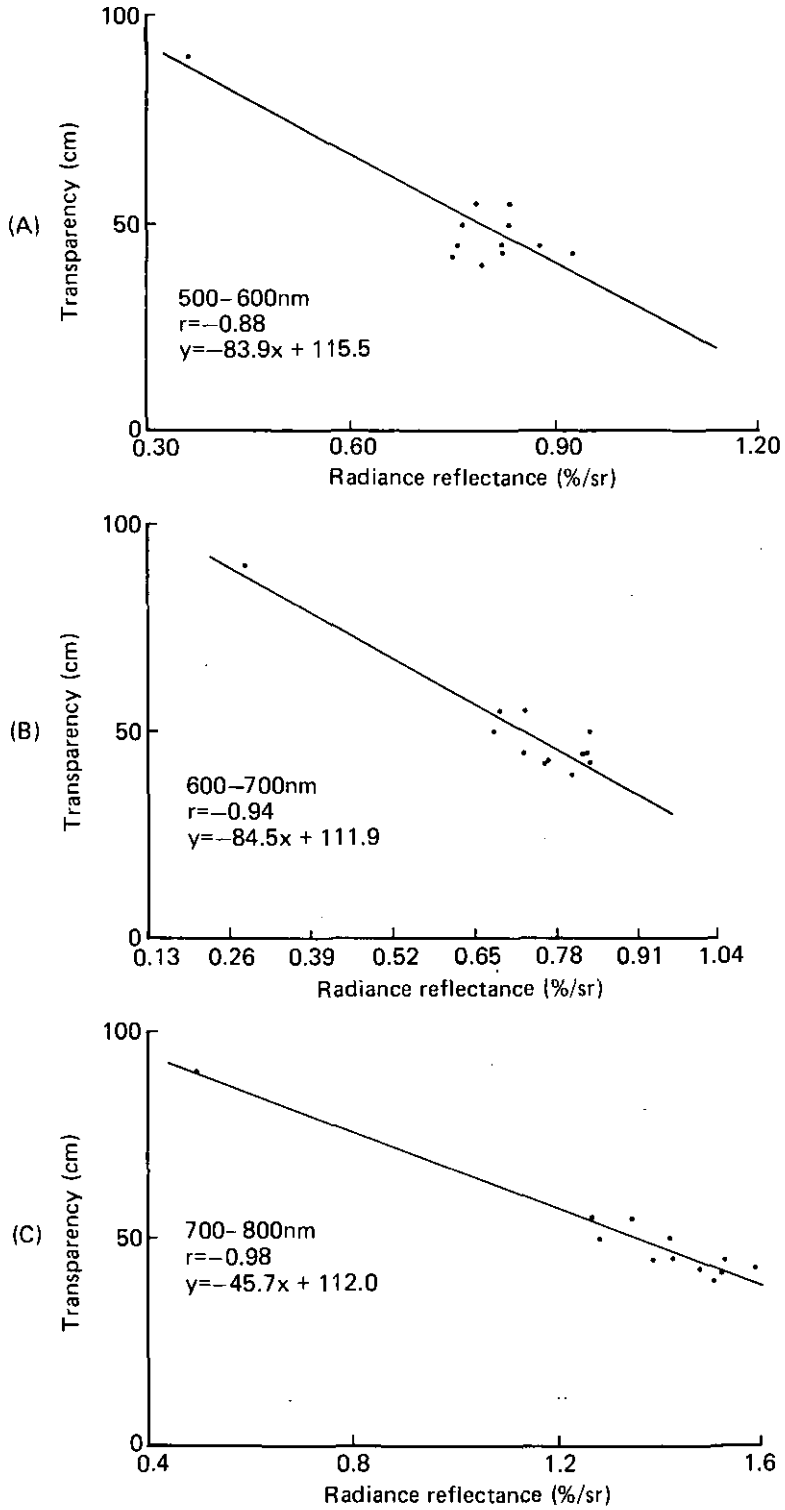

Fig. 3.16 Relation between transparency and radiance reflectance just above water surface.
(A): 500-600nm. (B): 600-700nm. (C): 700-800nm.

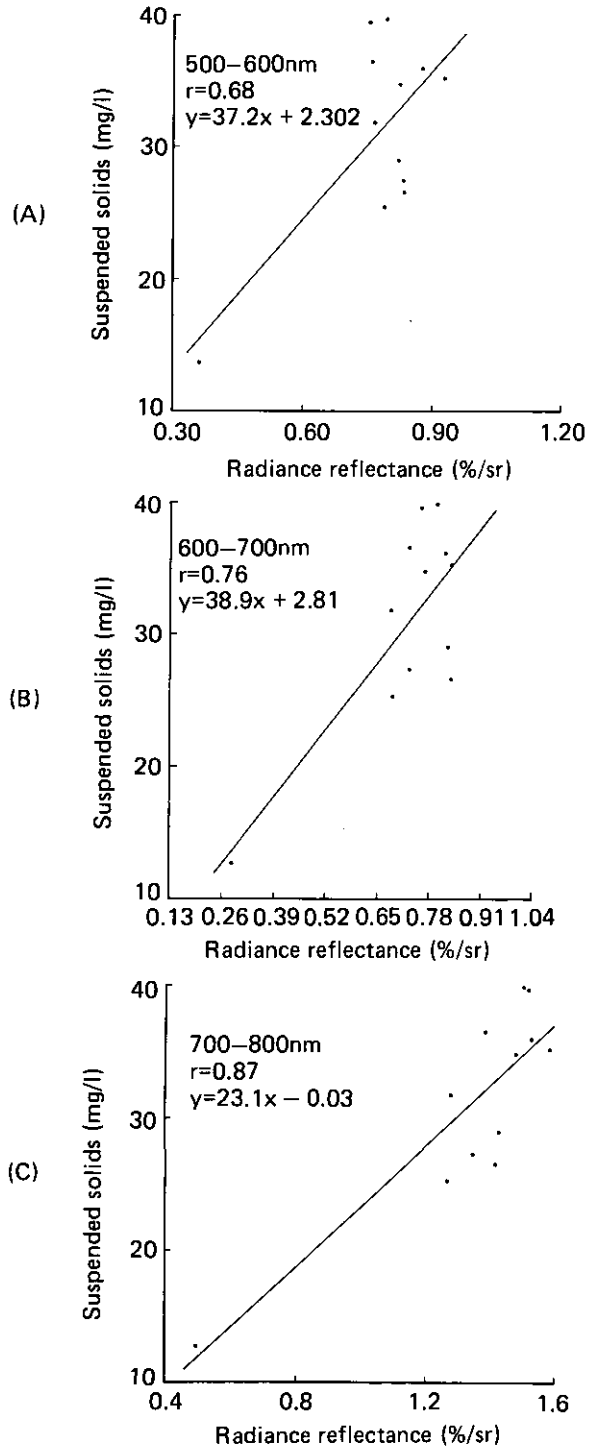

Fig. 3.17 Relation between suspended solids and radiance reflectance just above water surface.
(A): 500-600nm. (B): 600-700nm. (C): 700-800nm.

3.5 CONCLUSIONS

Linear least-square regression analysis was used to evaluate the relationships between various water quality parameters and the radiance reflectance at the water surface. The results showed that there is a quantitative relationship between the concentration of suspended solids and the Secchi depth transparency and the radiance reflectance at the water surface. The best spectral range for using this quantitative relationship would be between 700 and 800 nm for suspended solids and between 500 and 800 nm for transparency, and the results indicate that it should be possible quantitatively to determine concentration of suspended solids in surface water or Secchi depth transparency from remote platforms.

The radiance U_O measured at the water surface consits of the radiance U_W just above water surface and the radiance U_R reflected from the water surface by sky light as stated in Eq. 3.2. The ratio of U_R to U_O, therfore, shows the fraction of the radiance reflected from the water surface by skylight included in the total radiance from the water surface. This ratio is plotted in Fig. 3.18 showing that the component U_R was dependent on the wavelength and that influence of this type of radiance increased at both ends of wavelength rnge of 400 to 420 and 640 to 720 nm.

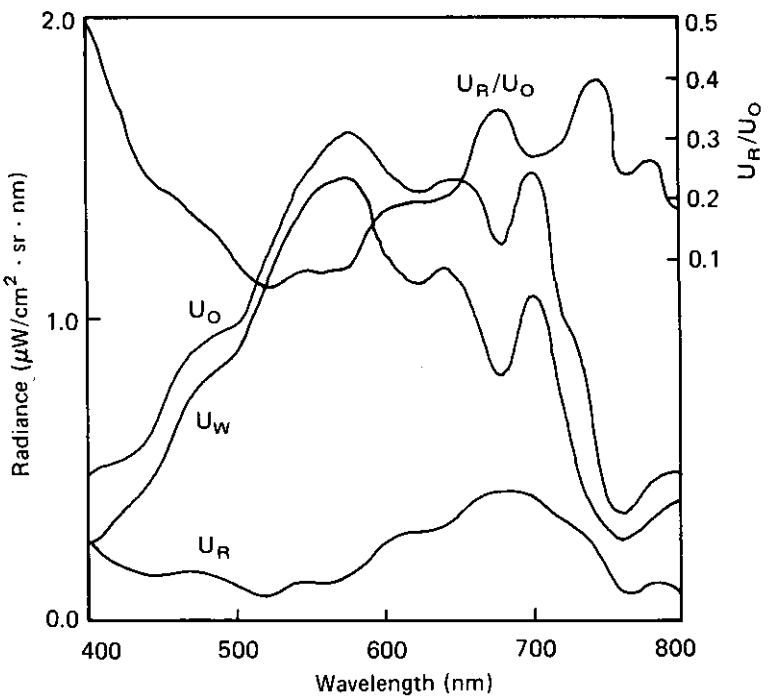

Fig. 3.18 Relation between U_O, U_W, U_R, and U_R/U_O at ground truth point 2.

Regression analysis between water quality and radiance reflectance at the water surface, and between water quality and radiance reflectance just above the water surface differed only slightly. Therefore, the component of total radiance due to light reflected from the water surface need not be considered, from our experiments, for water quality measurement by LANDSAT remote sensing.

CHAPTER

4

Measuring water quality from LANDSAT MSS data

4.1 INTRODUCTION

Suspended solids and phytoplankton are a serious problem in streams, lakes and estuaries, and they degrade aquatic ecosystems and prevent the recreational use of many bodies of water. These two water quality parameters are measured at many bodies of water as laboratory experiments, for water resource management, or for other purposes. These measurements, however, have only limited usefulness, since they represent point samples and do not give an overall view of the body of water. Measurements of water surface reflectance from a satellite or an airplane have shown the potential use of such a remote platform to give qualitative as well as quantitative measures of suspended solids or phytoplankton in the surface water over a large area of a body of water.

The invention of a multispectral scanner (Lowe *et al.* 1966, Polcyn 1967) has brought about a new dimension in airborne and spaceborne surveying of both marine and land resources. By utilizing the simultaneous registry of several bands in the visible and in the infrared region with an airborne multispectral scanner, Polcyn and Wezernak (1970) were able to map industrial discharge from several different industrial plants. Multispectral data were also utilized to map large oil-slicks occurring offshore due to leaks from oil-drilling platforms, pipelines, or accidental spills from ships.

The Earth Resorces Technology Satellite, ERTS, (NASA, 1971), later renamed as LANDSAT was not designed for ocean observations; however, very early in the mission Charnell and Maul (1973) reported that features of oceanographic significance were visible from ERTS imagery, and Szekielda (1973) reported good agreement between the ratio of band 4 to band 5 and the surface chlorophyll-*a* measured by ship. Williamson and Graban (1973) found from ERTS-1 images that suspended inorganic particles from two rivers draining into Chesapeake Bay had different reflectance. Maul and Gordon (1975) developed techniques of using ERTS-1 data to distinguish between the coastal water and the Gulf Stream and between coastal water and plankton bloom. Strong *et al.* (1974), using satellite data of Lake Michigan, reported that the band 4 and band 5 data of ERTS-1 can detect suspended solids. They also investigated the surface current and water color of Lake Michgan using ERTS-1 and VHRR-IR data. Yost *et al.* (1973) have compared ERTS-1 satellite data with water sample data collected in New York Bight and were able to determine the absolute value of total suspended solids with MSS band 5 and band 6 data. Also Yarger *et al.* (1973) showed that MSS band 5 and the band ratio of band 4 to band 5 could be used for reliable measurement of the suspended solids to at least 900 ppm in a reservoir in Kansas. Kritikos *et al.* (1974) also used ERTS-1 multispectral data for measurement of the water quality of the Potomac River and showed that the image of band 5 could easily determine the

concentration of suspended solids in the body of water. By utilizing ERTS-1 data, some related work has been done by the followdng investigators: Klemas (1973), Bowker (1973), and Ruggles (1973). They have studied the dispersion of high sedimentation plumes from ERTS-1 images. Wezernak (1973), Yarger (1973), and Schuburt (1973) also have investigated the surveillance of areas with high sedimentation in various bodies of water. The coastal land use and the water properties of Delaware Bay have been studied by Klemas *et al.* (1973, 1974 a, 1974 b) using ERTS-1 satellite and Skylab-ERED data. They concluded that ERT-1 and Skylab-ERED provided data suitable for mapping coastal vegetation, land use, coastal erosion, current circulation, frontal system, water turbidity, surface slicks, and waste disposal plumes.

Multiple regression techniques were used by Johnson (1975) to correlate ERTS-1 data with measured values of suspended solids in the Potomac River. He was able to plot the suspended solid contours for the river, and he suggested that atmospheric calibration with a different ERTS scene of the deeper water area of Chesapeake Bay might make more accurate detection of suspended solids possible. Thomson *et al.* (1975) used the ratio of band 4 to band 5 of ERTS-1 data to classify the limnological characteristics of lakes in the area of James Bay.

Gordon *et al.* (1975) showed that the suspended particle concentration in the Gulf of Mexico can be estimated from MSS band 5 images taken by the ERTS-1 satellite; while band 4 is strongly influenced by yellow substances. Rouse and Coleman (1976) investigated the discharge plume from the Mississipi River into the Louisiana Bight from ERTS-1 band 5 images. In Nigeria, Abiodun (1976) has examined the distribution of suspended solids at the initial stage of the annual flood in Lake Kainji using ERTS-1 spectral data. He delineated the suspended solid concentration clearly into five levels. Johnson and Norris (1977) used Skylab multispectral scanner data to study the spectral signature of the water at the confluence of the Falkland and the Brazil Current off the east coast of Argentina. Klemas and Polis (1977) investigated the tidal current of Delaware Bay using a suspended solid distribution map derived from ERTS-1 and LANDSAT-2 satellite images. Strong (1978) utilised LANDSAT, Skylab, and NOAA satellite data to observe chemical whitings several meters below the water surface in Lake Michigan and concluded that the whitings can be detected from LANDAST band 4.

Abiodun and Adeniji (1978) showed that the movement of the water of Lake Kainji over two years could be detected with LANDSAT band 5 images. Smith *et al.* (1978) reported that the ratio of LANDSAT band 5 to band 7 showed the pattern of discharge from volcanoes into Hamersley Basin. Munday and Alfoldi (1979) confirmed that the LANDSAT band 5 data could be used to measure suspended solids in bodies of water. Klemas (1980) observed the tidal front of Delaware Bay with LANDSAT satellite band 5 data. Thomas (1980) monitored the motion of non-uniformly distributed suspended solids in a New Zealand tidal basin and penetration depth for MSS band 5 over the tidal basin was founded. Finley and Baumgardner (1980) observed the plumes of turbid surface water in the vicinity of Aranso Pass by utilizing LANDSAT images.

Khorram (1981) reported that, for assessing water quality parameters within the San Francisco Bay-Delta, LANDSAT MSS data and U-2 color and color infrared photographs were combined with *in situ* data such as that for turbidity and suspended solids. They developed regression models between the LANDAST digital

data and each of the water quality parameter measurements. The results showed that the areas of relatively high concentration of suspended solids were clearly discernible from LANDAST MSS data. The water quality measurement of freshwater lakes in Australia has been investigated by Carpenter and Crmpenter (1983). To estimate water quality they have developed multiple regression models in which they accounted for the sun elevation and the time of sample collection. These models were used successfully to estimate water quality for three lakes on different occasions.

Gordon *et al.* (1983) developed algorithms for measuring phytoplankton pigments from the data obtained by the Coastal Zone Color Scanner (CZCS) on NIMBUS-7. These algorithms were applied to data from the Middle Atlantic Bight and from the Sargasso Sea. Caraux and Austin (1983) also used NIMBUS-7 data to monitor seasonal changes in phytoplankton pigment distribution in the Gulf of Lions in the Mediterranean Sea; the characteristics of boundaries between water masses with different phytoplankton content were also noted. The results demonstrated that phytoplankton distributions are a good indicator of seasonal variations of oceanic fronts, and coastal upwellings, cyclonic eddies, and of the plume of a river.

The Trophic State Index (TSI) proposed by Carlson (1977) indicates the eutrophic level of a lake or ocean and can be calculated from any of several parameters such as Secchi depth transparency, chlorophyll, and total phosphorus. Lillesand *et al.* (1983) estimated the TSI from LANDSAT data for 60 Minnesota lakes. They formulated statistical models relating values of the TSI to LANDSAT data, and the results showed that TSI estimates from LANDSAT data were reliably close to those obtained by the Secchi depth transparency method.

Verdin (1985) reported that with corrections for sun angle and atmospheric effects in LANDSAT data, he was able to estimate the Secchi depth transparency and chlorophyll concentration of the Flaming Gorge Reservoir in Wyoming, without concurrent surface sampling. Khorram (1985) developed water quality models to map salinity, turbidity, suspended solid, and chlorophyll-*a* concentration in San Fransisco Bay and Delta. Khorram and Cheshire (1985) developed similar water quality models for the Neuse River estuary in North Carolina. These latter two models still required extensive ground truth measurements.

The work of these many researchers has used, basically, regression analysis between water quality parameters and LANDSAT MSS data for estimating the water quality of many bodies of water. Consequently, ground truth measurements taken at the time of LANDSAT overpass are essential. However, techniques for correcting LANDSAT data for atmospheric effects were later introduced in an effort to develop more gentral water quality models or medels which do not require any ground truth measurements. Further research work is needed to develop an easy and simple way to determine the effect of the atmosphere on LANDSAT data and to developed generalized water quality models of inland bodies of water and oceans.

The object of the investigation reported in this chapter was to use remotely sensed data (LANDSAT data), combined with *in situ* data, to assess water quality parameters such as suspended solids, chlorophyll-*a*, and transparency and to locate regions of highly polluted water within Lake Kasumigaura. Our investigation was based on the relationships between water quality parameters and the spectral reflectance of the water surface which we developed in Chapter 3.

4.2 DESCRIPTION OF DATA ACQUISITION

The water quality data comprised measurements of suspended solid, of algal pigment (chlorophyll-*a* and phaeopigments) concentration, of the Secchi depth transparency, of the surface temperature of the water as well as of fundamental meteorological conditions such as temperature, wind direction and speed, and visibility. These measurements were made at a time and at a point on the lake which corresponded to an overflight of LANDSAT. These data were acquired on 24 November 1981, 3 March 1982, and 25 October 1983. Typical ground truth points are shown in Fig. 4.1, and Table 4.1 summarizes the acquired data. The water quality data are listed in Table 4.2. The concentration of suspended solids changes from 3.5 mg/*l* in the clean water area in the center of the lake to 39.8 mg/*l* in the most polluted place while chlorophyll-*a* changes from 6.9 μg/*l* to 124.4μg/*l*.

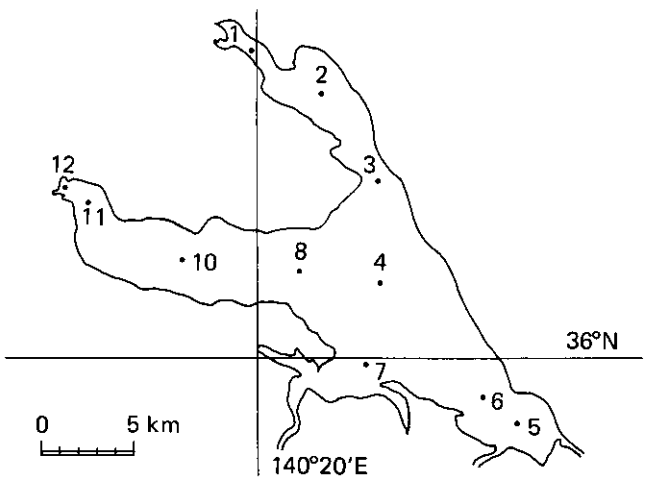

Fig. 4.1 Location of sampling points for ground truth at Lake Kasumigaura (24 Nov. 1981).

Table 4.1 Summary of data acquisition in Kasumigaura experiment.

Date	24 November 1981	3 March 1982	25 October 1983
LANDSAT	L-2, MSS Path 115, Row 35	L-3, MSS Path 115, Row 35	L-3, MSS Path 107, Row 35
Spectral measurement	Water surface, Under water*, White reflector	Water surface, Under water*, White reflector	Water surface, Under water, White reflector
Water quality	Temperature, Transparency, Suspended solids	Temperature, Transparency, Suspended solids	Temperature, Transparency Suspended solids
Number of ground truth point	11	13	12
Weather condition	Strong haze	Clear	Clear

* Measured by OCS (Kishino *et al.*, 1984)

Table 4.2 Summary of water quality samples collected.

Date	Ground truth point	Temperature (℃)	Transparency (cm)	Suspended solids (mg/l)	Chlorophyll-*a* (μg/l)	Phaeophytin (μg/l)
24 Nov.	0	10.1	60.0	17.5	12.5	4.1
1981	1	9.8	80.0	11.0	47.1	8.7
	2	10.3	85.0	13.5	105.5	3.7
	3	10.8	60.0	20.0	124.4	11.6
	4	10.6	90.0	12.5	74.8	9.1
	5	11.1	90.0	11.5	70.1	5.9
	6	11.1	85.0	12.5	61.8	3.9
	7	11.1	75.0	13.5	76.1	4.8
	8	11.6	85.0	10.3	75.3	5.9
	10	10.3	65.0	17.5	73.6	5.7
	11	9.0	45.0	36.0	31.6	5.6
3 Mar.	1	6.5	95.0	10.2	34.4	0.4
1982	2	6.5	135.0	6.2	22.4	1.8
	3	6.3	135.0	9.8	22.5	2.9
	4	6.2	135.0	9.8	23.9	2.5
	5	6.2	130.0	8.7	23.7	5.1
	6	6.0	150.0	3.5	12.4	1.3
	7	5.9	130.0	5.3	13.3	2.2
	8	5.7	115.0	6.8	8.6	2.8
	9	5.9	140.0	4.5	10.2	2.8
	10	6.2	140.0	5.2	9.7	0.8
	11	6.0	120.0	4.7	9.0	0.3
	12	6.2	45.0	28.5	11.1	0.1
	13	6.9	45.0	23.0	6.9	0.4
25 Oct.	1	16.8	90.0	12.7	56.3	10.3
1983	2	16.1	50.0	31.8	50.5	13.9
	3	16.3	55.0	27.3	49.2	7.1
	4	16.6	55.0	25.3	53.6	6.4
	5	16.0	45.0	36.5	55.4	4.6
	6	16.0	45.0	36.0	60.4	2.6
	7	16.2	43.0	34.8	55.5	2.6
	9	16.3	43.0	35.2	47.2	3.3
	10	16.2	42.0	39.5	58.2	3.6
	11	16.2	40.0	39.8	38.9	3.8
	12	16.3	50.0	26.5	16.2	0.2
	13	16.7	45.0	29.0	26.9	2.0

The LANDSAT MSS data used were identified as Path 115, Row 35 for LANDSAT-2 and 3 data, and Path 107, Row 35 for LANDSAT-4 data. The data were received and used as sets of multispectral digital radiance values on computer compatible tape (CCT). These data were distributed by the National Space Development Agency of Japan.

The LANDSAT MSS data were obtained from four spectral bands. Band 4 in 500 to 600 nm (visible green); band 5 is 600 to 700nm (visible red); band 6 in 700 to 800 nm and band 7 is 800 to 1100 nm (both near infrared), and the resolution at ground

level was approximately 80×80 m.

To determine the position for ground truth mesurements is one of the most important factors for remote sensing. Here, a handheld mariner's compass was used for reading the magnetic compass diretion of several ground objects located at the lakeside. The accuracy of this measurement is between 50 to 100 meters under relatively calm weather conditions, an accuracy satisfactory for coordination with LANDSAT remote sensing.

Digital levels for a ground truth point are extracted from the CCT by first locating the ground station coordinate on a CCT generated gray level map. Then the 9 pixels (3×3 pixels) which correspond to a 240×240 meter square area on the water surface at the coordinate are averaged. From the CCT count for 25 Oct. 1983 experiment, however, 25 pixels (5×5 pixels) were extracted and averaged. In Table 4.3, the CCT counts corrsponding to each ground truth point are listed.

4.3 REGRESSION ANALYSIS BETWEEN WATER QUALITY PARAMETERS AND LANDSAT MSS DATA

For apparently practical reasons but without theoretical justification, a linear relationship between the water quality parameters measured at the ground truth point and the upwelling radiance detected by LANDSAT has often been used to measure water quality in water bodies. A series of regression analyses were run to determine the best relationships between each water quality parameter measured at ground truth points and the mean CCT count computed from LANDSAT band 4, 5, and 6. The dependent variables were water quality parameters and the independent variables were CCT count from each band. Again, it was assumed that the distribution of the values utilized for regression analysis is a normal distribution for each pair of measurements.

Table 4.4 shows the correlation coefficients calculated from the regression analysis and from the significance test. The underscored values in the table are statistically significant at the 5% level. The transparency and amount of suspended solids are well correlated with the LANDSAT data band 4, 5, and 6, while chlorophyll-*a* showed no significant correlation with any of the LADSAT bands. The regression lines for transparency and the concentration of suspended solids are illustrated in Figs. 4.2, 4.3, and 4.4. As can be seen from these figures, a few of the measuremest values are abnormally high or low when compared with other values. At these points on the lake, one point in the 24 Nov. 1981 and two points in the 3 Mar. 1982 experiment, the water quality was highly turbid from recent dredging. One point, in the 25 Oct. 1983 experiment, at the center of the lake, the water was very clear, and so these water quality values were expected to appear as outliers in the regression analysis.

Table 4.3 LANDSAT CCT count at the ground truth points.

Date	Ground truth point	LANDSAT CCT count Band 4	Band 5	Band 6	
24 Nov.	0	12.66	11.55	6.66	Averaged
1981	1	10.60	8.88	4.55	3×3 pixels
	2	10.73	8.77	5.66	
	3	10.91	9.66	6.33	
	4	10.88	9.88	5.88	
	5	10.77	8.33	4.44	
	6	10.93	9.00	5.66	
	7	10.88	9.22	5.11	
	8	11.22	10.11	6.22	
	10	11.77	10.55	6.66	
	11	13.82	12.88	7.88	
3 Mar.	1	15.31	8.88	3.77	Averaged
1982	2	14.55	8.66	4.11	3×3 pixels
	3	14.46	8.11	3.11	
	4	14.44	8.22	3.66	
	5	14.82	8.88	4.13	
	6	13.63	7.47	3.80	
	7	14.77	7.88	3.80	
	8	15.22	8.55	3.77	
	9	14.82	8.23	3.48	
	10	14.20	8.15	3.23	
	11	15.39	8.40	3.93	
	12	19.45	14.15	7.43	
	13	17.88	13.11	7.22	
25 Oct.	1	10.42	7.90	4.94	Averaged
1983	2	12.44	10.80	7.50	5×5 pixels
	3	12.60	10.90	7.15	
	4	13.08	11.28	7.18	
	5	12.67	11.90	8.01	
	6	13.17	12.03	8.05	
	7	13.66	12.15	8.43	
	9	13.56	12.41	8.37	
	10	13.47	12.12	8.69	
	11	13.75	12.66	8.79	
	12	13.85	13.31	7.82	
	13	13.42	12.26	8.22	

Table 4.4 Coefficients of correlation between water quality parameters and LANDSAT CCT count.

Date	24 Nov. 1981			3 Mar. 1982			25 Oct. 1983		
LANDSAT band	4	5	6	4	5	6	4	5	6
Transparency	−0.81	−0.82	−0.78	−0.96	−0.95	−0.91	−0.91	−0.91	−0.98
Suspended solids	0.80	0.79	0.79	0.94	0.97	0.92	0.73	0.74	0.93
Chlorophyll-*a*	−0.53	−0.43	−0.25	−0.30	−0.27	−0.31	−0.40	−0.47	−0.19
Number of ground truth point	11			13			12		
LANDSAT	L-2			L-3			L-4		

Underscored values are statistically significant at the 5% level.

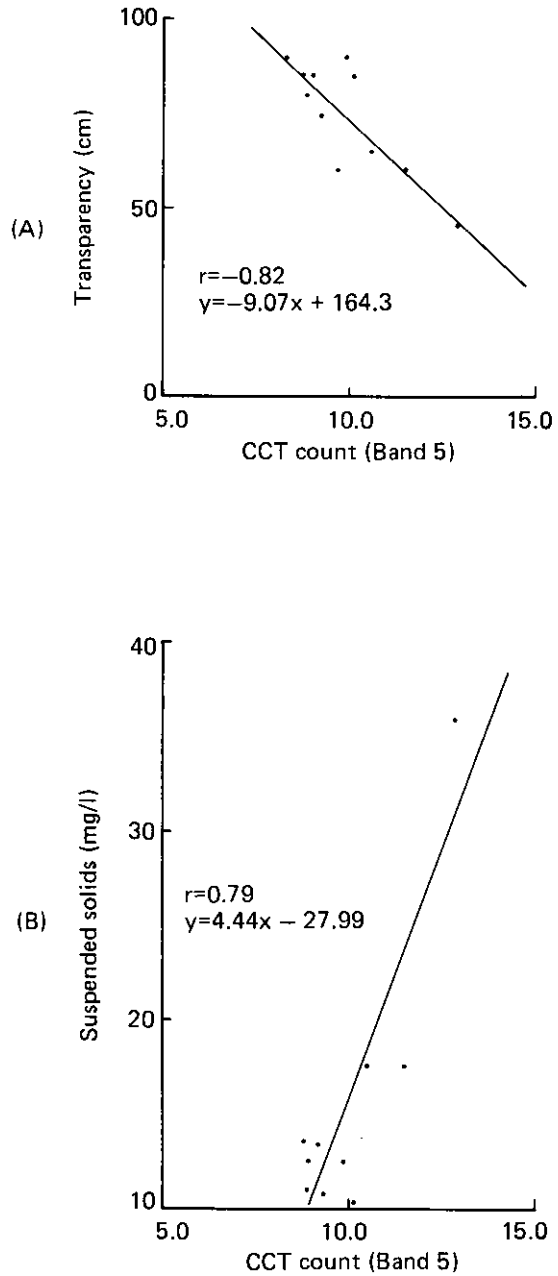

Fig. 4.2 Relation between water quality and LANDSAT CCT count band 5 (24 Nov. 1981). (A): Transparency. (B): Suspended solids.

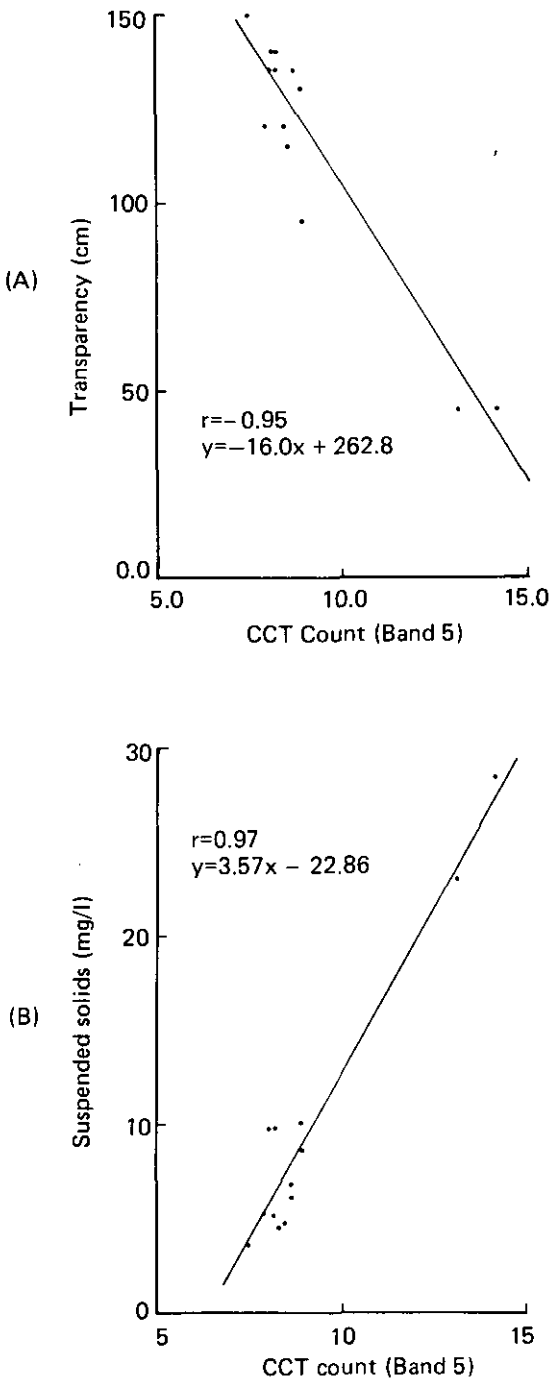

Fig. 4.3 Relation between water quality and LANDSAT CCT count band 5 (3 Mar. 1982). (A): Transparency. (B): Suspended solids.

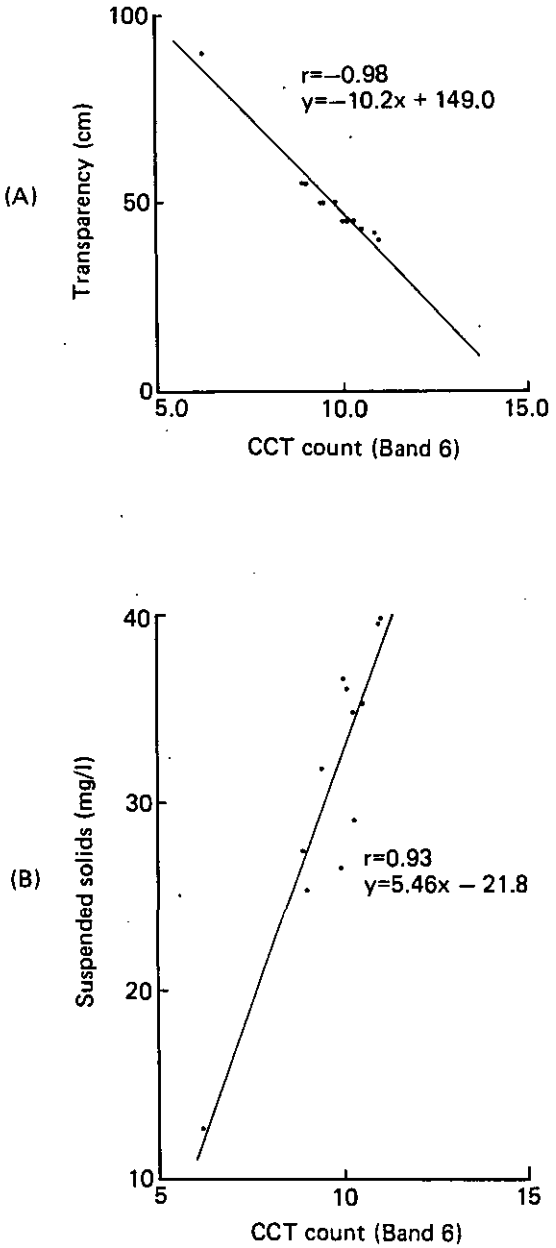

Fig. 4.4 Relation between water quality and LANDSAT CCT cont band 6 (25 Oct. 1983). (A): Transparency. (B): Suspended solids.

4.4 ESTIMATING THE WATER QUALITY DISTRIBUTION OF LAKE KASUMIGAURA

In the previous section, the best-fit regression models, for mapping water quality parameters from the LANDSAT data were obtained. These regression medels were then extended to map the selected water quality parameters for all of Lake Kasumigaura. Fig. 4.5 shows examples of distribution maps for suspended solids which were derived from LANDSAT data. In Fig. 4.5 (A), the concentration

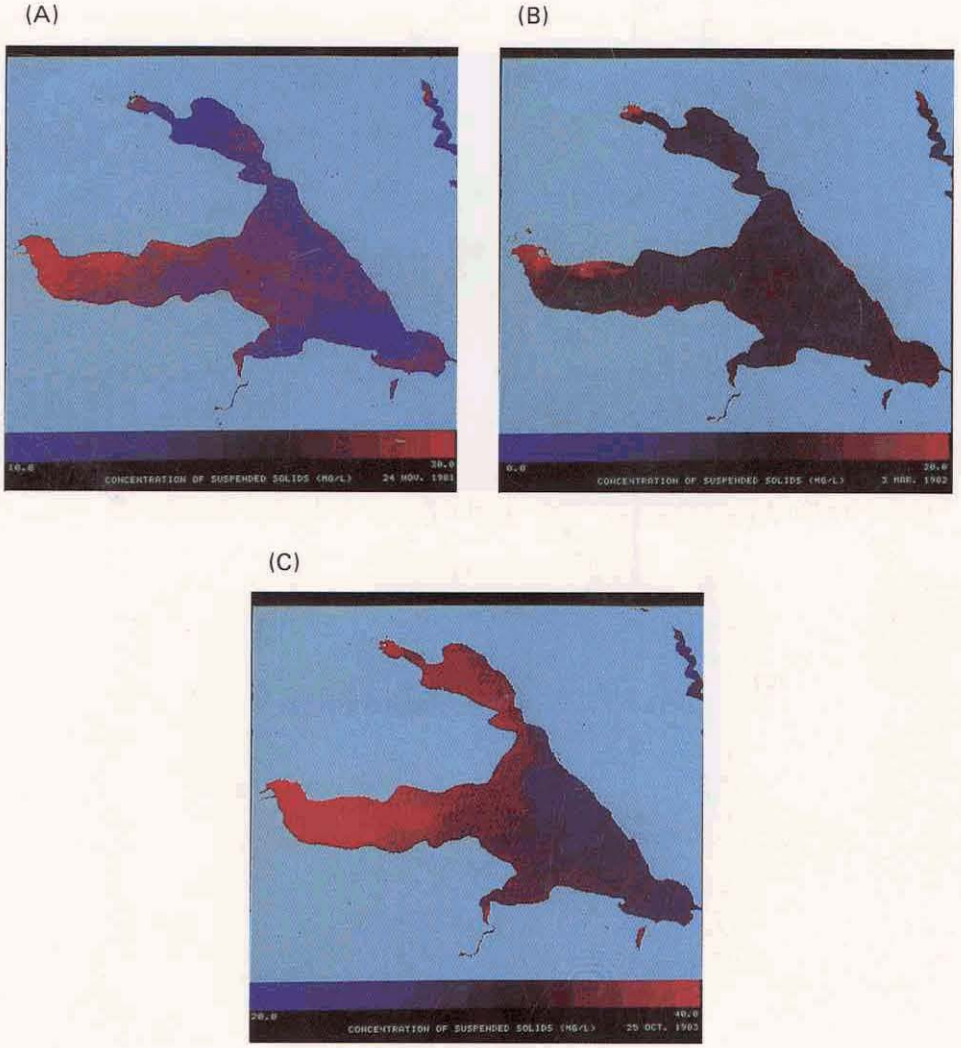

Fig. 4.5 Estimated distribution of suspended solids in Lake Kasumigaura. (A): 10-30mg/*l* (24 Nov. 1981). (B): 0-20mg/*l* (3 Mar. 1982). (C): 20-40mg/*l* (25 Oct. 1983).

levels of polluted areas are brighter red, the least pollnted areas are brighter blue, and the concentration range of 10 to 30 mg/l is represented by 16 color levels. Fig. 4.5 (B) represents the concentration range of 0 to 20 mg/l ; Fig. 4.5 (C), the range of 10 to 40 mg/l.

4.5 CONCLUSIONS

LANDSAT MSS data are not well suited for the remote sensing of water quality since the spectral band of the multispectral scanner are located mostly in that part of the spectrum where water absorbs strongly. Moreover, the sensitivity of the detectors is set for generally more strongly reflecting land areas. However, by using a simple linear regression technique on data obtained over water area and data from LANDSAT, we have shown that Secchi depth transparency and concentration of suspended solids can be estimated with accuracy from LANDSAT MSS data. Experiments on three different dates showed that transparency and amount of suspended solids were well correlated with LANDSAT MSS band 4, 5, and 6 data. On the other hand, as can be concluded from Table 4.4, chlorophyll-a was not well correlated with the same LANDSAT data. Band 7 data has been excluded from this analysis because band 7 can have only a very weak response to variations in water area. Some more nuanced models using, for exmple nonlinear regreession or multiple linear regression might be able to correlate water quality with LANDSAT data but we judged such methods to have little physical signficance here.

For the transparency and suspended solid analysis, the correlation coefficients obtained from the experiment on 24 Nov. 1981 showed values slightly lower than those of the other two experiments. This may have been a result of the condition of the atmosphere between LANDSAT and the water surface because it was a very hazy day the time of LANDSAT overflight, when the visibility was recorded as less than 2 km around the lake. There was, it seems, the possibility that haze over the lake affected the CCT counts extracted from the LANDSAT data. An atmospheric correction, therefore, to the LANDAST data might be needed to develop weather-independent regressions suitable for estimating water quality parameters.

The models generated allowed the extrapolation of point-sample data to produce distribution maps for the entire lake from LANDAST data. These distribution maps corresponded closely to the actual observed conditions of the water at various parts of the lake.

CHAPTER

5

Evaluation of atmospheric effects on LANDSAT MSS data

5.1 INTRODUCTION

The characteristics of the earth's surface can be accurately measured by comparing the remotely sensed characteristics of unknown regions with those for regions in which the same characteristics have been independently measured at what are called "ground truth points". As the number of ground truth points required beomes fewer, this method becomes more efficient and valuable. As described in Chapter 4, we used this method to measure the water quality of Lake Kasumigaura. The regression models, however, derived from the regression analysis between water quality parameters and LANDSAT MSS data seem to be heavily dependent on weather conditions. That is, depending on the weather when the LANDAST data was taken, the slope and the y-intercept of the regression lines showed different values from one another. Because of the low reflectance of water, the atmospheric path radiance forms a large part of the total radiance detected by LANDSAT MSS, and so the differences in the medel may be largely caused by the atmosphere between the water surface and the LANDSAT sensor. It has been known that the back-scattered radiance from water surface comprises only 10 to 50% of the total radiance detected by the LANDSAT sensor. LANDSAT data distributed for users have not, in general, been corrected for atmosphric scattering or path radiance. The difficulty in making an accurate correction for such atmospheric effects is a major obstacle to the use of remote sensing for determining the water quality of bodies of water.

A number of approaches to determining the required correction for path radiance are currently being explored. Turner and Spencer (1972), O'Neill *et al.* (1978), and Dave (1978) have used a radiative transfer model to compute the path radiance. Gordon *et al.* (1973) and Rogers *et al.* (1973) measured path radiance by the Duntley method (Duntley, 1973) of correction for atmospheric effects. Fraser *et al.* (1977) estimated the atmospheric radiance for LANDAST-1 MSS by utilizing the radiance detected over the deep ocean area where the radiance of the atmosphere is several times stronger than the ocean radiance. Gordon (1978) has proposed a method for correcting the aerosol influence on remotely sensed data by measuring the radiance of the wavelength range of 0.7 μm or longer, where the ocean becomes a black body. He assumed that the scattering effects due to molecules and aerosols in the atmosphere are independent of one another and that the aerosol effects are linearly dependent on optical thickness. These hypotheses were verified by Viollier *et al.* (1980) by accurately calculating diverse terms of atmospheric perturbation, and developing simple formulas to facilitate quick and accurate correction. Gordon *et al.* (1980) applied this method to remove the aerosol effect from the radiance measured by the NIMBUS-7 Coastal Zone Color Scanner (CZCS) over Southern California, Chesapeake Bay, and the Gulf of Mexico. The phytoplakton pigment concentrations derived from the corrected CZCS radiances agreed well with surface

measurements. Under the assumption that the radiance observed in LANDSAT band 7 (0.8–1.1 μm) over water is nearly equal to the path radiance of atmosphere, Onitsuka *et al.* (1981) developed algorithms for path radiance correction of LANDSAT images acquired over Japanese coastal weters. The corrected images showed some interesting features which were not evident in the original LANDAST images. MacFarlane and Robinson (1984) presented atmospheric corrections for LANDAST-3 data collected over the Solent area on the south coast of England during the period 1979 to 1980. The Rayleigh scattering was calculated from the incident solar irradiance, the Rayleigh scattering function, the Rayleigh optical thickness, the radiance transmittance, the optical thickenss of the ozone, and the Fresnel reflectivity. The actual equations used were derived by Sturn (1981, 1983). Another factor, the aerosol scattering component, can be calculated from the LANDSAT CCT band 7 digital data by assuming there is no radiance reflected from the water surface in band 7.

These methods have been shown to be effective for determining the path radiance at a specific geographic location. In Japan, however, significant spatial inhomogeneities in the optical characteristics of the atmosphere are expected, and so the above methods are not expected to be so useful to correct data taken over Japan.

In this chapter, we attempt to estimate the atmospheric effects, especially that of path radiance and transmittance by an empirical analysis based on the radiance detected by LANDSAT and that measured at the water surface. We also present some corrections of LANDSAT MSS data which we made.

5.2 ESTIMATING THE PATH RADIANCE AND THE TRANSMITTANCE OF THE ATMOSPHERE

The response of each LANDSAT MSS band to upwelling radiance over water can be expressed as

$$L = \tau \cdot U_o + P \qquad 5.1$$

where L is apparent radiance detected by LANDSAT, P is atmospheric path radiance. U_o is upwelling radiance above the water surface, and τ is the atmospheric transmittance (see Fig. 5.1). The radiance reflectance R_o at the water surface is given as

$$R_o = \frac{U_o}{H} \qquad 5.2$$

where H is the total incident solar irradiance at water surface. Then using Eq. 5.1 R_o can be written as

$$R_o = \frac{L-P}{\tau \cdot H} \quad . \qquad 5.3$$

The total incident solar irradiance H is estimated with the following expression

$$H = \pi \cdot \rho \cdot W \qquad 5.4$$

where W is the upwelling radiance reflected by a white reflector placed at the ground truth point. The surface of the while reflector is assumed to be a lambertian surface and ρ is the reflectivity of the white reflector. Now using Eq. 5.3 and 5.4 radiance

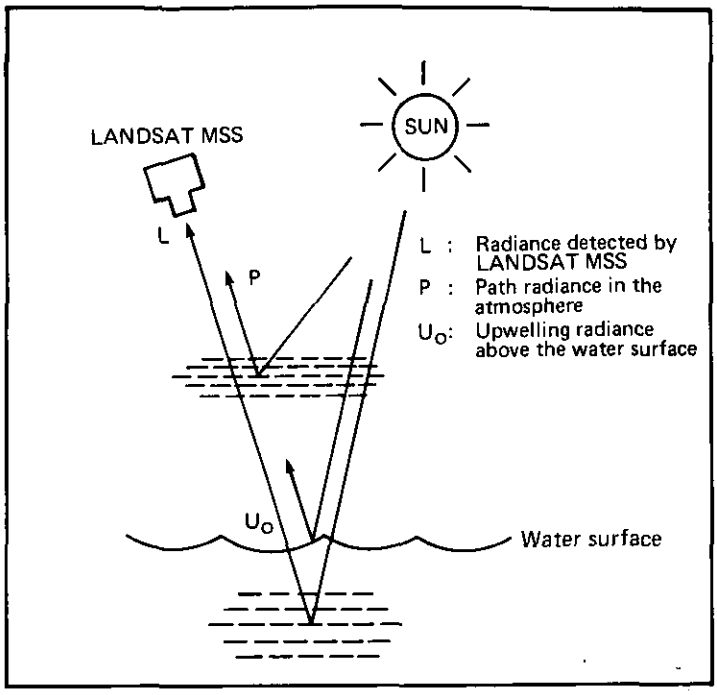

Fig. 5.1 Schematic flow diagram of remote sensing of water quality. Three spectral components detected by remote sensor.

reflectiance R_o can be expressed as

$$R_o=\frac{L-P}{\tau \cdot \pi \cdot \rho \cdot W} \quad . \qquad 5.5$$

All terms in Eqs. 5.1 to 5.5 are dependent on the wavelength.

In order to obtain the path radiance P and the transmittance τ of the atmosphere between LANDSAT and the water surface for Eq. 5.1, a linear regression analysis was introduced in this study.

As described before in Chapter 4, on 24 November 1981, 3 March 1982, and 25 October 1983, the dates when LANDSAT acquired the information used in this study, the radiance of the water surface and the upwelling radiance reflected from a white reflector were measured whth the high-speed spectroradiometer at the time when LANDSAT passed over that spot.

Table 5.1 Radiance corresponding to maximum and minimun sensitivity for each band of LANDSAT-2, 3, and 4.

Band	Wavelength(nm)	LANDSAT-2		LANDSAT-3		LANDSAT-4	
		L_{max}	L_{min}	L_{max}	L_{min}	L_{max}	L_{min}
4	500- 600	2.63	0.08	2.50	0.04	2.38	0.04
5	600- 700	1.76	0.06	2.00	0.03	1.64	0.04
6	700- 800	1.52	0.06	1.65	0.03	1.42	0.05
7	800-1100	3.91	0.11	4.50	0.03	3.49	0.12

(mw/cm² · sr)

Before estimating the path radiance and the transmittance, the absolute radiance detected by LANDSAT had to be derived. The digital 7-bit count N of LANDSAT is converted into radiance L by assigning 127 to the known maximum value L_{max} and zero to the minimum value L_{min}. Thus, L is given by

$$L=\frac{L_{max}-L_{min}}{127}\cdot N+L_{min}. \qquad 5.6$$

The value of L_{max} and L_{min} in each band of LANDSAT-2, 3, and 4 are shown in Table 5.1.

Table 5.2 Coefficients of correlation between radiance detectded by LANDSAT and radiance at water surface.

LANDSAT band	24 Nov. 1981	3 Mar. 1982	25 Oct. 1983
4	0.91	0.99	0.87
5	0.90	0.99	0.85
6	0.85	0.96	0.86

Underscored values are statistically significant at the 5% level.

The values of upwelling radiance U_o and W used in this study were calculated from the measured radiance values at the ground truth points by integrating over the wavelength ranges equivalent to those of LANDSAT. The radiance U_o and W were measured approximately from one hour before and to one hour after actual LANDSAT overflight. For eliminating the influence of the sun angle effect, the radiance U_o was normalized by following equation

$$U_o^N=U_o\cdot\frac{W^N}{W} \qquad 5.7$$

where U_o^N is normalized upwelling radiance at the water surafce and W^N is the radiance value of the white reflector measured at the exact time (9:30 A.M.) of LANDSAT overflight.

In order to estimate the path radiance P and the transmittance τ in Eq. 5.1, a regression analysis was performed on the data set of $\{L\}$ and $\{U_o^N\}$, to determine the constants a and b in

$$L=a\cdot U_o^N+b \quad . \qquad 5.8$$

Here again it was assumed that the measured values L and U_o are normally distributed for each pair of data sets.

From Eqs. 5.1 and 5.8, the transmittance τ and the path radiance P are expressed as

$$\tau=a \qquad p=b \quad . \qquad 5.9$$

Figs. 5.2, 5.3, and 5.4 show the relationships between the radiance detected by LANDSAT and the radiance at the water surface. The calculated coefficients of correlation are listed in Table 5.2 and the derived transmittance and path radiance are summarized in Table 5.3. As can be seen from Figs. 5.2, 5.3 and 5.4, all the computed values of the sample correlation coefficients (r) are larger than the 95% level of confidence critical values (r_c), 0.60, 0.55, and 0.58 for the 24 Nov. 1981, 3 Mar. 1982, and 24 Oct. 1983 experiments respectively. Therefore, the hypothesis that each pair of data sets are independent of each other should be rejected.

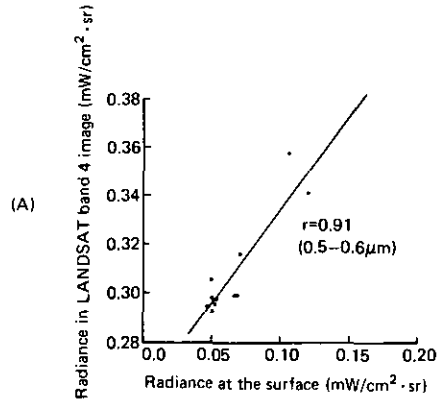

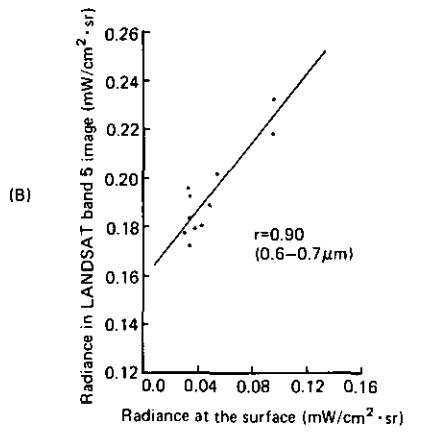

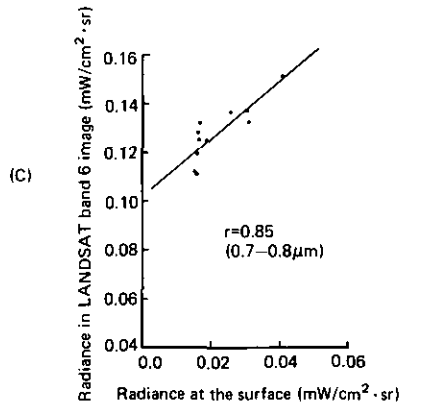

Fig. 5.2 Relation between radiance detected by LANDSAT and upwelling radiance at water surface (24 Nov. 1981).
(A): Band 4. (B): Band 5. (C): Band 6.

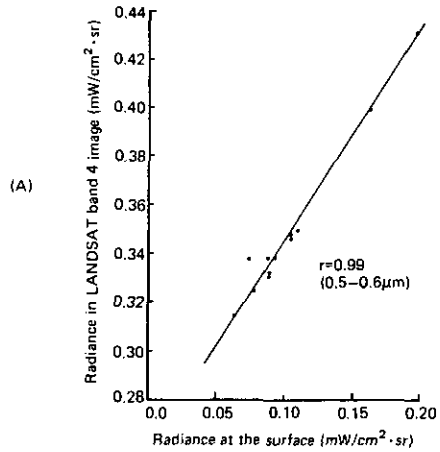

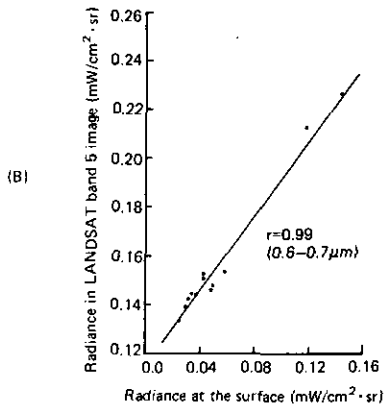

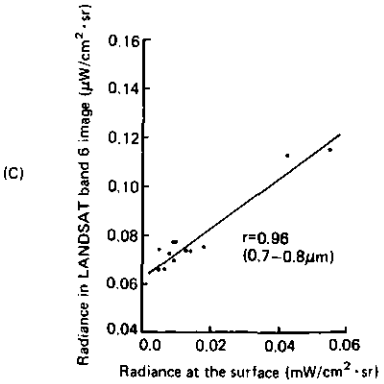

Fig. 5.3 Relation between radiance detected by LANDSAT and upwelling radiance at water surface (3 Mar. 1982).
(A): Band 4. (B): Band 5. (C): Band 6.

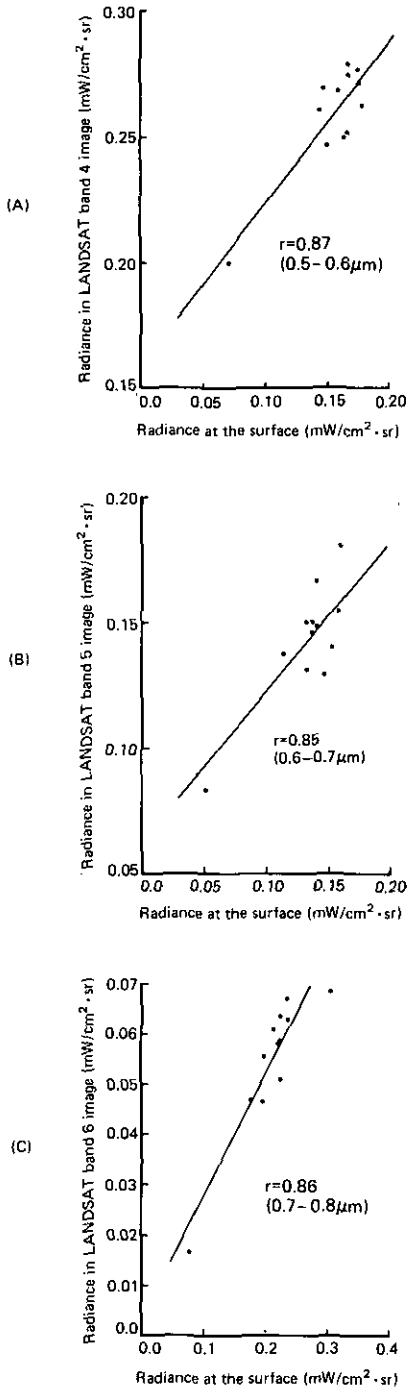

Fig. 5.4 Relation between radiance detected by LANDSAT and upwelling radiance at water surface (25 Oct. 1983).
(A): Band 4. (B): Band 5. (C): Band 6.

Table 5.3 Estimated transmittance and path radiance.

	24 Nov. 1981		3 Mar. 1982		25 Oct. 1983	
	a	b ($mW/cm^2 \cdot sr$)	a	b ($mW/cm^2 \cdot sr$)	a	b ($mW/cm^2 \cdot sr$)
Band 4	0.77(±0.27)	0.26(±0.02)	0.86(±0.10)	0.26(±0.01)	0.65(±0.26)	0.16(±0.04)
Band 5	0.72(±0.26)	0.16(±0.01)	0.78(±0.08)	0.11(±0.01)	0.60(±0.27)	0.06(±0.04)
Band 6	1.17(±0.56)	0.10(±0.01)	1.01(±0.21)	0.06(±0.01)	0.48(±0.20)	0.02(±0.02)

5.3 ESTIMATING THE RADIANCE REFLECTANCE OF THE WATER SURFACE FROM LANDSAT DATA

From Eqs 5.5 and 5.9 the radiance reflectance at water surface of the lake can be expressed as

$$R_o = \frac{L - b}{a \cdot \pi \cdot \rho \cdot W} \quad . \qquad 5.10$$

Using this equation, the distribution of radiance reflectance R_o is calculated from the LANDSAT data in this section. For the value of the radiance W reflected by a white reflector, the value W^N measured at the time of LANDSAT overpass was used, and the reflectivity ρ of the white reflector was assumed to be 1.0. On the other hand, the calculated values at the ground truth point 6, for example, on 3 Mar. 1982 from LANDSAT band 6 gave the value: a=0.78, b=0.11 ($mW/cm^2 \cdot sr$), L=0.13 ($mW/cm^2 \cdot sr$), W=2.66 ($mW/cm^2 \cdot sr$), and R_o=0.31 (%/sr).

Figs. 5.5 to 5.7 show the original uncorrected LANDSAT band 5 images and the estimated distribution of radiance reflectance from water surface of Lake Kasumigaura. In Figs. 5.5 (B), 5.6 (B), and 5.7 (B), the radiance reflectance range from 0 to 30 (%/sr) is represented by 127 color levels. These images give much clearer detail than the original images because path radiance has been eliminated.

(A)

(B)

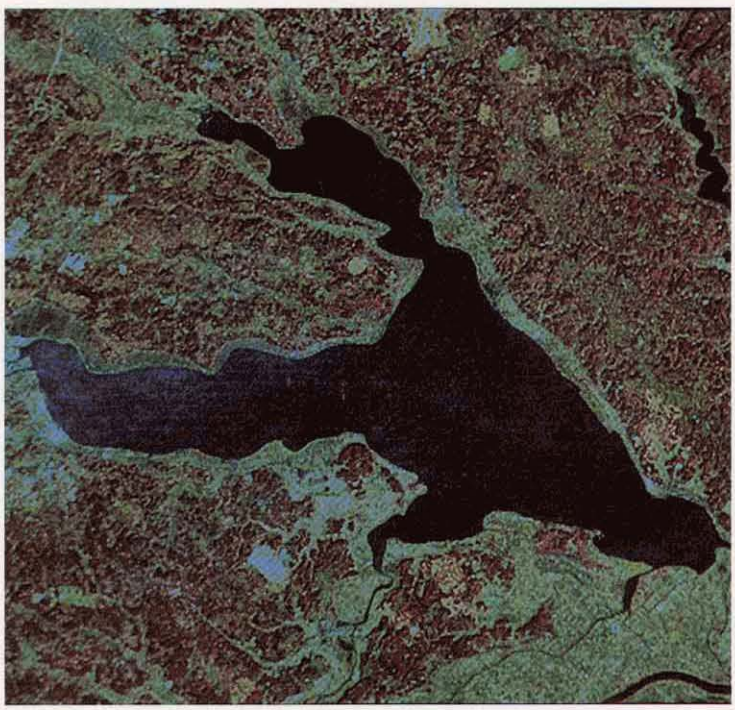

Fig. 5.5 Distribution of radiance reflectance (24 Nov. 1981). (A): Original image from LANDSAT MSS band 5. (B): Estimated pattern of radiance reflectance at water surface.

(A)

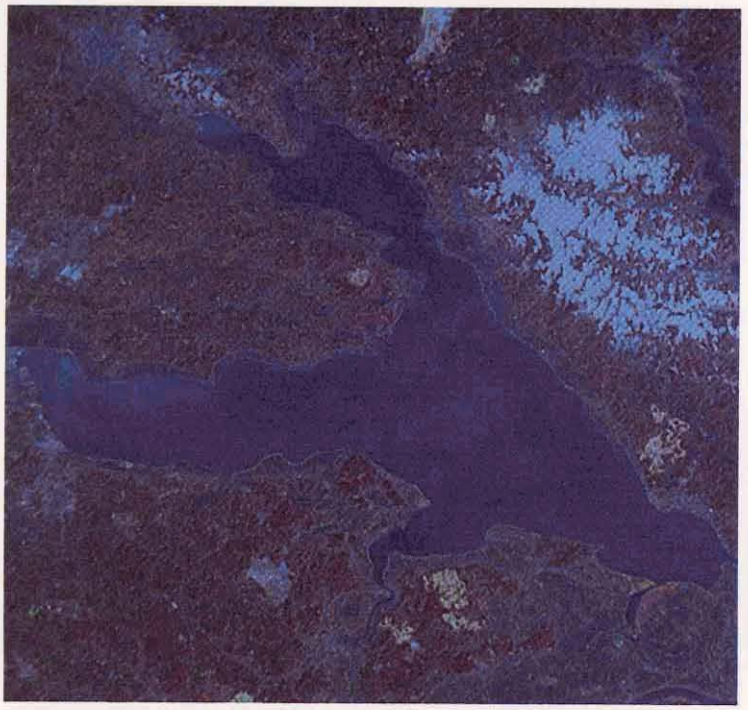

(B)

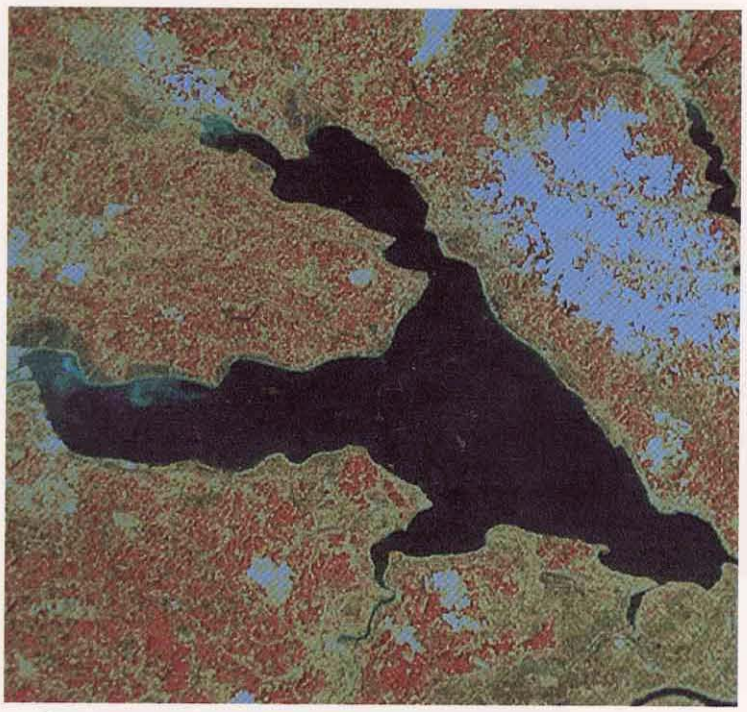

Fig. 5.6 Distribution of radiance reflectance (3 Mar. 1982). (A): Original image from LANDSAT MSS band 5. (B): Estimated pattern of radiance reflectance at water surface.

(A)

(B)

Fig. 5.7 Distribution of radiance reflectance (25 Oct. 1983). (A): Original image from LANDSAT MSS band 5. (B): Estimated pattern of radiance reflectance at water surface.

5.4 ESTIMATING THE WATER QUALITY DISTRIBUTION BY THE RADIANCE REFLECTANCE

In the previous chapter, the distribution of water quality in Lake Kasumigaura was estimated from linear regressions between the water quality parameters and the LANDSAT CCT count corresponding to the point where the water quality parameters were actually measured on the lake. The Secchi depth transparency and the concentration of suspended solids are well estimated from LANDSAT band 4, 5, and 6 data. However, the regression medels developed are not independent of the weather conditions such as clouds, haze or humidity occuring on the date of observation. Therefore, ground truth measurements were required for calibrating the models for quantitative water quality measurement.

In this section, we present a similar linear regression between the water quality parameters and the radiance reflectance derived from the original LANDSAT data.

Table 5.4 shows the coefficients of correlation obtained by linear regression. The underscored values are statistically significant at the 5% level. Compared to the results presented in Table 4.4, the coefficients of correlation for transparency and for concentration of suspended solids have improved, especially in the band 5 and 6 for the date 24 Nov. 1981. This means that using the radiance reflectance from which has been eliminated the effect of the atmosphere, one is better able to estimate water quality. The model derived by this analysis is shown in Fig. 5.8. The regression lines for each of the three wavelength bands have been plotted separately in Figs. 4.2 to

Table 5.4 Coefficients of correlation between water quality parameters and radiance reflectance at water surface calculated from LANDSAT CCT count.

Date	24 Nov. 1981			3 Mar. 1982			25 Oct. 1983		
LANDSAT band	4	5	6	4	5	6	4	5	6
Transparency	−0.79	−0.85	−0.95	−0.95	−0.97	−0.96	−0.90	−0.93	−0.97
Suspended solids	0.67	0.77	0.92	0.92	0.96	0.94	0.73	0.76	0.94
Chlorophyll-*a*	−0.44	−0.48	−0.35	−0.34	−0.30	−0.36	−0.24	−0.37	−0.20
No. of ground truth point	11			13			12		
LANDSAT	L-2			L-3			L-4		

Underscored values are statistically significant at the 5% level.

4.4, where it can be seen that each of the three regression lined have a different y-intercept and slope. On the other hand, in Fig. 5.8, the three regression lines can be seen to be much more nearly equivalent in their y-intercept and slope. To determine the degree to which the regression lines are equivalent, the statistical t test (Kawabata, 1982) was applied to the difference between the slopes and between the y-intercepts. This statistical test for comparing three regression models showed that under the 95% confidence condition, the slope of the lines for the 24 Nov. 1981 and

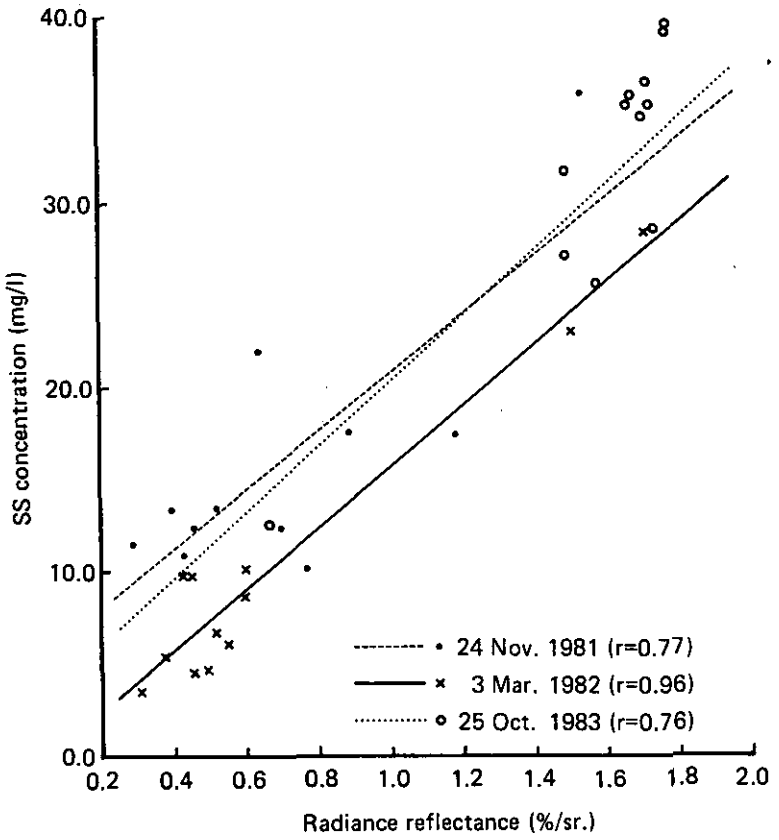

Fig. 5.8 Relation between concentration of suspended solids and radiance reflectance derived form LANDSAT data.

the 3 Mar. 1982 experiment is equivalent and the y-intercept of the lines for the 3 Mar. 1982 and the 25 Oct. 1983 experiment is equivalent. Therefore, three regression lines can be represented by one linear regression line. This simple relation can, then, be considered to be a generalized model for measuring the water quality of Lake Kasumigaura.

Maps for the distribution of suspended solids derived using these models are shown in Fig. 5.9.

(A)

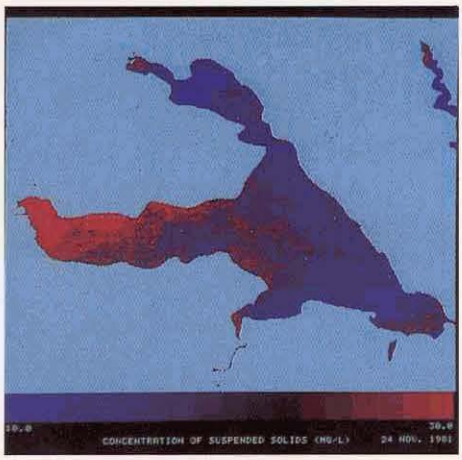

(B)

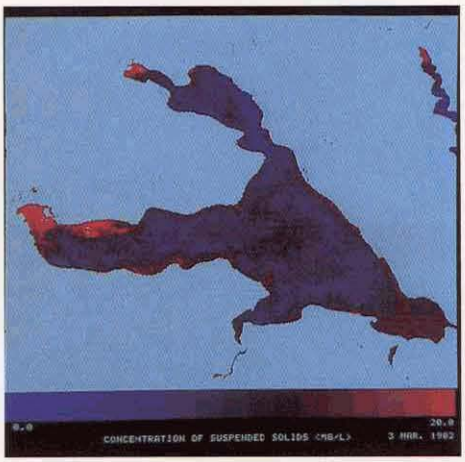

(C)

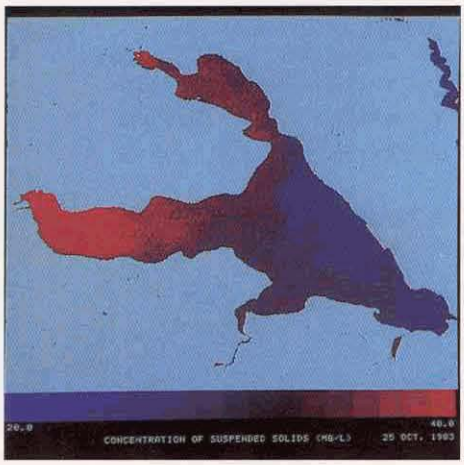

Fig. 5.9 Estimated distribution map of suspended solids.
(A): 10-30mg/l (24 Nov. 1981). (B): 0-20mg/l (3 Mar. 1982). (C): 20-40mg/l (25 Oct. 1983).

5.5 CONCLUSIONS

Effects such as the transmittance and the path radiance of the atmosphere have been estimated by a linear regression analysis between the radiance at the water surface and the radiance detected by LANDSAT. With values, the radiance reflectance at the water surface has been deduced from LANDAST MSS data. The derived distribution of the radiance reflectance gives much clearer detail than the original LANDSAT images. Models for estimating water quality (transparency and concentration of suspended solids) were developed by regression analysis between the water quality and the radiance reflectance. Finally, distribution maps for the concentration of suspended solids in Lake Kasumigaura were presented.

The correlation coefficients derived in Chapter 5 after making correction for the effects of the atmosphere, were much improved over those obtained in Chapter 4 where no correction for the atmosphere was applied. The values of the correlation coefficient increased, especially for the measurements made on 24 Nov. 1981. Since this was a very hazy day at the time of LANDSAT overpass, rather low correlation coefficients were expected. This result suggests that the atmospheric effects were eliminated by using the derived value of radiance reflectance instead of the original LANDSAT CCT data.

The regression models shown in Fig. 5.8. were statistically nearly equivalent to one another in slope and y-intercept. Therefore, there seems to be a possibility of developing models for measuring the water qualitity in Lake Kasumigaura which are independent of the date or season. It is also suggested that one regression medel for estimating the water quality can be formed by the whole data set of the water quality and the radiance reflectance at the water surface of the three Kasumigaura experiments.

CHAPTER 6

Discussions and conclusions

Measuring water quality by LANDSAT remote sensing was described in this report.

In remorte sensing, electromagnetic energy acts as a link between surface features of the earth and the remotely separated sensor. Therefore, it is essential to study the characteristics of the electromagnetic energy reflected by the object of interest. A high-speed spectroradiometer was developed to study the relationships between spectral reflectance and the surface features. The spectroradiometer operates in a wavelength range of 400 to 850 nm with a resolution of 2 nm, and its scanning cycle is approximately one second. Laboratory and field measurements with this instrument showed the appropriate accuracy and the speed of operation was especially well suited for measuring a shifting and changing surface such as water.

To investigate the relationships between various water quality parameters and upwelling radiance from the water surface, an experiment was carried out at Lake Kasumigaura on 25 Nov. 1983. The water quality parameters were measured, and at the same time, the upwelling radiance at the water surface and underwater were measured with this spectroradiometer. From the radiance measured underwater, the extinction coefficient of the lake water and the radiance just above water surface were calculated. The regression analysis between the water quality and the radiance at or just above the water surface showed signficant correlation between Secchi depth transparency or concentration of suspended solids and these radiances. However, there were no differences detected between the radiance at the water surface and just above the water surface, thus showing that reflection at the water surface need not be considered. Secchi depth transparency and concentration of suspended solids were well estimated in the wavelength range of 500 to 800 nm.

Water quality models were developed for three different weather coditions by use of regression analysis betwees the water quality parameters and the LANDSAT CCT count. The medels showed good ability to estimate Secchi depth transparency and concentration of suspended solids from the data of LANDSAT band 4, 5, and 6. However, there was a difference between the model derived for a clear day and for a hazy day. Therefore some correction of the LANDSAT data for atmospheric effcts was required to develop a water quality model which would be independent of the weather conditions.

In order to estimate the atmospheric effects on the LANDSAT MSS data, the transmittance and the path radiance of the atmosphere were estimated using a linear regression between the radiance detected by LANDSAT MSS and the radiance at water surface. The LANDSAT MSS data were converted from CCT count to absolute radiance data using the sensitivity parameters of the sensor given by the Eq. 5.6. The radiance reflectance at the water surface was defined by the Eq. 5.10 and the distribution of the radiance reflectance was calculated from the estimated transmittance and path radiance, and radiance detected by LANDSAT MSS. The

results showed that the distribution maps for radiance reflectance appeared to be clearer in detail than the images from the original LANDSAT data. This was the evidence that the path radiance had been successfully eliminated from the LANDSAT MSS data.

The derived radiance reflectance of the water surface was correlated with various water quality parameters to formulate models for estimating the water quality independently of the effects of the atmosphere on the remotely sensed data. Distribution maps for suspended solids for three different days and weather conditions were presented. The resultant maps agreed well with the actual characteristics of the water of Lake Kasumigaura.

A series of similar remote sensing experiments were performed on Lake Kasumigaura during the years 1979 to 1981 (Yasuoka & Miyazaki 1979, 1982 a, 1982 b). The correlation coefficients derived between water quality parameters and LANDSAT MSS data are listed in Table 6.1. The water quality parameters were not always well correlated with LANDSAT MSS data. On 20 Feb. 1979 and 13 Aug. 1980, the Secchi depth transparency and the concentration of suspended solids were well estimated from LANDSAT MSS data, while the concentration of suspended solids could not be estimated from the data for 14 Dec. 1979, 19 Jan. 1980, and 6 Feb. 1980. This showed that the models derived for estimating water quality parameters varied with the weather condtions or the season of the year. In order to develop generalized models which are independent of the weather conditions, some correction of the LANDSAT MSS data for the effects of the atmosphere are definitely necessary.

Table 6.1 Coefficients of correlation between water quality parameters and LANDSAT CCT count obtained from previous experiments at Lake Kasumigaura.

Date	20 Feb. 1979			14 Dec. 1979			19 Jan. 1980			6 Feb. 1980		
LANDSAT band	4	5	6	4	5	6	4	5	6	4	5	6
Transparency	−0.93	−0.94	−0.95	−0.00	−0.19	−0.53	−0.39	−0.64	−0.90	−0.30	−0.13	−0.71
Suspended solids	0.91	0.89	0.90	0.18	0.18	0.23	−0.17	0.33	0.49	−0.01	0.01	0.04
Chlorophyll-*a*	−0.10	−0.15	−0.06	−0.52	−0.47	−0.04	−0.21	0.08	0.59	−0.24	−0.40	−0.12
COD	−0.14	−0.42	−0.42	—	—	—	—	—	—	−0.57	−0.54	−0.31
Ground truth point	15			10			10			16		
LANDSAT	2			3			3			3		

Date	13 Aug. 1980			17 Dec. 1980			22 Jan. 1981		
LANDSAT band	4	5	6	4	5	6	4	5	6
Transparency	−0.86	−0.88	−0.95	−0.40	−0.60	−0.71	−0.42	−0.64	−0.44
Suspended solids	0.77	0.81	0.95	0.70	0.72	0.74	0.39	0.61	−0.41
Chlorophyll-*a*	0.72	0.72	0.90	−0.07	−0.12	−0.19	0.27	0.42	0.30
COD	—	—	—	0.21	−0.01	0.31	−0.19	0.33	0.38
Ground truth point	22			22			15		
LANDSAT	2			2			2		

Underscored values are statistically significant at the 5% level.

In this report, the models developed by correcting LANDSAT data for the atmosphere gave a similar slope and y-intercept for varied conditions (see Fig. 5.8). This suggested that there is a possibility of developing generalized models for measuring water quality from LANDSAT data. However, this requires that one measures the upwelling radiance of water surface at the time of LANDSAT overpass in order to estimate the transmittance and the path radiance of the atmosphere. This would require special instrumentation to measure the surface radiance.

The final goal of this study is to formulate a single model to estimate the water quality parameters of Lake Kasumigaura by LANDSAT data without any ground truth measurements. The data for visibility in the Lake Kasumigaura area provided by a local meteorological station may possibly be used for calculating transmittance and path radiance or some simulation models for calculating transmittance and path radiance, for example LOWTRAN 5 (Kneizys *et al.* 1980) may possibly be used. These methods, which were neither described nor used in this report, may be an alternative way to measure radiance at ground truth points. Finally, a series of additional studies are needed at various seasons of the year and under various weather conditions in order to develop generalized models for water quality estimation which are applicable to Lake Kasumigaura all year round. The latest LANDSAT-5 satellite carries a Thematic Mapper (TM) with 30-meter resolution and with six visible and infrared bands each having a narrower range than the four MSS bands. It also has one thermal band. In the future, from the LANDSAT TM data we may be able to get better results for chlorophyll detection due to the increased spatial (from 80 to 30 meter), spectral (from 4 to 7 bands), and radiometric (from 7 to 8 bit) resolution of the data.

ACKNOWLEDGMENTS

The author wishes to acknowledge partial financial support from the Special Research Project on Environmental Science, Grant-in-Aid for Scientific Research, Ministry of Education.

I also wish to acknowledge Dr. Y. Yasuoka for many useful discussions and guidance as well as practical assistance in these experiments, Dr. H. Shimizu for his efficient help in the development of the spectroradiometer, Dr. M. Watanabe for assistance in the Microcosm experiments, and Mr. N. Okami, Mr. M. Kishino and Dr. S. Sugihara for fruitful discussions and field support.

The LANDSAT MSS data used were distributed by the National Space Development Agency of Japan.

References

Abiodun, A. A. (1976): Satellite survey of paticulate distribution patterns in Lake Kainji. Remote Sensing Environ., **5**, 106-123.

Abiodun, A. A. and H. A. Adeniji (1978): Movement of water columns in lake Kainji. Memote Sensing Environ., **7**, 227-234.

Adams, M. J., G. J. Ewen and R. V. Birnie (1985): A portable two-band radiometer. Int. J. Remote Sensing, **6**, 963-966.

Aranuvachapun, S. and R. I. Perry (1981): Spectral variations of coastal water irradiance as a measure of phytoplankton pigments. Int. J. Remote Sensing, **2**, 199-312.

Austin, R. W. (1974): Remote sensing of spectral radiance on optical aspects of oceanography. N.G. Jerlor and E. Steeman, (*Eds.*), Neilsen, Academic Press, London and New York.

Booth, C. R. and P. Dustan (1979): Diver-operable multiwavelength radiometer. Soc. Photo. Instr. Eng., **196**, 33-39.

Bowker, D. (1973): Correlation of ERTS multispectral imagery with suspended matter and chlorophyll in lower Chesapeake Bay. Symp. Significant Results Obtained from ERTS-1, NASA, 1291-1298.

Bukata, R. P., J. E. Bruton and J. H. Jerome (1983): Use of chromaticity in remote measurements of water quality. Remote Sensing Environ., **13**, 166-177.

Burr, A. H. and M. J. Duncan (1972): Portable spectroradimeter for underwater environments. Limnol. Oceanogr., **17**,466-475.

Caraux, D. and R. W. Austin (1983): Delineation of seasonal changes of chlorophyll frontal boundaries in Mediterranean coastal waters with Nimbus-7 Coastal-Zone Color Scanner data. Remote Sensing Environ., **13**, 239-249.

Carlson, R. E. (1977): A trophic state index for lakes. Limnol. Oceanogr., **22**, 361-369.

Carpenter, D. J. and S. M. Carpenter (1983): Modeling inland water quality using LANDSAT data. Remote Sensing Environ., **13**, 345-352.

Charnell, R. L. and G. A. Maul (1973): Oceanic obsevation of New York Bight by ERTS-1. Nature, **242**, (5398), 451-452.

Chiu, H. -Y. and W. Collins (1978): A spectroradiometer for airborne remote sensing. Photogramm. Eng. Remote Sensing, **44**, 507-517.

Clarke, G. L., G. C. Ewing and C. J. Lorenzen (1969): Remote measurement of ocean color as an index of biological productivity. Proc. of the 6th Remote Sensing Conf., Univ. of Michigan.

Clarke, G. L., G.C. Ewing and C. J. Lorenzen (1970): Spectra of backscattered light from sea obtained from aircraft as a measurement of chlorophyll concentration. Science, **67**, 1119-1121.

Dave, J. V. (1978): Extensive datasets of the diffuse radiaion in realistic atmospheric models with aerosols and common absorbing gases. Solar Energy, **21**, 361-370.

Doda, D. D. and A. E. S. Green (1978): Spectral sunphotometry using a compact spectrometer. Remote Sensing Environ., **7**, 97-104.

Duntley, S. Q. (1960): The visibility of submerged objects. Cambridge Press, London.

Duntley, S. Q. (1973): Measuring earth-to-space contrast transmittance from ground stations. Appl. Opt., **12**, 1317-1324.

Finley R. J. and R. W. Baumgardner Jr. (1980): Interpretation of surface-water circulation,

Aransas Press, Texas, using LANDSAT imagery. Remote Sensing Environ., **10**, 3-22.
Fraser, R. S., O. P. Bahethi and A. H. Al-Abbas (1977): The effect of the atmosphere on the classification of satellite observations to identity surface features. Remote Sensing Environ., **6**, 229-249.
Gordon, H. R. (1978): Removal of atmospheric effects from satellite imagery of oceans. Appl. Opt., **17**, 1631-1636.
Gordon, H. R., O. B. Brown and M. M. Jacobs (1975): Computed relationships between the inherent and apparent optical properties of a flat homogeneous ocean. Appl. Opt., **14**, 417-427.
Gordon,H. R., D. K. Clark, J. L. Mueller and W. A. Hovis (1980): Phytoplankton pigments from the Nimbus-7 Coastal Zone Color Scanner: Comparisons with surface measurements. Science, **210**, 63-66.
Gordon, H. R., D. K. Clark, J. W. Brown, O. B. Brown, R. H. Evans and W. W. Broenkow (1983): Phytoplankton pigment concentrations in the Middle Atlantic Bight: comparison of ship determinations and CZCS estimates. Appl. Opt., **22**, 20-36.
Gorden, J. I., J. L. Harris Jr. and S. Q. Duntley (1973): Measuring earth-to-space contrast transmittance from ground stations. Appl. Opt., **12**, 1317-1325.
Gower, J. F. R., S. Lim and G. A. Borstad (1984): The information content of different optical spectral ranges for remote chlorophyll estimation in coastal waters. Int. J. Remote Sensing, **5**, 349-364.
Grum. F. and G. W. Luckey (1968): Optical sphere paint and a working standard of reflectance. Appl. Opt., **7**, 2289-2294.
Johnson, R.W. (1975): Quantitative sediment mapping from remotely sensed multispectral data. Proc. of the 4th Annual Remote Sensing of Earth Resources Conf., Tullahoma, Tenn. 565-576.
Johnson R. W. and D. R. Norris (1977): A multispectral analysis of the interface between the Brazil and Folkland Current from Skylab. Remote Sensing Environ., **6**, 271-288.
Kawabata, K. (1982): Regression and correlation. Handbook of applied statistics. T. Okuno, *(Ed.)*, Youkendou, Tokyo, (in Japanese).
Khorram, S. (1981): Use of ocean color scanner data in water quality mapping. Photogramm. Eng. Remote Sensing, **47**, 667-676.
Khorram, S. (1985): Development of water quality models applicable throughout the entire San Francisco Bay and Delta. Photogramm. Eng. Remote Sensing, **51**, 53-62.
Khorram, S. and H. M. Cheshire (1985): Remote sensing of water quality in the Neuse River Estuary, North Carolina. Photogamm. Eng. Remote Sensing, **51**, 329-341.
Kishino, M., C. R. Booth and N. Okami (1984): Under water radiant energy absorbed by phytoplankton, detritus, disslved organic matter, and pure water. Limnol. Oceanogr., **29**, 340-349.
Klemas, V. (1973): Applicability of ERTS-1 imagery to the study of suspended sediment and aquatic fronts. Symp. Signficant Results Obtained from ERTS-1, NASA, 615-624.
Klemas,V. (1980): Remote sensing of coastal fronts and thier effects on oil dispersion. Int. J. Remote Sensing, **1**, 11-29.
Klemas, V., J. F. Borchardt and W. M. Tresure (1973): Suspended sediment observations from ERTS-1. Remote Sensing Environ., **2**, 205-223.
Klemas, v., M. Otley, M. Philpot, C. Wethe and R. Rogers (1974a): Correlation of coastal water turbidity and circulation with ERTS-1 and Skylab imagery. Proc. of the 9th Int. Symp. Remote Sensing Environ., Environmental Research Institute of Michigan, Ann Arbor, Mich.

Klemas, V., D. Bartlett, W. Philpot, R. Rogers and L. Reed (1974 b): Coastal and estuarine studies with ERTS-1 and Skylab. Remote Sensing Environ., **3**, 153-174.

Klemas, V. and D. F. Polis (1977): A study of density fronts and their effects on coastal pollutants. Remote Sensing Environ., **6**, 95-126.

Kneizys, F. X., E. P. Shettle, W. O. Gallery, J. H. Chetwynd Jr., L. W. Abrew, J. E.A. Selby, R.W. Fenn and R. A. McClatchey (1980): Atmospheric transmittance/radiance: Computer code LOWTRAN 5. AFGL-TR-80-0067, Environmental Research Paper, No. 697, Optical Physics Division, Project 7670, Air Force Geophysics Laboratory.

Kritikos, H., L. Yorinks and H. Smith (1974): Suspended solids analysis using ERTS-1 data. Remote Sensing Environ., **3**, 69-78.

Lillesand, T.M., W. L. Johnson, R. L. Devell, O.M. Lindstrom and D. E. Meisner (1983): Use of LANDSAT data to predict the trophic state of Minnesota lakes. Photogramm. Eng. Remote Sensing, **49**, 219-229.

Lowe, D.S., J.G. Braithwaite and V.L. Larrowe (1966): An investigative study of spectrum-matching system. Report No. 8201-1-F, Institute of Science and Technology, Univ. Michigan, Ann Arbor, Mich.

MacFarlane, N. and I. S. Robinson (1984): Atmospheric correction of LANDSAT MSS data for a multidate suspended sediment algorithm. Int. J. Remote Sensing, **5**, 561-676.

Maul, G. A. and H. R. Gordon (1975): On the use of the earth reasources technolgy satellite (LANDSAT-1) in optical oceanography. Remote Sensing Environ., **4**, 95-128.

McKim, H. L., J. C. Merry and R. W. Layman (1984): Water quality monitoring using an airborne spectroradiometer. Photogramm. Eng. Remote Sensing, **50**, 353-360.

Miller, J. R., G. G. Shepherd and R. A. Koehler (1971): A four channel scanning photometer for remote sensing. Can. Aeronaut. Space J., **18**, 325-330.

Milton, G. J. (1980): A portable multiband radiometer for ground data collection in remote sensing. Int. J. Remote Sensing, **1**, 153-165.

Miyazaki, T., H. Shimizu and Y. Yasuoka (1981): High-speed spectroradiometer. Basic Research on Environmental Information Collection by Remote Sensing, Res. Rep. Special Research Project on Environmental Science, Ministly of Education, Culture and Science, Japan, 3-14, (in Japanese).

Miyazaki, T. and M. Watanabe (1984): Measurement of underwater irradiance of Microcosm by underwater spectroradiometer. Preprint of the 10th Remote Sensing Symposium, Tokyo, 159-160, (in Japanese).

Miyrabø, H. K., O. Lillesæten and T. Høimyr (1982): Portable field spectrometer for reflectance measurements 340-2500 nm. Appl. Opt., **21**, 2855-2858.

Mueller, J. L. (1972): Remote measurement of chlorophyll concentration and Secchi-depth using the principal components of the ocean's color spectrum. 4 th Annual Earth Resources Program Review, NASA Manned Spacecraft Center, Huston, Texas, 4, 105, 1-13.

Munday, J. C. and T. T. Alfoldi (1979): LANDSAT test of diffuse reflectance models for aquatic suspended solid measurement. Remote Sensing Environ., 8,169-183.

NASA (1971): ERTS data user handbook. Document No. 71SD4249, Washington D.C.

Okami, N., M. Kishino and T. Miyazaki (1982): Correlation studies between spectral radiance reflectance and water qualities in Lake Kasumigaura. J. Remote Sensing Soc. Jpn, **2**, 21-31, (in Japanese).

O'Neill, N. T., J. R. Miller and F. J. Ahern (1978): Radiative transfer calculations for remote sensing applications. Proc. of the 5th Canadian Symp. Remote Sensing, 572-576.

Onitsuka, M., K. Ohta, N. Okami and J. R. Miller (1981): An approach to path radiance

correction in MSS images. Proc. of the 15th Int. Symp. Remote Sensing Environ., Environmental Research Institute of Michigan, Ann Abor, Mich., 681-689.

Polcyn, F.C. (1967): Investigations of spectrum-matching sensing in agriculture. Report No. 6590-7-P, Institute of Science and Technology, Univ. Michigan, Ann Arbor,Mich.

Polcyn, F.C. (1972): Modern approach to coastal zone survey. Tools for Coastal Zone Management, 41-57, Washington D.C.

Polcyn, F. C. and C. T. Wezernak (1970): Pollution surveillance and data acquistion using multispectral remote sensing. Water Resources Bull., J. Am. Water Res. Assoc., **6**, 920-934.

Rouse, L. J. and J. M. Coleman (1976): Circulation observation in the Louisiana Bight using LANDSAT imagery. Remote Sensing Enliron., **5**, 55-66.

Raggles, R. (1973): Plume development in Long Island Sound observed by remote sensing. Symp. Significant Results Obtained from ERTS-1, NASA, 1299-1304.

Rogers, R. H., K. Peacock and N. J. Shah (1973): A technique for correcting ERTS data for solar and atmospheric effects. Paper 1-7, 3rd ERTS Symposium, Washington D. C.

Schuburt, J. (1973): Digital analysis of Potomac River Basin ERTS-1 imagery. Symp. Significant Results Obtained from ERTS-1, NASA, 659-664.

Smith, R. E., A. A. Green, G. Robinson and F.R. Honey (1978): Use of LANDSAT-1 imagery in exploration for Keweenawan-type copper deposits. Remote Sensing Environ., **7**, 129-144.

Snedecor, G.W. and W.G. Cochran (1980): Statistical methods.The Iowa State University Press, Ames, Iowa, USA.

Strong, A. E. (1978): Chemical whiting and chlorophyll distribution in the Grate Lakes as viewed by LANDSAT. Remote Sensing Environ. **7**, 61-72.

Strong, A. E., H. G. Stumpf, J. L. Hart and J. A. Pritchard (1974): Extensive summer upwelling on Lake Michigan during 1973 observed by NOAA-2 and ERTS-1 satellites. Proc. of the 9th Int. Symp. Remote Sensing Environ., Environmental Research Institute of Michigan, Ann Arbor, Mich., 923-932.

Sturm, B. (1981): Atmospheric correction of remotely sensed data and quantitative determination of suspended sediment in marine water bodies. In Remote Sensing in Meteorology, Oceanography, and Hydrology, A. P. Cracknell *(Ed.)*, Chichester, Ellis Horwood.

Sturm, B. (1983): Selected topics of CZCS data evaluation. In Remote Sensing Application in Marine Science and Technology, A. P. Cracknell *(Ed.)*, Dordrecht Reidel.

Szekielda, K. H. (1973): Proc. Amer. Soc. Photogramm., Fall Convention, Part II, Falls Church, Va., 667-719.

Suits, G. (1973): Preliminary results of water reflectance calculations using AQUACAN. Environmental Research Institute of Michigan Memo.

Thomas, I. L. (1980): Suspended sediment dynamics from repetitve LANDSAT data. Int. J. Remote Sensing, **1**, 285-292.

Thomson, K. P. B., C. Pare and M. D. Roy (1975): Digital analysis of multispectral satellite data applied to lake surveillance problem in large hydro electric development. 3rd Canadian Symp. Remote Sensing, Edmonton, Alberta.

Turner, R. E. and M. M. Spencer (1972): Atmospheric model for correcting the spacecraft data. Proc. of the 8th Int. Symp. Remote Sensing Environ. Environmental Research Institute of Michigan, Ann Arbor, Mich., 895-934.

Verdin, J. P. (1985): Monitoring water quality conditions in a large western reservoir with LANDSAT imagery. Photogramm. Eng. Remote Sensing, **51**, 343-353.

Viollier, M., P. Y. Deschamps and P. Lecomte (1978): Airborne remote sensing of chlorophyll content under cloudy sky as applied to the tropical water in the Gulf of Guinea. Remote Sensing Environ., **7**, 235-248.

Viollier, M., D. Tanrē and P. Y. Deschamps (1980): An algorithm for remote sensing of water color from space. Baundary-Layer Meteorol., **18**, 147-267.

Wezernak, C. (1973): Monitoring ocean dumping with ERTS-1 data. Symp. Significant Results Obtained from ERTS-1, NASA, 635-642.

Williams, J. (1970): Optical properties of the sea. U. S. Naval Institute, Annapolis, 39.

Williamson, A. N. and W. E. Graban (1973): Sediment concentration mapping in tidal estuaries. 3rd ERTS-1 Symp. Washington D. C.

Yarger, H.L. (1973): Water turbidity detection using ERTS-1 imagery. Symp. Significant Results Obtained from ERTS-1, NASA, 651-658.

Yarger, H. L., R. McCauley, G. W. James and L. M. Magnuson (1973): Quantitative water quality with ERTS-1. Proc. of the 3rd. ERTS-1 Sympos. 1(B) 1637-1652, Goddard Space Flight Center, Maryland.

Yasuoka, Y. and T. Miyazaki (1979): Classification of water quality characteristics by remote sensing. Preprint of the 5th Remote Sensing Symp., Tokyo, 103-106, (in Japanese).

Yasuoka, Y. and T. Miyazaki (1982 a): Assessment and evaluation of water quality by remote sensing. Research Report in Researches Related to the UNESCO's Man and the Bioshere Program in Japan, 14-9 (5-9), 171-176.

Yasuoka, Y. and T. Miyazaki (1982 b): Evaluation of quantitave water quality measurement by remote sensing. Preprint of the 8th Remote Sensing Symp., Tokyo, 9-12, (in Japanese).

Yasuoka, Y. and T. Miyazaki (1982 c): Remote sensing of water quality in the lake -Atmospheric correction and water quality estimation by regression analysis-. J. Remote Sensing Soc. of Japan, **2**, 51-62, (in Japanease).

Yost, E, R. Hollman, J. Alexander, and R. Nuzzi (1973): An interdisciplinary study of the estuarine and coastal oceanography of Block Island Sound and adjacent New York coastal waters. Proc of the 3rd. ERTS-1 Symp. 1(B) 1607-1618, Goddard Space Flight Center, Maryland.

LANDSAT リモートセンシングによる霞ヶ浦の水質計測

宮崎 忠国[1]

本研究は人工衛星(LANDSAT)リモートセンシングを利用した霞ヶ浦湖水の水質計測手法の開発について述べたものである。

リモートセンシングは人工衛星や航空機を利用して上空から地表の物質の種類や状態を知る技術である。地表の物質はその種類や状態により固有の電磁波の反射特性を持っているため，対象物の反射特性を計測することによってその物質の種類や状態を知ることが出来る。リモートセンシングでは計測対象物質の量や状態とその物質の反射特性との間の関係を知ることが最も大切である。このため，リモートセンシングにおける基礎データの収集を目的として高速ラジオスペクトロメータの開発を行った。この高速ラジオスペクトロメータは，分光部にグレーティングを，光検知部に光電子増倍管を利用し，波長分解能 2nm で，400 から 850nm の波長範囲を 1 秒間で測定する。フィールドや実験室内での測定結果から，本装置はリモートセンシング実験の光学的基礎データの収集，特に水のような動きの速い対象物の光学的データの収集に最適であることが判明した。本装置を利用して，霞ヶ浦湖水の分光特性を計測した結果，水面直上の上方向放射輝度と浮遊懸濁物(SS)の量は波長領域 500～800nm で良い相関があることが判明し，リモートセンシングによる SS の定量的計測の可能性が示された。しかし，クロロフィル-a に関しては，良い結果は得られなかった。次に，LANDSAT により得られたデータと水質の関係を調べ，定量的水質計測のための統計モデルの作成を行った。この結果，透明度と SS の量は LANDSAT バンド 4，5 及び 6 で計測可能であるという結果を得た。さらに，定量的水質計測に大きな影響を及ぼす大気散乱光についてその影響の評価を行った。LANDSAT データと水面で測定した分光反射輝度データから大気の散乱光と透過率を推定し，得られた大気散乱光と透過率を用いて LANDSAT データの大気補正を行った。大気補正された LANDSAT 画像は原画像に比べて画像が細部で鮮明となった。また大気補正された LANDSAT データによる水質計測モデルは時期の異なった実験に対してほぼ一様なモデルが開発され，時期や季節によらない安定な水質計測モデルの開発の可能性が示された。最後に，LANDSAT による霞ヶ浦全域の SS 濃度図の作成を行った。

1．国立公害研究所環境情報部　〒305　茨城県筑波郡谷田部町小野川 16 番 2

国立公害研究所特別研究成果報告

第 1 号　陸水域の富栄養化に関する総合研究――霞ケ浦を対象域として――昭和51年度．(1977)

第 2 号　陸上植物による大気汚染環境の評価と改善に関する基礎的研究――昭和51／52年度　研究報告．(1978)

(改　称)

国立公害研究所研究報告

※第 3 号　A comparative study of adults and immature stages of nine Japanese species of the genus *Chironomus* (Diptera, Chironomidae). (1978)
(日本産ユスリカ科　*Chironomus*　属9種の成虫，サナギ，幼虫の形態の比較)

第 4 号　スモッグチャンバーによる炭化水素――窒素酸化物系光化学反応の研究――昭和52年度中間報告．(1978)

第 5 号　芳香族炭化水素――窒素酸化物系の光酸化反応機構と光酸化二次生成物の培養細胞に及ぼす影響に関する研究．――昭和51，52年度　研究報告．(1978)

第 6 号　陸水域の富栄養化に関する総合研究(II)――霞ケ浦を中心として――昭和53年度．(1979)

※第 7 号　A morphological study of sdults and immature stages of 20 Japanese species of the family Chironomidae (Diptera). (1979)
(日本産ユスリカ科20種の成虫，サナギ，幼虫の形態学的研究)

※第 8 号　大気汚染物質の単一および複合汚染の生体に対する影響に関する実験的研究――昭和52，53年度　研究報告．(1979)

第 9 号　スモッグチャンバーによる炭化水素――窒素酸化物系光化学反応の研究――昭和53年度中間報告．(1979)

第 10 号　陸上植物による大気汚染環境の評価と改善に関する基礎的研究――昭和51～53年度　特別研究報告．(1979)

※第 11 号　Studies on the effects of air pollutants on plants and mechanisms of phytotoxicity. (1980)
(大気汚染物質の植物影響およびその植物毒性の機構に関する研究)

第 12 号　Multielement analysis stdies by flame and inductively coupled plasma spectroscopy utilizing computer-controlled instrumentation. (1980)
(コンピュータ制御装置を利用したフレームおよび誘導結合プラズマ分光法による多元素同時分析)

第 13 号　Studies on chironomid midges of the Tama River. (1980)
Part 1. The distribution of chironomid species in a tributary in relation to the degree of pollution with sewage water.
Part 2. Description of 20 species of Chironominae recovered from a tributary.
(多摩川に発生するユスリカの研究
――第1報　その一支流に見出されたユスリカ各種の分布と下水による汚染度との関係――
――第2報　その一支流に見出されたChironominae 亜科の20種について――)

第 14 号　有機廃棄物，合成有機化合物，重金属等の土壌生態系に及ぼす影響と浄化に関する研究――昭和53，54年度　特別研究報告．(1980)

※第 15 号　大気汚染物質の単一および複合汚染の生体に対する影響に関する実験的研究――昭和54年度　特別研究報告．(1980)

第 16 号　計測車レーザーレーダーによる大気汚染遠隔計測．(1980)

※第 17 号　流体の運動および輸送過程に及ぼす浮力効果――臨海地域の気象特性と大気拡散現象の研究――昭和53，54年度　特別研究報告．(1980)

第 18 号　Preparation, analysis and certification of PEPPERBUSH standard reference material. (1980)
(環境標準試料「リョウブ」の調製，分析および保証値)

※第 19 号　陸水域の富栄養化に関する総合研究（III）――霞ケ浦（西浦）の湖流――昭和53，54年度．(1981)

第 20 号　陸水域の富栄養化に関する総合研究（IV）――霞ケ浦流域の地形，気象水文特性およびその湖水環境に及ぼす影響――昭和53，54年度．(1981)

第 21 号　陸水域の富栄養化に関する総合研究（V）――霞ケ浦流入河川の流出負荷量変化とその評価――昭和53，54年度．(1981)

第 22 号　陸水域の富栄養化に関する総合研究（VI）――霞ケ浦の生態系の構造と生物現存量――昭和53，54年度．(1981)

第 23 号　陸水域の富栄養化に関する総合研究（VII）――湖沼の富栄養化状態指標に関する基礎的研究――昭和53，54年度 (1981)

第 24 号　陸水域の富栄養化に関する総合研究（VIII）――富栄養化が湖利用に及ぼす影響の定量化に関する研究――昭和53，54年度．(1981)

第 25 号　陸水域の富栄養化に関する総合研究（IX）――*Microcystis*（監藻類）の増殖特性――昭和53，54年度．(1981)

第 26 号　陸水域の富栄養化に関する総合研究（X）――藻類培養試験法によるＡＧＰの測定――昭和53，54年度．(1981)

第 27 号　陸水域の富栄養化に関する総合研究（XI）――研究総括――昭和53，54年度．(1981)

第 28 号　複合大気汚染の植物影響に関する研究――昭和54，55年度　特別研究報告．(1981)

第 29 号　Studies on chironomid midges of the Tama River. (1981)
Part 3. Species of the subfamily Orthocladiinae recorded at the summer survey and their distribution in relation to the pollution with sewage waters.
Part 4. Chironomidae recorded at a winter survey.
(多摩川に発生するユスリカ類の研究
――第３報　夏期の調査で見出されたエリユスリカ亜科Orthocladiinae 各種の記載と，その分布の下水汚染との関係について――
――第４報　南浅川の冬期の調査で見出された各種の分布と記載――)

※第 30 号　海域における富栄養化と赤潮の発生機構に関する基礎的研究――昭和54，55年度　特別研究報告．(1982)

第 31 号　大気汚染物質の単一および複合汚染の生体に対する影響に関する実験的研究――昭和55年度　特別研究報告．(1981)

第 32 号　スモッグチャンバーによる炭化水素－窒素酸化物系光化学反応の研究――環境大気中における光化学二次汚染物質生成機構の研究（フィールド研究１）――昭和54年度　特別研究中間報告．(1982)

第 33 号　臨海地域の気象特性と大気拡散現象の研究――大気運動と大気拡散過程のシミュレーション――昭和55年度　特別研究報告．(1982)

※第 34 号　環境汚染の遠隔計測・評価手法の開発に関する研究――昭和55年度　特別研究報告．(1982)

第 35 号　環境面よりみた地域交通体系の評価に関する総合解析研究．(1982)

第 36 号　環境試料による汚染の長期モニタリング手法に関する研究――昭和55，56年度　特別研究報告．(1982)

第 37 号　環境施策のシステム分析支援技術の開発に関する研究．(1982)

第 38 号　Preparation, analysis and certification of POND SEDIMENT certified reference meterial．(1982)
（環境標準試料「池底質」の調製，分析及び保証値）

※第 39 号　環境汚染の遠隔計測・評価手法の開発に関する研究――昭和56年度　特別研究報告．(1982)

第 40 号　大気汚染物質の単一及び複合汚染の生体に対する影響に関する実験的研究――昭和56年度特別研究報告．(1983)

※第 41 号　土壌環境の計測と評価に関する統計学的研究．(1983)

※第 42 号　底泥の物性及び流送特性に関する実験的研究．(1983)

※第 43 号　Studies on chironomid midges of the Tama River．(1983)
Part 5．An observation on the distribution of Chironominae along the main stream in June with description of 15 new species.
Part 6．Description of species of the subfamily Orthocladiinae recovered from the main stream in the June survey.
Part 7．Additional species collected in winter from the main stream.
（多摩川に発生するユスリカ類の研究
――第５報　本流に発生するユリカ類の分布に関する６月の調査成績とユスリカ亜科に属する15新種等の記録――
――第６報　多摩本流より６月に採集されたエリユスリカ亜科の各種について――
――第７報　多摩本流より３月に採集されたユスリカ科の各種について――）

第 44 号　スモッグチャンバーによる炭化水素―窒素酸化物系光化学反応の研究――環境大気中における光化学二次汚染物質生成機構の研究（フィールド研究２）――昭和54年度　特別研究中間報告．(1983)

第 45 号　有機廃棄物，合成有機化合物，重金属等の土壌生態系に及ぼす影響と浄化に関する研究――昭和53～55年度　特別研究報告．(1983)

第 46 号　有機廃棄物，合成有機化合物，重金属等の土壌生態系に及ぼす影響と浄化に関する研究――昭和54，55年度　特別研究報告　第１分冊．(1983)

第 47 号　有機廃棄物，合成有機化合物，重金属等の土壌生態系に及ぼす影響と浄化に関する研究――昭和54，55年度　特別研究報告　第２分冊．(1983)

※第 48 号　水質観測点の適正配置に関するシステム解析．(1983)

第 49 号　環境汚染の遠隔計測・評価手法の開発に関する研究――昭和57年度　特別研究報告．(1984)

※第 50 号　陸水域の富栄養化防止に関する総合研究（Ⅰ）――霞ケ浦の流入負荷量の算定と評価――昭和55～57年度　特別研究報告．(1984)

※第 51 号　陸水域の富栄養化防止に関する総合研究（Ⅱ）――霞ケ浦の物質循環とそれを支配する因子――昭和55～57年度　特別研究報告．(1984)

※第 52 号　陸水域の富栄養化防止に関する総合研究（Ⅲ）――霞ケ浦高浜入における隔離水界を利用した富栄養化防止手法の研究――昭和55～57年度　特別研究報告．(1984)

第 53 号　陸水域の富栄養化防止に関する総合研究（Ⅳ）――霞ケ浦の魚類及び甲かく類現存量の季節変化と富栄養化――昭和55～57年度　特別研究報告．(1984)

第 54 号　陸水域の富栄養化防止に関する総合研究（Ⅴ）――霞ケ浦の富栄養化現象のモデル化――昭和55～57年度　特別研究報告．(1984)

第 55 号　陸水域の富栄養化防止に関する総合研究（Ⅵ）――富栄養化防止対策――昭和55～57年度特別研究報告．(1984)

第 56 号　陸水域の富栄養化防止に関する総合研究（Ⅶ）――湯ノ湖における富栄養化とその防止対策――昭和55～57年度　特別研究報告．(1984)

※第 57 号　陸水域の富栄養化防止に関する総合研究（Ⅷ）――総括報告――昭和55～57年度　特別研究報告．（1984）

第 58 号　環境試料による汚染の長期的モニタリング手法に関する研究――昭和55～57年度　特別研究総合報告．（1984）

第 59 号　炭化水素－窒素酸化物－硫黄酸化物系光化学反応の研究――光化学スモッグチャンバーによるオゾン生成機構の研究――大気中における有機化合物の光酸化反応機構の研究――昭和55～57年度　特別研究報告（第１分冊）．（1984）

第 60 号　炭化水素－窒素酸化物－硫黄酸化物系光化学反応の研究――光化学エアロゾル生成機構の研究――昭和55～57年度　特別研究報告（第２分冊）．（1984）

第 61 号　炭化水素－窒素酸化物－硫黄酸化物系光化学反応の研究――環境大気中における光化学二次汚染物質生成機構の研究（フィールド研究１）――昭和55～57年度　特別研究報告（第３分冊）．（1984）

第 62 号　有害汚染物質による水界生態系のかく乱と回復過程に関する研究――昭和56～58年度　特別研究中間報告．（1984）

※第 63 号　海域における富栄養化と赤潮の発生機構に関する基礎的研究――昭和56年度　特別研究報告．（1984）

※第 64 号　複合大気汚染の植物影響に関する研究――昭和54～56年度　特別研究総合報告．（1984）

第 65 号　Studies on effects of air pollutant mixtures on plants － Part 1．（1984）
（複合大気汚染の植物に及ぼす影響――第１分冊）

※第 66 号　Studies on effects of air pollutant mixtures on plants － Part 2．（1984）
（複合大気汚染の植物に及ぼす影響――第２分冊）

第 67 号　環境中の有害物質による人の慢性影響に関する基礎的研究――昭和54～56年度　特別研究総合報告．（1984）

※第 68 号　汚泥の土壌還元とその環境影響に関する研究――昭和56～57年度　特別研究総合報告．（1984）

※第 69 号　中禅寺湖の富栄養化現象に関する基礎的研究．（1984）

第 70 号　Studies on chironomid midges in lakes of the Nikko National Park．（1984）
Part Ⅰ．Ecological studies on chironomids in lakes of the Nikko National Park．
Part Ⅱ．Taxonomical and morphological studies on the chironomid species collected from lakes in the Nikko National Park．
（日光国立公園の湖沼のユスリカに関する研究
――第１部　日光国立公園の湖のユスリカの生態学的研究――
――第２部　日光国立公園の湖沼に生息するユスリカ類の分類学的，形態学的研究――）

※第 71 号　リモートセンシングによる残雪及び雪田植生の分布解析．（1984）

第 72 号　炭化水素－窒素酸化物－硫黄酸化物系光化学反応の研究　環境大気中における光化学二次汚染物質生成機構の研究（フィールド研究２）――昭和55～57年度　特別研究報告（第４分冊）．（1985）

※第 73 号　炭化水素－窒素酸化物－硫黄酸化物系光化学反応の研究――昭和55～57年度　特別研究総合報告．（1985）

※第 74 号　都市域及びその周辺の自然環境に係る環境指標の開発に関する研究．環境指標――その考え方と作成方法――昭和59年度　特別研究報告．（1984）

第 75 号　Limnological and environmental studies of elements in the sediment of Lake Biwa．（1985）
（琵琶湖底泥中の元素に関する陸水学及び環境化学的研究）

第 76 号　Study on the behavior of monoterpenes in the atmosphere. (1985)
（大気中モノテルペンの挙動に関する研究）
第 77 号　環境汚染の遠隔計測・評価手法の開発に関する研究――昭和58年度　特別研究報告. (1985)
第 78 号　生活環境保全に果たす生活者の役割の解明. (1985)
第 79 号　Studies on the method for long term environmental monitoring —— Research report in 1980-1982. (1985)
（環境汚染による汚染の長期的モニタリング手法に関する研究）
第 80 号　海域における赤潮発生のモデル化に関する研究――昭和57/58年度　特別研究報告. (1985)
第 81 号　環境影響評価制度の政策効果に関する研究――地方公共団体の制度運用を中心として. (1985)
第 82 号　植物の大気環境浄化機能に関する研究――昭和57～58年度　特別研究報告. (1985)
第 83 号　Studies on chironomid midges of some lakes in Japan. (1985)
（日本の湖沼に発生するユスリカ類の研究）
第 84 号　重金属環境汚染による健康影響評価手法の開発に関する研究――昭和57～59年度　特別研究総合報告. (1985)
第 85 号　Studies on the rate constants of free radical reactions and related spectroscopic and thermochemical parameters. (1985)
（フリーラジカルの反応速度と分光学的及び熱力学的パラメーターに関する研究）
第 86 号　GC/MSスペクトルの検索システムに関する研究. (1986)
第 87 号　光化学二次汚染物質の分析とその細胞毒性に関する基礎的研究――昭和53～58年度　総合報告. (1986)
第 88 号　都市域及びその周辺の自然環境等に係る環境指標の開発に関する研究II. 環境指標――応用例とシステム. (1986)
第 89 号　Measuring the water quality of Lake Kasumigaura by LANDSAT remote sensing. (1986)
（LANDSAT リモートセンシングによる霞ケ浦の水質計測）
第 90 号　ナショナルトラスト運動にみる自然保護運動にむけての住民意識と行動――知床国立公園内100平方メートル運動と天神崎市民地主運動への参加者の分析を中心として. (1986)
第 91 号　Economic analysis of man's utilization of environmental resources in aquatic environments and national park regions. (1986)
（人間による環境資源利用の経済分析――水環境と国立公園地域を対象にして）
第 92 号　アオコの増殖及び分解に関する研究. (1986)
第 93 号　汚泥の土壌還元とその環境影響に関する研究（I）――昭和58～59年度　特別研究総合報告（第1分冊）. (1986)
第 94 号　汚泥の土壌還元とその環境影響に関する研究（II）――昭和58～59年度　特別研究総合報告（第2分冊）. (1986)
第 95 号　自然浄化機能による水質改善に関する総合研究（I）――汚濁負荷の発生と流出・流達――昭和58～59年度　特別研究報告. (1986)
第 96 号　自然浄化機能による水質改善に関する総合研究（II）――水草帯・河口域・池沼の生態系構造と機能――昭和58～59年度　特別研究報告. (1986)

※　残部なし

Report of Special Research Project the National Institute for Environmental Studies

No. 1 * Man activity and aquatic environment—with special references to Lake Kasumigaura —Progress report in 1976. (1977)

No. 2 * Studies on evaluation and amelioration of air pollution by plants —Progress report in 1976-1977. (1978)

[Starting with Report No. 3, the new title for NIES Reports was changed to:]

Research Report from the National Institute for Environmental Studies

※No. 3 A comparative study of adults and immature stages of nine Japanese species of the genus *Chironomus* (Diptera, Chironomidae). (1978)

No. 4 * Smog chamber on photochemical reactions of hydrocarbon-nitrogen oxides system —Progress report in 1977. (1978)

No. 5 * Studies on the photooxidation products of the alkylbenzene-nitrogen oxides system, and on their effects on Cultured Cells —Research report in 1976-1977. (1978)

No. 6 * Man activity and aquatic environment—with special references to Lake Kasumigaura —Progress report in 1977-1978. (1979)

※No. 7 A morphological study of adults and immature stages of 20 Japanese species of the family Chironomidae (Diptera). (1979)

※No. 8 * Studies on the biological effects of single and combined exposure of air opllutants —Research report in 1977-1978. (1979)

No. 9 * Smog chamber studies on photochemical reactions of hydrocarbon-nitrogen oxides system —Progress report in 1978. (1979)

No. 10* Studies on evaluation and amelioration of air pollution by plants —Progress report in 1976-1978. (1979)

※No. 11 Studies on the effects of air pollutants on plants and mechanisms of phytotoxicity. (1980)

No. 12 Multielement analysis studies by flame and inductively coupled plasma spectroscopy utilizing computer-controlled instrumentation. (1980)

No. 13 Studies on chironomid midges of the Tama River.(1980)
Part 1. The distribution of chironomid species in a tributary in relation to the degree of pollution with sewage water.
Part 2. *Description of 20 species of Chironominae recovered from a tributary.*

No. 14* Studies on the effects of organic wastes on tha soil ecosystem—Progress report in 1978-1979. (1980)

※No. 15* Studies on the biological effects of single and combined exposure of air pollutants —Research report in 1977-1978. (1980)

No. 16* Remote measurement of air pollution by a mobile laser radar. (1980)

※No. 17* Influence of buoyancy on fluid motions and transport processes —Meteorological characteristics and atmospheric diffusion phenomena in the coastal region—Progress report in 1978-1979. (1980)

No. 18 Preparation, analysis and certification of PEPPERBUSH standard reference material. (1980)

※No. 19* Comprehensive studies on the eutrophication of fresh-water areas—Lake current of Kasumigaura (Nishiura)— 1978-1979. (1981)

No. 20* Comprehensive studies on the eutrophication of fresh-water areas—Geomorphological and hydrometeorological characteristics of Kasumigaura watershed as related to the lake environment— 1978-1979. (1981)

No. 21* Comprehensive studies on the eutrophication of fresh-water areas—Variation of pollutant load by influent rivers to Lake Kasumigaura— 1978-1979. (1981)

No. 22* Comprehensive studies on the eutrophication of fresh-water areas—Structure of ecosystem and standing crops in Lake Kasumigaura— 1978-1979. (1981)

No. 23* Comprehensive studies on the eutrophication of fresh-water areas—Applicability of trophic state indices for lakes — 1978-1979. (1981)

No. 24* Comprehensive studies on the eutrophication of fresh-water areas—Quantitative analysis of eutrophication effects on main utilization of lake water resources— 1978-1979. (1981)

No. 25* Comprehensive studies on the eutrophication of fresh-water areas—Growth characteristics of Blue-Green Algae, *Mycrocystis* — 1978-1979. (1981)

No. 26* Comprehensive studies on the eutrophication of fresh-water areas—Determination of argal growth potential by algal assay procedure— 1978-1979. (1981)

No. 27* Comprehensive studies on the eutrophication of fresh-water areas—Summary of researches — 1978-1979. (1981)

No. 28* Studies on effects of air pollutant mixtures on plants—Progress repot in 1979-1980. (1981)

No. 29 Studies on chironomid midges of the Tama River. (1981)
Part 3. Species of the subfamily Orthocladiinae recorded at the summer survey and their distribution in relation to the pollution with sewage waters.
Part 4. Chironomidae recorded at a winter survey.

※No. 30* Eutrophication and red tides in the coastal marine environment—Progress report in 1979-1980. (1982)

No. 31* Studies on the biological effects of single and combined exposure of air pollutants —Research report in 1980. (1981)

No. 32* Smog chamber studies on photochemical reactions of hydrocarbon-nitrogen oxides system —Progress report in 1979 —Research on the photochemical secondary pollutants formation mechanism in the environmental atmosphere (Part 1). (1982)

No. 33* Meteorological characteristics and atmospheric diffusion phenomena in the coastal region—Simulation of atmospheric motions and diffusion processes —Progress report in 1980. (1982)

※No. 34* The development and evaluation of remote measurement methods for environmental pollution—Research report in 1980. (1982)

No. 35* Comprehensive evaluation of environmental impacts of road and traffic. (1982)

No. 36* Studies on the method for long term environmental monitoring —Progress report in 1980-1981. (1982)

No. 37* Study on supporting technology for systems analysis of environmental policy —The evaluation laboratory of Man-Environment Systems. (1982)

No. 38 Preparation, analysis and certification of POND SEDIMENT certified reference material. (1982)

※No. 39* The development and evaluation of remote measurement methods for environmental pollution—Research report in 1981. (1983)

No. 40* Studies on the biological effects of single and combined exposure of air pollutants —Research report in 1981. (1983)

※No. 41* Statistical studies on methods of measurement and evaluation of chemical condition of soil. (1983)

※No. 42* Experimental studies on the physical properties of mud and the characteristics of mud transportation. (1983)

※No. 43 Studies on chironomid midges of the Tama River. (1983)

Part 5. An observation on the distribution of Chironominae along the main stream in June, with description of 15 new species.

Part 6. Description of species of the subfamily Orthocladiinae recovered from the main stream in the June survey.

Part 7. Additional species collected in winter from the main stream.

No. 44* Smog chamber studies on photochemical reactions of hydrocarbon-nitr ogen oxides system—Progress report in 1979 —Research on the photochemical secondary pollutants formation mechanism in the environmental atomosphere (Part 2). (1983)

No. 45* Studies on the effect organic wastes on the soil ecosystem —Outlines of special resarch project— 1978-1980. (1983)

No. 46* Stusies on the effect of organic wastes on the soil ecosystem —Research report in 1979-1980, Part 1. (1983)

No. 47* Studies on the effect of organic wastes on the soil ecosystem —Research report in 1979-1980, Part 2 (1983)

※No. 48* Study on optimal allocation of water quality monitoring points. (1983)

No. 49* The development and evaluation of remote measurement method for environmental pollution —Research report in 1982. (1984)

※No. 50* Comprehensive studies on the eutrophication control of freshwaters—Estimation of input loading of Lake Kasumigaura.— 1980-1982. (1984)

※No. 51* Comprehensive studies on the eqtrophication control of freshwaters—The function of the ecosystem and significanse of sediment in nutrient cycle in Lake Kasumigaura. — 1980-1982.(1984)

※No. 52* Comprehensive studies on the eutrophication control of freshwaters—Enclosure experiments for restoration of highly eutrophic shallow Lake Kasumigaura. — 1980-1982. (1984)

No. 53* Comprehensive studies on the eutrophication control of freshwaters—Seasonal changes of hte biomass of fishes and crustacia in Lake Kasumigaura. — 1980-1982. (1984)

No. 54* Comprehensive studies on the eutrophication control of freshwaters—Modeling the eutrophicatión of Lake Kasumigaura. — 1980-1982.(1984)

No. 55* Comprehensive studies on the eutrophication control of freshwaters—Measures for eutrophication control.— 1980-1982.(1984)

No. 56* Comprehensive studies on the eutrophication control of freshwaters—Eutrophicattion in Lake Yunoko. — 1980-1982. (1984)

※No. 57* Comprehensive studies on the eutrophication control of freshwaters—Summary of researches. — 1980-1982. (1984)

No. 58* Studies on the method for long term environmental monitoring—Outlines of special research project in 1980-1982. (1984)

No. 59* Studies on photochemical reactions of hydrocarbon-nitrogen oxides-sulfer oxides system —Photochemical ozone formation studies by the evacuable smog chamber —Atomospheric photooxidation mechanisms of selected organic compqunds —Research report in 1980-1982, Part1. (1984)

No. 60* Studies on photochemical reactions of hydrocarbon-nitrogen oxides-sulfer oxides system —Formation mechanisms of photochemical aerozol —Research report in 1980-1982, Part2. (1984)

No. 61* Studies on photochemical reactions of hydrocarbon-nitrogen oxides-sulfer oxides system —Research on the photochemical secondary pollutants formation mechanism in the environmental atmosphere (Part 1) —Research report in 1980-1982, Part 3. (1984)

No. 62* Effects of toxic substances on aquatic ecosystems —Progress report in 1980-1983. (1984)

※No. 63* Eutrophication and red tides in the coastal marine environment —Progress report in 1981. (1984)

※No. 64* Studies on effects of air pollutant mixtures on plants—Final report in 1979-1981. (1984)

No. 65 Studies on effects of air pollutant mixtures on plants—Part 1. (1984)

※No. 66 Studies on effects of air pollutant mixtures on plants—Part 2. (1984)

No. 67* Studies on unfavourable effects on human body regarding to several toxic materials in the environment, using epidemiological and anaiytical techniques —Project research report in 1979-1981. (1984)

※No. 68* Studies on the environmental effects of the application of sewage sludge to soil —Research report in 1981-1982. (1984)

No. 69* Fundamental studies on the eutrophication of Lake Chuzenji—Basic research report. (1984)

No. 70 Studies on chironomid midges in lakes of the Nikko National Park—Part 1. Ecological studies on chironomids in lakes of the Nikko National Park. —Part II. Taxonomical and morphological studies on the chironomid species collected from lakes in the Nikko National Park. (1984)

※No.71* Analysis on distributions of remnant snowpack and snow patch vegetation by remote sensing. (1984)

No.72* Studies on photochemical reactions of hydrocarbon-nitrogen oxides-sulfur oxides-system—Research on the photochemical secondary pollutants formation mechanism in the environmental atmosphere. —Research report in 1980-1982. (1985)

※No.73* Studies on photochemical reactions of hydrocarbon-nitrogen oxides-sulfur oxides-system—Final report in 1980-1982. (1985)

※No.74* A comprehensive study on the development of indices system for urban and suburban environmental quality—Environmental indices-Basic notion and formaftioln (1984)

No.75 Limnological and environmental studies of elements in the sediment ofe Lake Biwa. (1985)

No.76 A Study on the behavior of monoterpenes in the atmosphere. (1985)

No.77* The development and evaluation of remote measurement methods for environmental pollution Research Report in 1983 (1985)

No.78* Study on residents' role in conserving the living environment. (1985)

No.79 Studies on the method for long term environmental monitoring—Research report in 1980-1982. (1985)

No.80* Modeling of red tide blooms in the coastal sea—Research report 1982-1983. (1985)

No.81* A study on effects of implementing environmental impact assessment procedure—With particular reference to implementation by local governments. (1985)

No.82* Studies on the role of vegetation as a sink of air pollutants —Research report in 1982-1983. (1985)

No.83 Studies on chironomid midges of some lakes in Japan. (1985)

No.84 A comprehensive study on the development of assessment techniques for health effects due to envirqnmental heavy metal exposure —Final report in 1982-1984. (1985)

No.85 Studies on the rate constants of free radical reactions and related spectroscopic and thermochemical parameters. (1985)

No.86* A novel retrieval system for identifications of unknown mass spetra. (1986)

No.87* Analysis of the photochemical secondary pollutants and their toxicity on caltured cells —Research report in 1978-1983. (1986)

No.88* A comprehensive study on the development of indices system for urban and suburban environmental quality II—Enviromental indices—Applications and systems. (1986)

No.89 Measuring the water quality of Lake Kasumigaura by LANDSAT remote sensing. (1986)

* in Japanese

※ out of stock

〔昭和60年5月8日受領〕
〔昭和60年11月26日受理〕

RESEARCH REPORT FROM
THE NATIONAL INSTITUTE FOR ENVIRONMENTAL STUDIES, JAPAN
No.89

国立公害研究所研究報告　第89号

(R—89—'86)

昭和61年2月28日発行

発行　環境庁　国立公害研究所

茨城県筑波郡谷田部町小野川16番2

印刷　HEC印刷株式会社
茨城県日立市大みか町5－1－26

Published by the National Institute for Environmental Studies
Yatabe-machi, Tsukuba, Ibaraki 305, Japan
February 1986